Over de zoutcrisis in de Middellandse Zee tijdens het Messinien (2)

Voor de werkgroep Algemene Geologie Kring Rijnland

Tom Kleijn 15 december 2015

Inhoud

- Inleiding
- Het Messinien en MSC
- Watercirculatie in MZ.
- De zeestraten tussen de AO en de MZ
- De aanloop naar de zoutcrisis en de eerste afzettingen van de zoutcrisis

DISTRIBUTION OF EMERGED LAND AND SEA 6 MILLION YEARS AGO

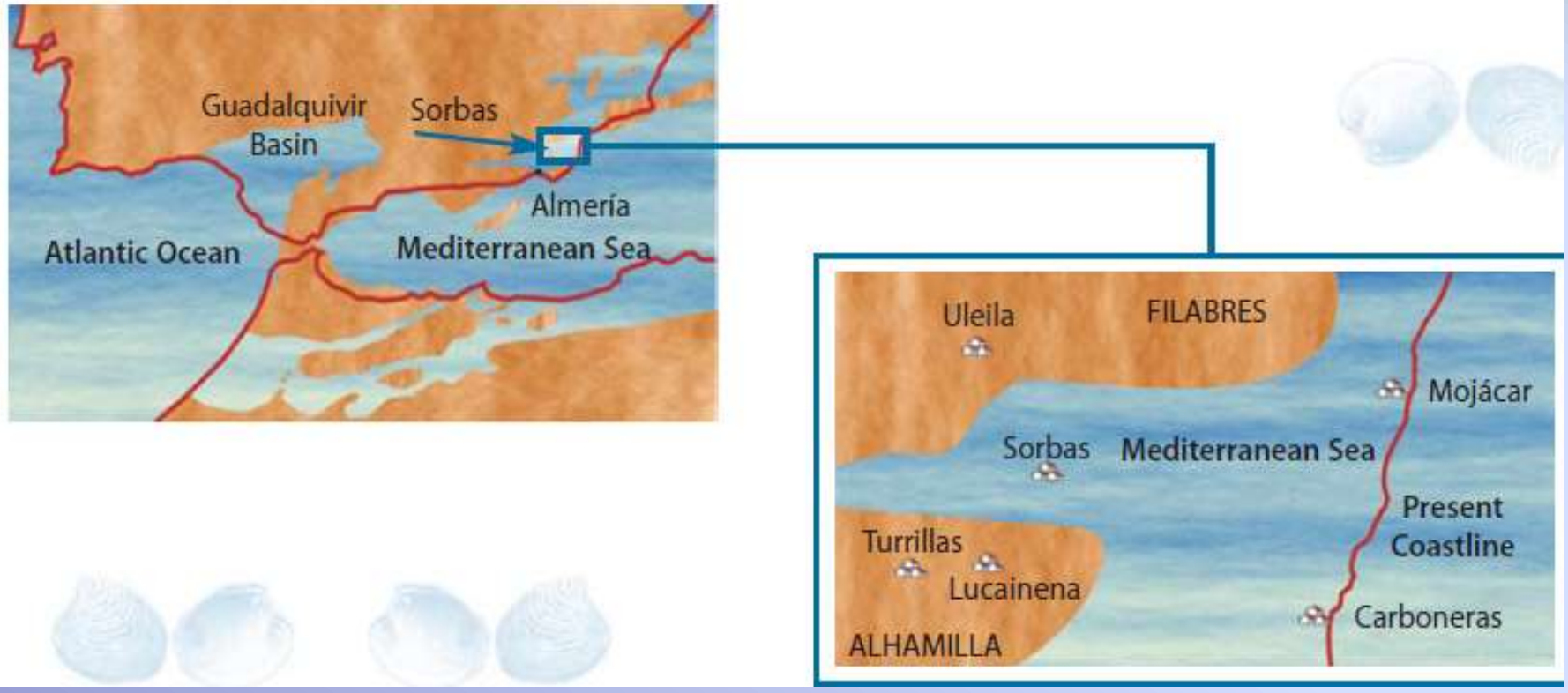


S
MSC onset
Perales section
(Sierro et al., 2001)
Lower Evaporites
Transition to the Gypsum
UA34
UA33
UA32
UA31
UA30
UA29
UA28
UA27
PRIMARY LOWER GYPSUM
(Yesares Formation)
PLG2
PLG1
UA34
UA33
UA32
UA31
UA30
UA29
UA28
PRE-EVAPORITIC
(Abad Formation)
IBERIAN PLATE
BETICS
RIF

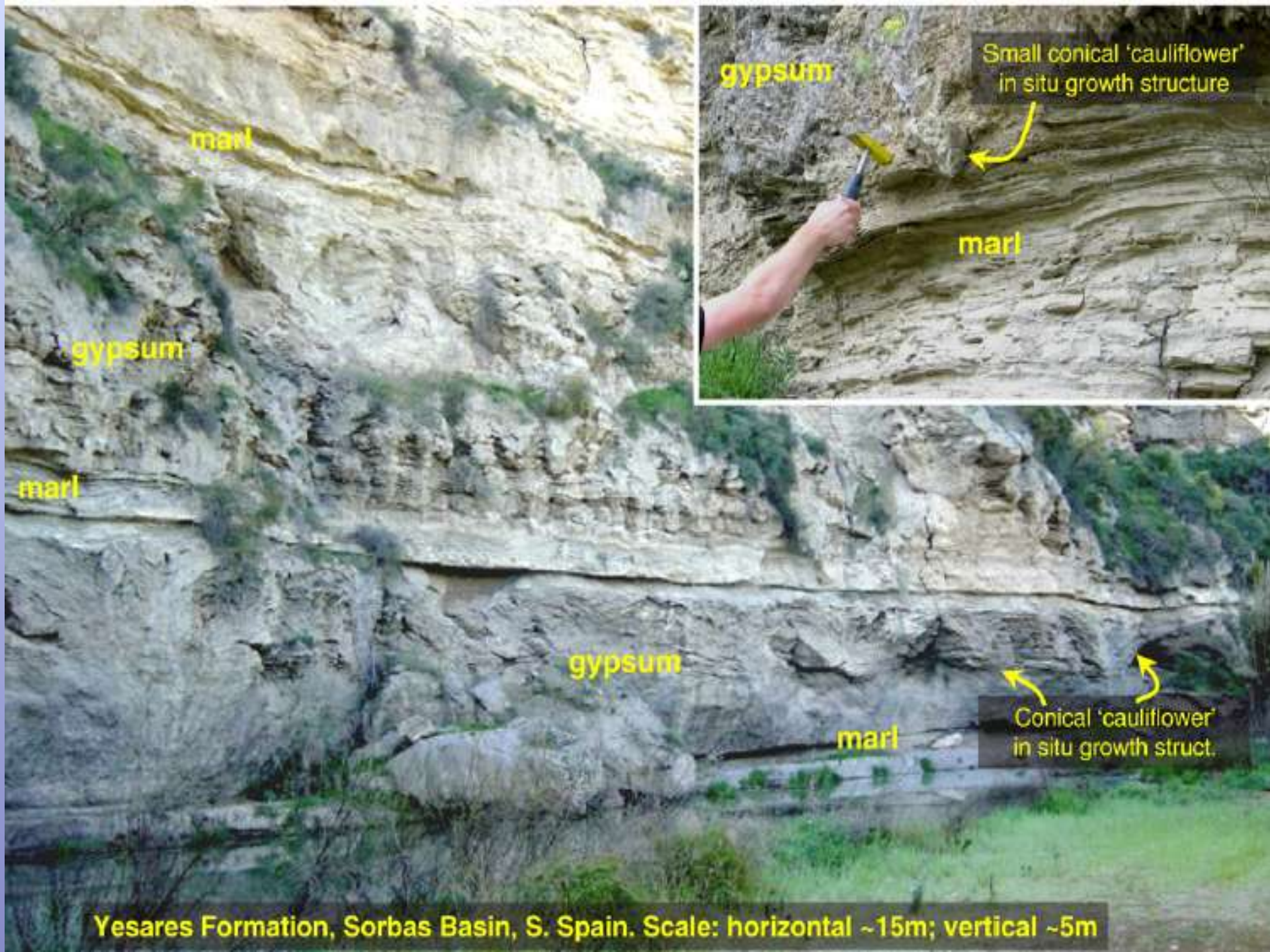
marl
gypsum
marl
gypsum
marl
gypsum
Small conical 'cauliflower' in situ growth structure
marl
Conical 'cauliflower' in situ growth struct.
Yesares Formation, Sorbas Basin, S. Spain. Scale: horizontal ~15m; vertical ~5m

Wanneer?

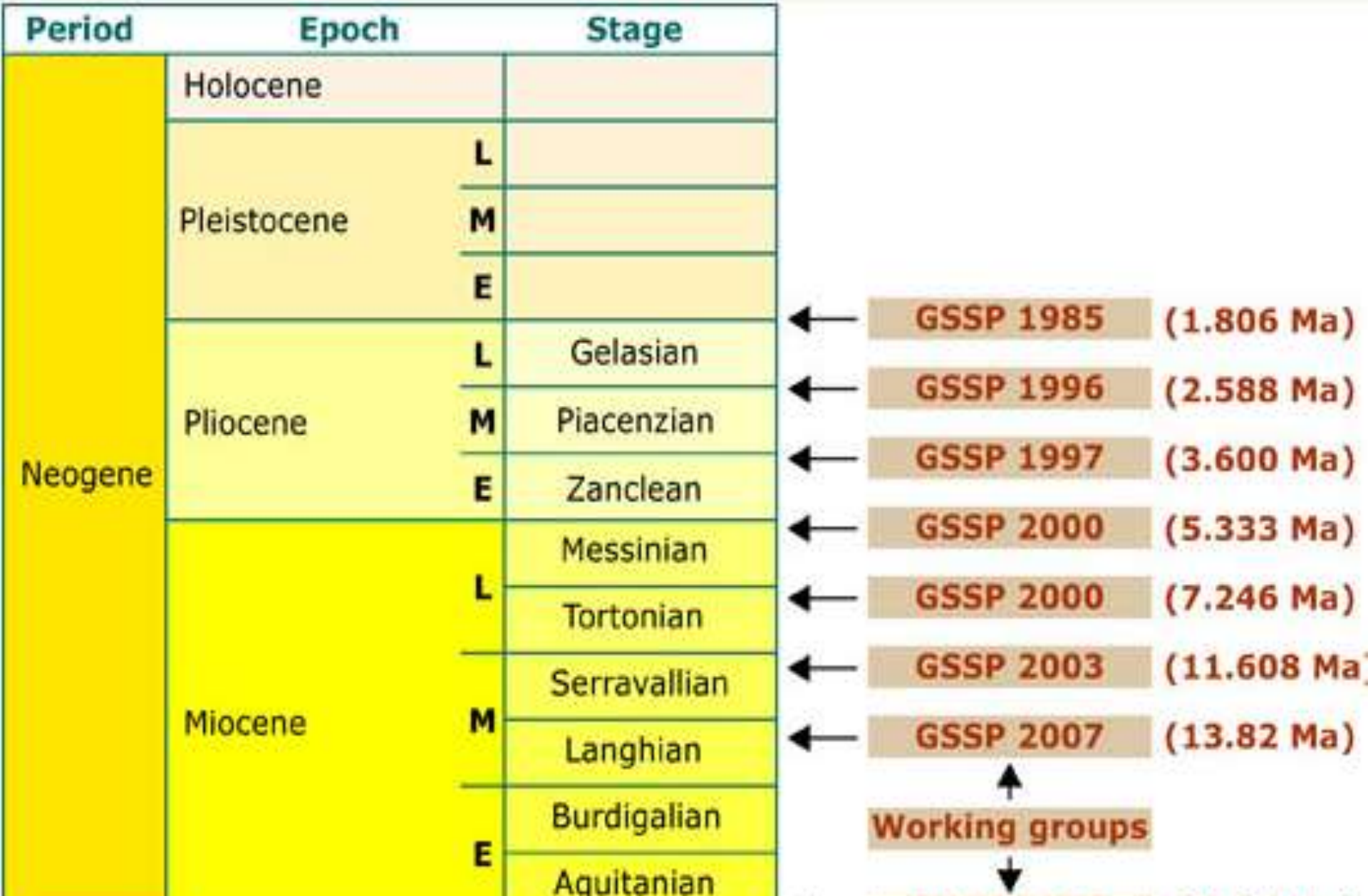
Period
Epoch
Stage
Neogene
Holocene
Pleistocene
L
M
E
Pliocene
L
M
E
Gelasian
Piacenzian
Zanclean
Miocene
L
M
E
Messinian
Tortonian
Serravallian
Langhian
Burdigalian
Aquitanian
GSSP 1985 (1.806 Ma)
GSSP 1996 (2.588 Ma)
GSSP 1997 (3.600 Ma)
GSSP 2000 (5.333 Ma)
GSSP 2000 (7.246 Ma)
GSSP 2003 (11.608 Ma)
GSSP 2007 (13.82 Ma)
Working groups

De “Golden Spikes” voor het Messinien

GSSP's

Map of GSSP's

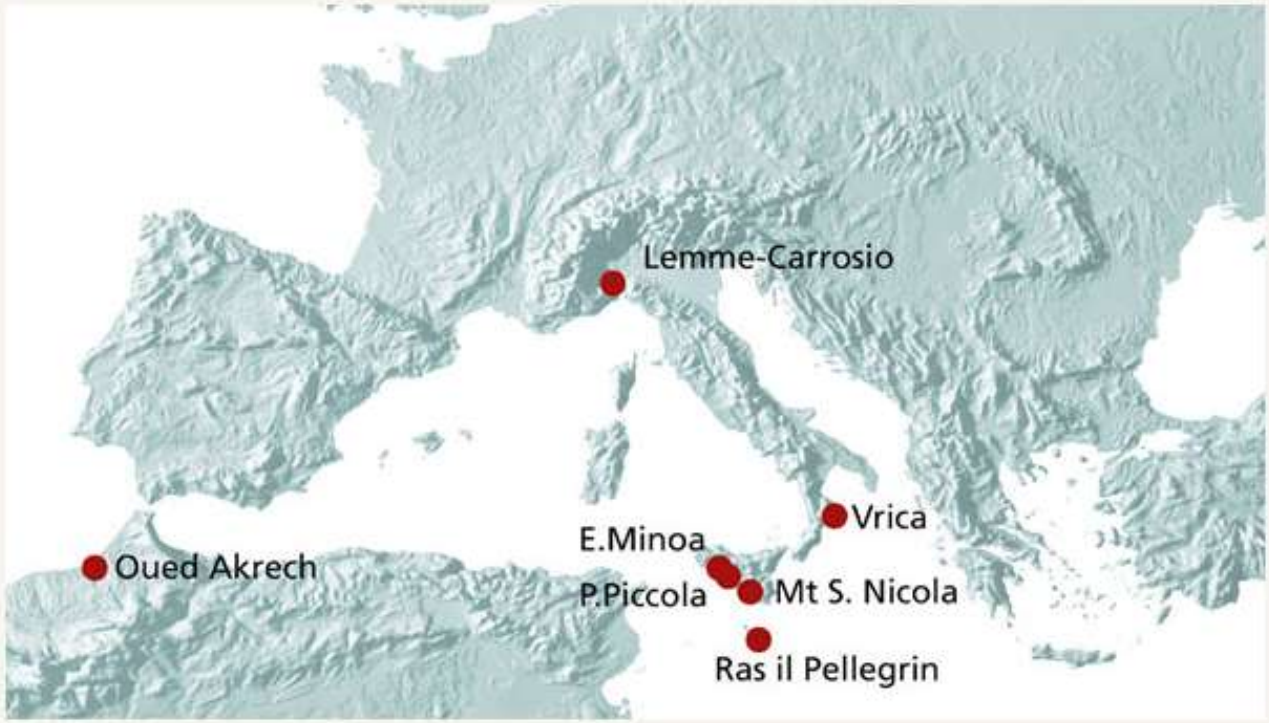

Stage	Section	Location
base Pleistocene	Vrica, near Crotone, Italy	39°05' N, 17°07' E
base Gelasian	Mt S. Nicola, near Gela, Sicily, Italy	37°04' N, 14°15' E
base Piacenzian	Punte Piccola, Sicily, Italy	37°17'20'' N, 13°29'36'' E
base Zanclean	Eraclea Minoa, Sicily, Italy	37°23'30'' N, 13°16'50'' E
base Messinian	Oued Akrech, Morrocco	33°56'13'' N, 6°48'45'' E
base Neogene	Lemme-Carrosio, northern Italy	44°39'32'' N, 8°50'11'' E
base Serravallian	Ras il Pellegrin	35°54'56'' N, 14°20'03'' E

Begin Messinien

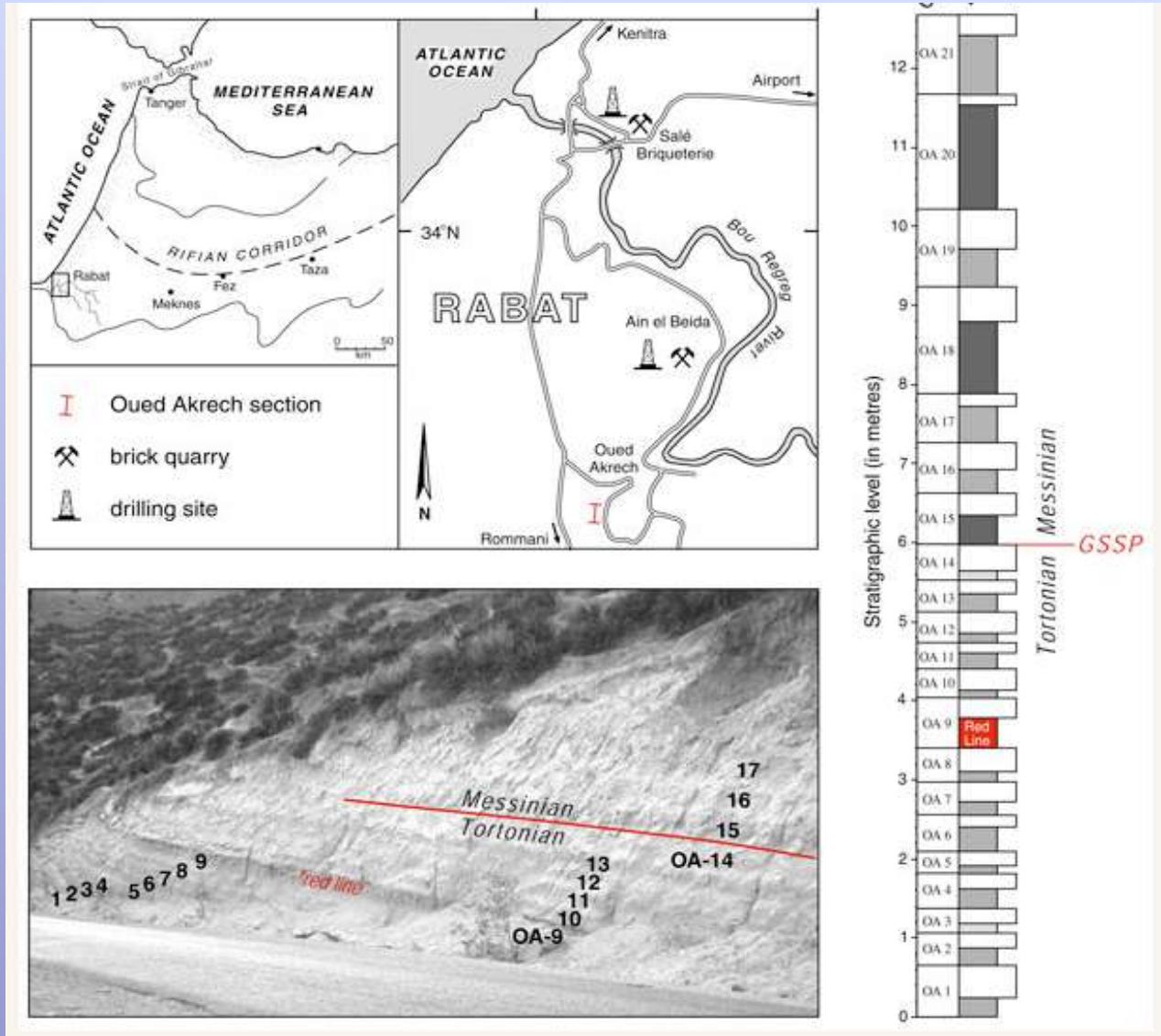

Het einde van het Messinien

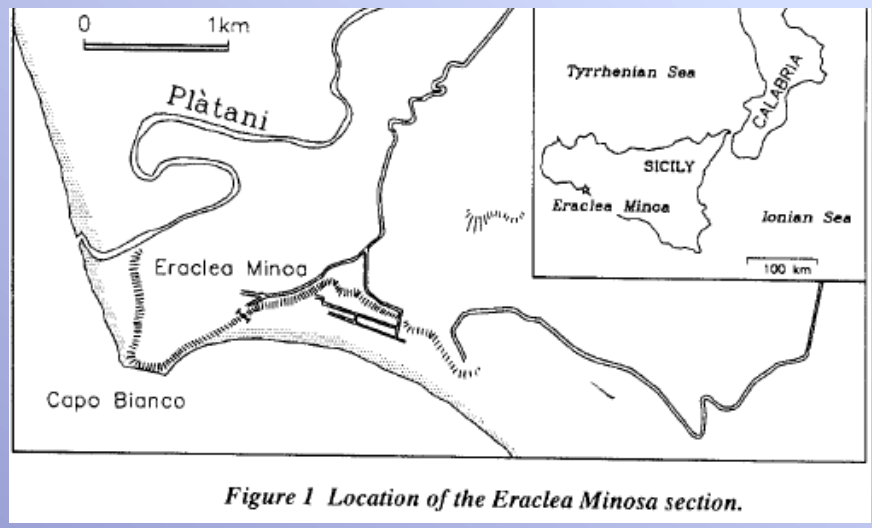

Figure 1 Location of the Eraclea Minosa section.

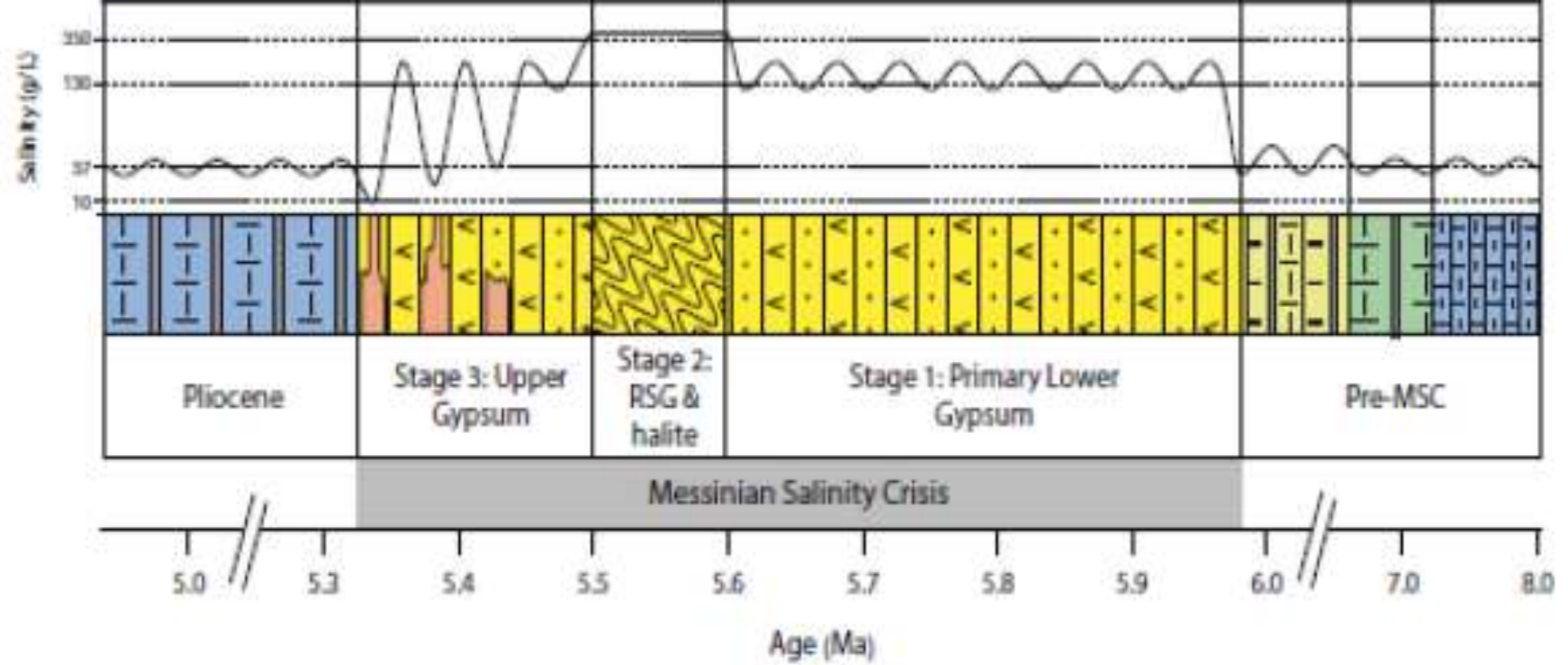

Indeling Messinien 7,246 Ma

Begin Messinien 7,246
Einde Messinien 5,33
Totale duur Messinien 1,913 milj. jaar
Aanloop naar MSC ruim 1,275 milj. jaar
Begin MSC 5,971Ma
Einde MSC 5,33 Ma
MSC totaal 638.000 jaar

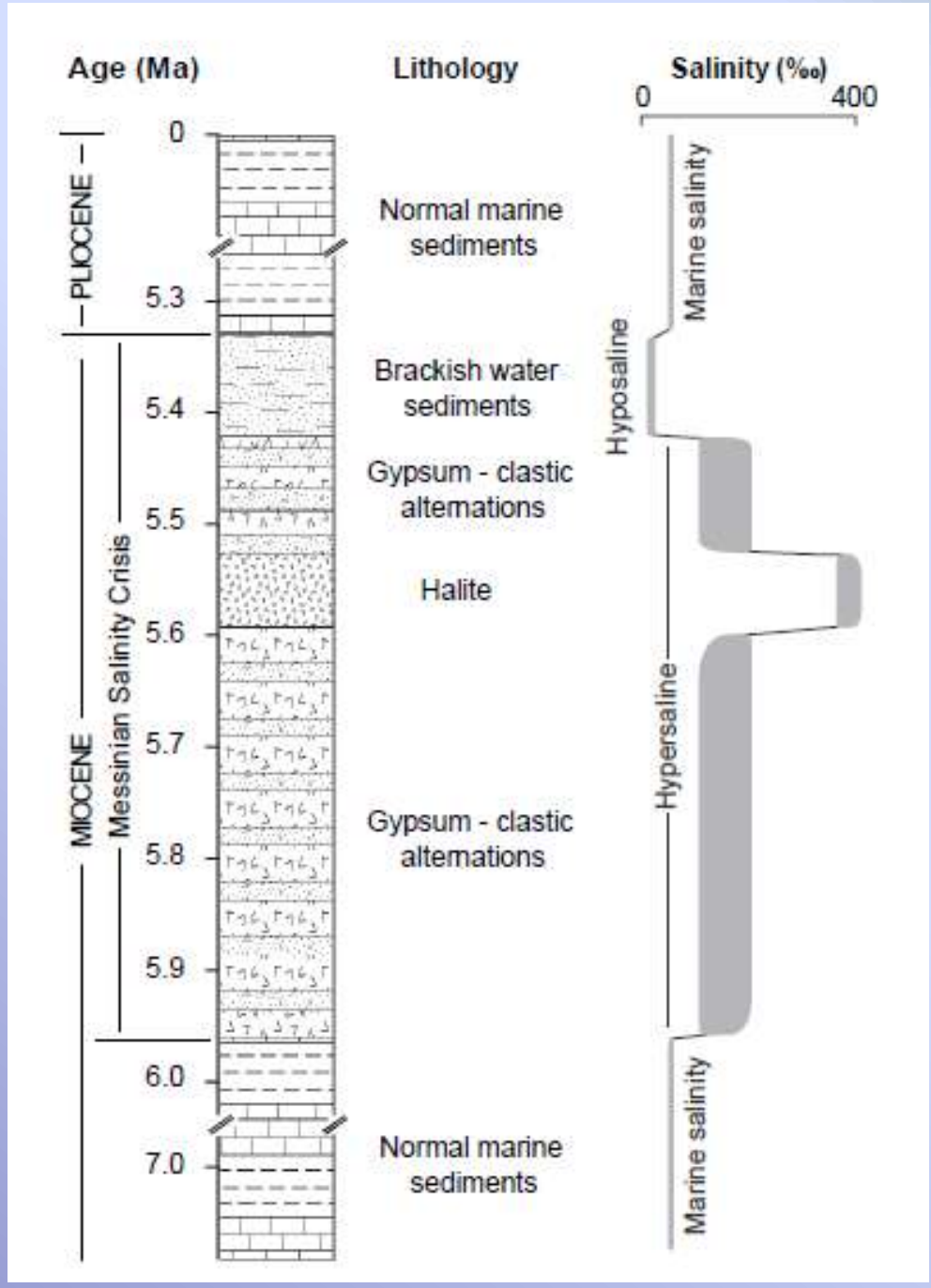
Age (Ma)
Lithology
Salinity (‰)
0
400
0
5.3
5.4
5.5
5.6
5.7
5.8
5.9
6.0
7.0
PLIOCENE
MIOCENE
Messinian Salinity Crisis
Normal marine sediments
Brackish water sediments
Gypsum - clastic alternations
Halite
Gypsum - clastic alternations
Normal marine sediments
Hyposaline
Marine salinity
Hypersaline
Marine salinity

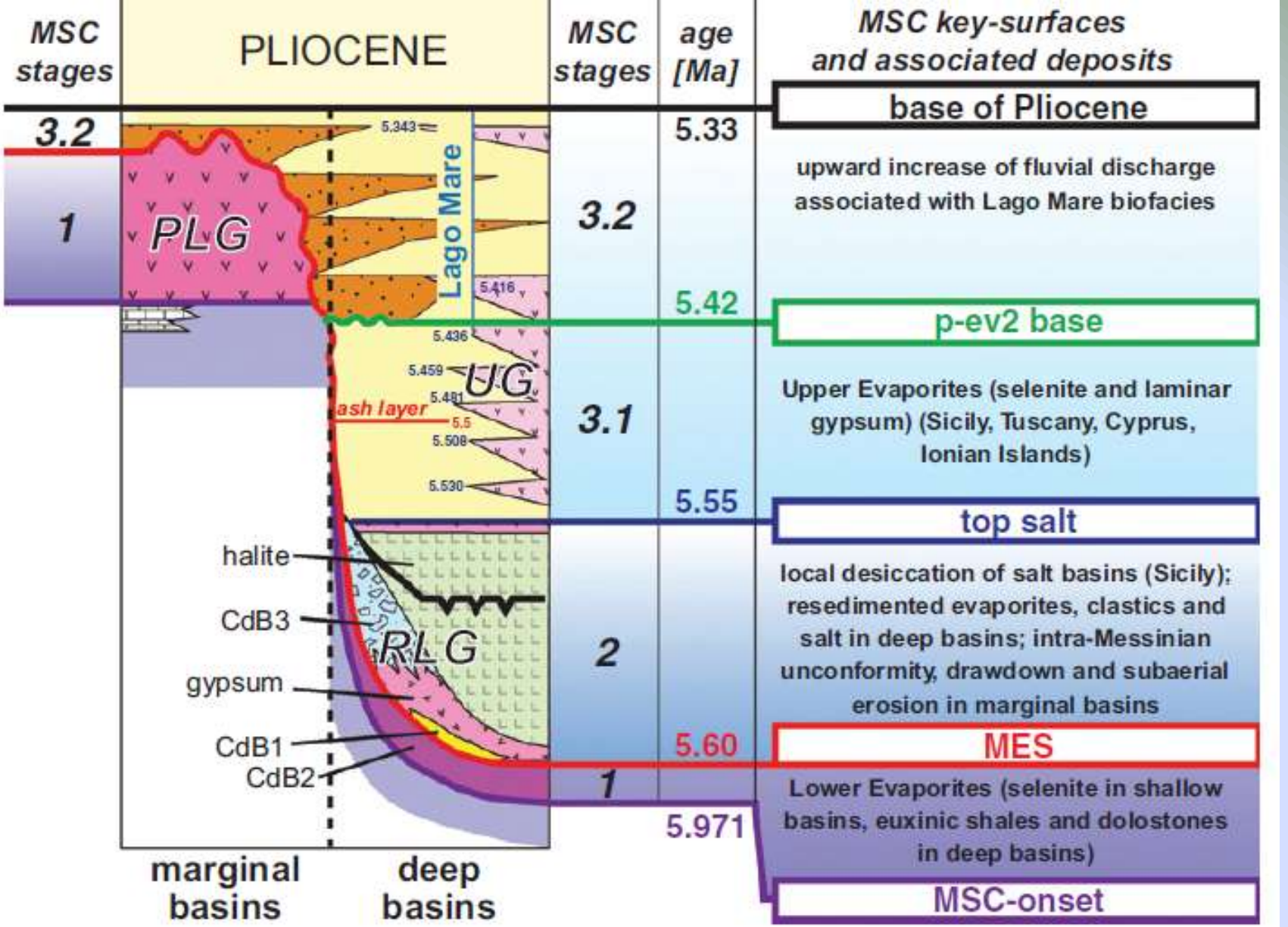

Fig. 1 The CIESM - Commission Internationale pour l'Exploration Scientifique de la mer Méditerranée (2008) Messinian salinity crisis stratigraphic framework (modified after: Roveri *et al.*, 2008a,b; Manzi *et al.*, 2011) showing the 5 key-surfaces

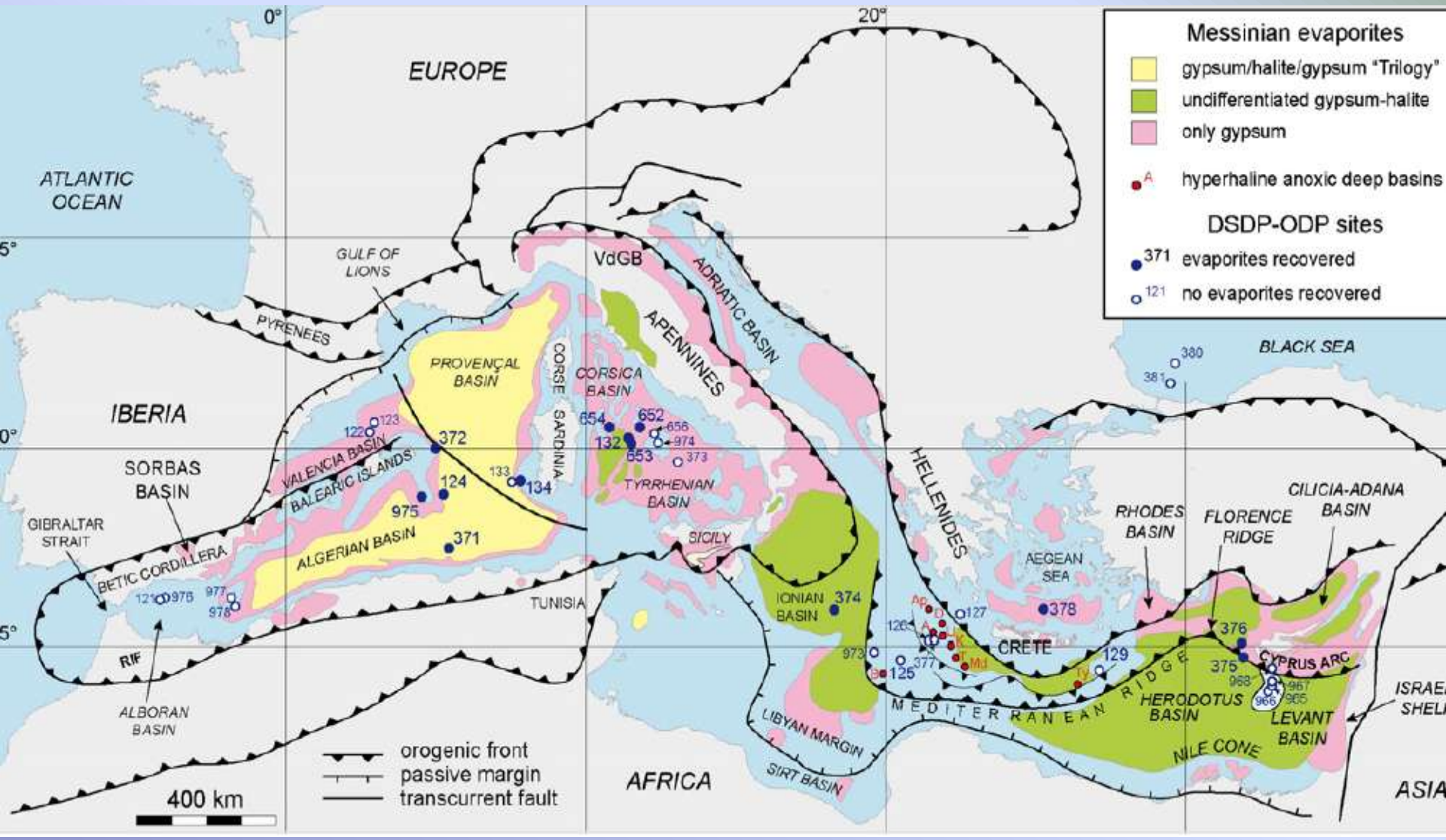
Messinian evaporites
gypsum/halite/gypsum "Trilogy"
undifferentiated gypsum-halite
only gypsum
hyperhaline anoxic deep basins
DSDP-ODP sites
371 evaporites recovered
121 no evaporites recovered
EUROPE
ATLANTIC OCEAN
IBERIA
AFRICA
ASIA
BLACK SEA
GULF OF LIONS
PYRENEES
PROVENÇAL BASIN
CORSE SARDINIA
CORSICA BASIN
APENNINES
ADRIATIC BASIN
VdGB
VALENCIA BASIN
BALEARIC ISLANDS
SORBAS BASIN
GIBRALTAR STRAIT
BETIC CORDILLERA
RIF
ALBORAN BASIN
ALGERIAN BASIN
TYRRHENIAN BASIN
SICILY
TUNISIA
IONIAN BASIN
HELLENIDES
AEGEAN SEA
CRETE
RHODES BASIN
FLORENCE RIDGE
CILICIA-ADANA BASIN
CYPRUS ARC
MEDITERRANEAN RIDGE
HERODOTUS BASIN
LEVANT BASIN
NILE CONE
LIBYAN MARGIN
SIRT BASIN
ISRAEL SHELF
orogenic front
passive margin
transcurrent fault
400 km

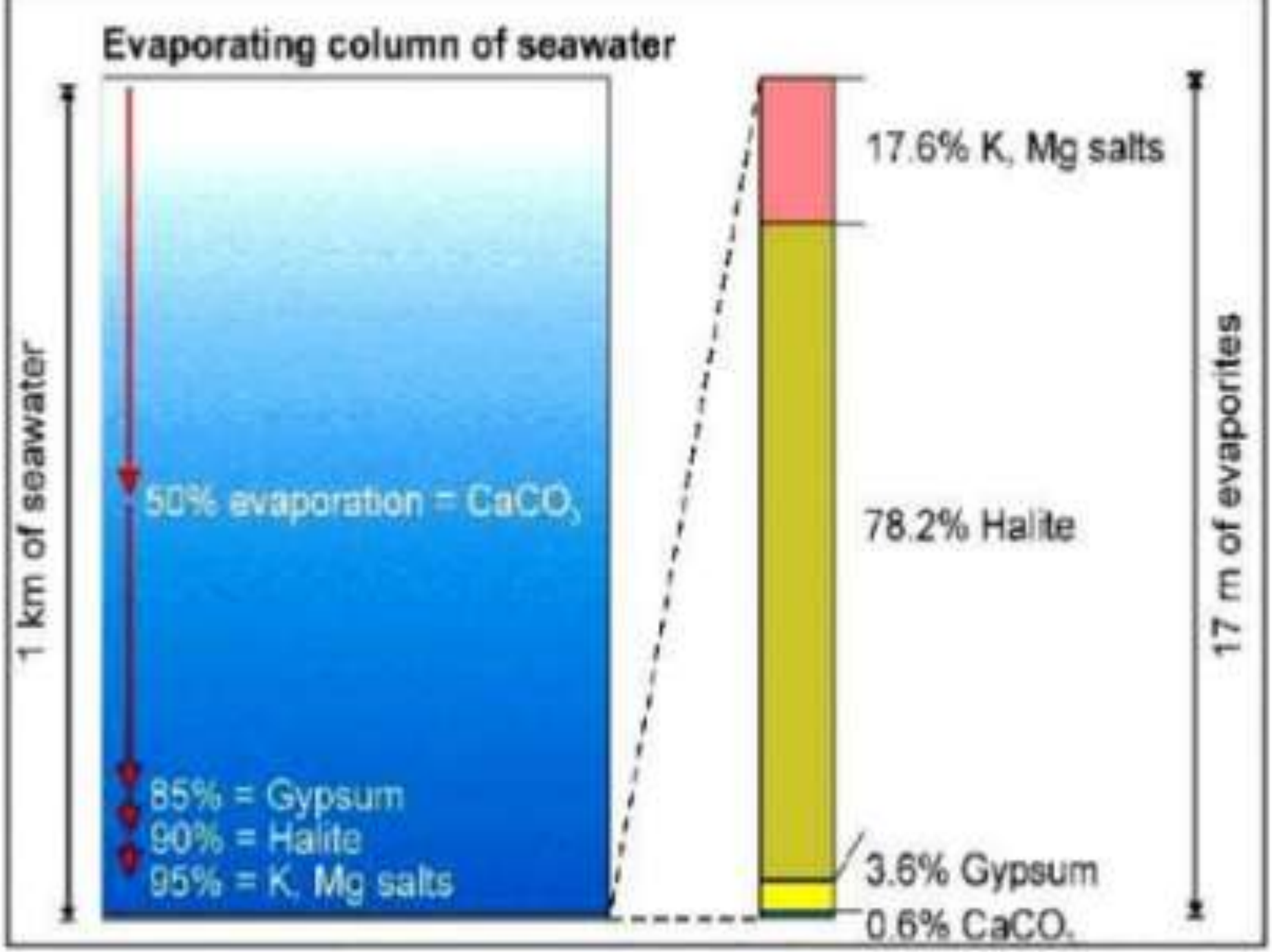
Evaporating column of seawater
1 km of seawater
50% evaporation = CaCO3
85% = Gypsum
90% = Halite
95% = K, Mg salts
17.6% K, Mg salts
78.2% Halite
3.6% Gypsum
0.6% CaCO3
17 m of evaporites

Luchttemperatuur boven de MZ

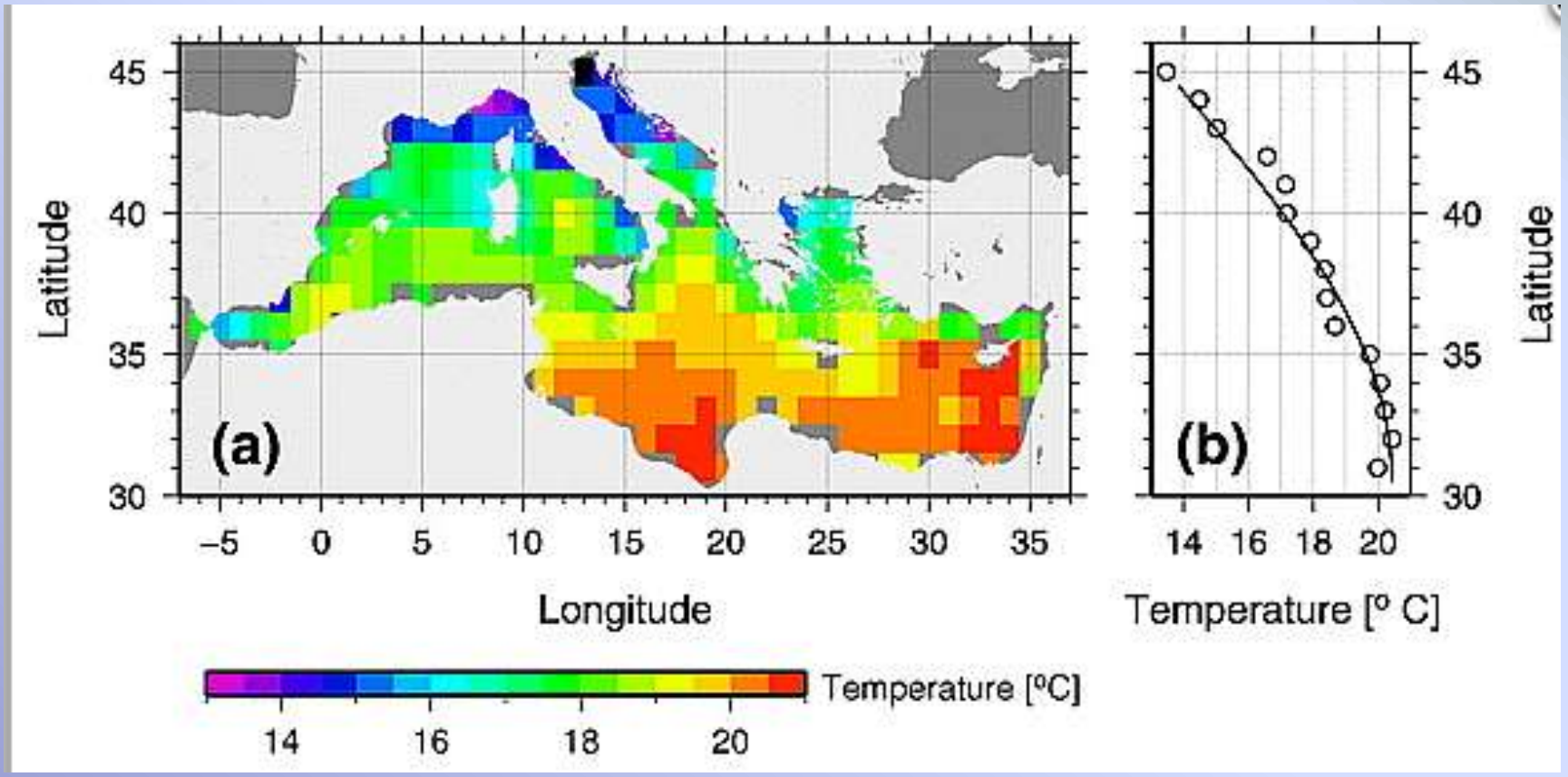

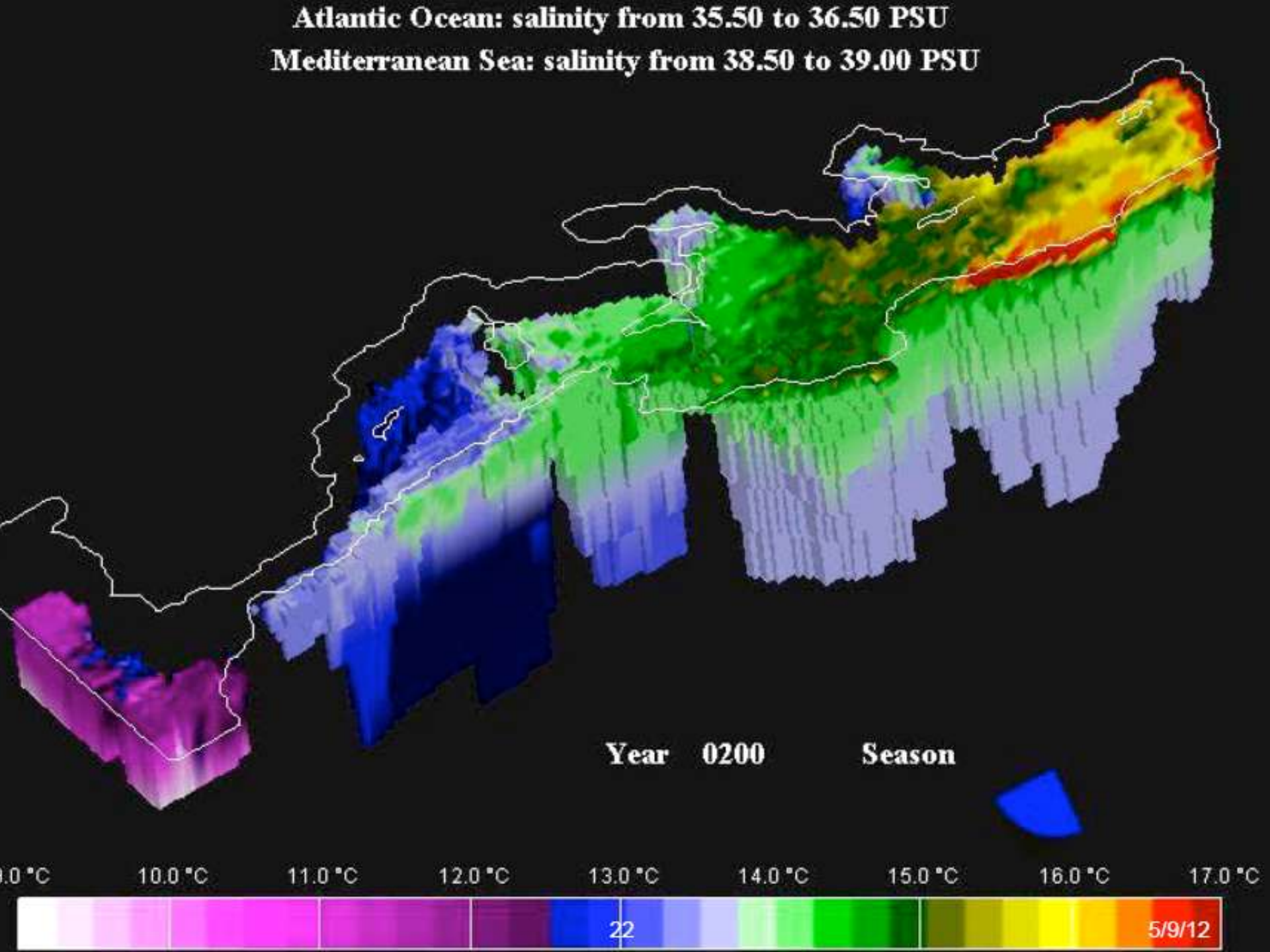
Atlantic Ocean: salinity from 35.50 to 36.50 PSU
Mediterranean Sea: salinity from 38.50 to 39.00 PSU
Year 0200 Season
10.0 °C
11.0 °C
12.0 °C
13.0 °C
14.0 °C
15.0 °C
16.0 °C
17.0 °C
22
5/9/12

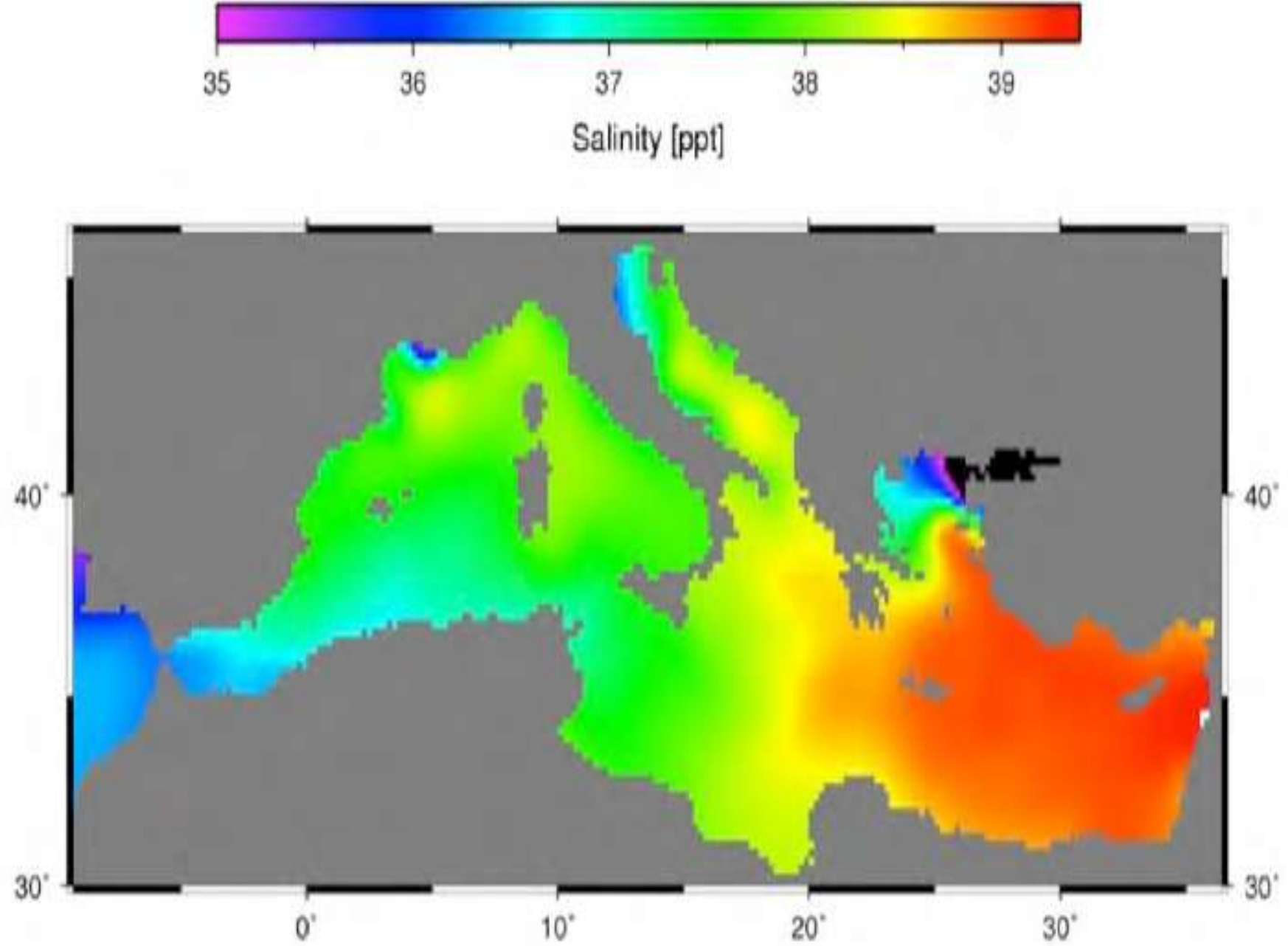

present-day sea surface salinity

Door klimaat een anti estuarine stroming in de MZ

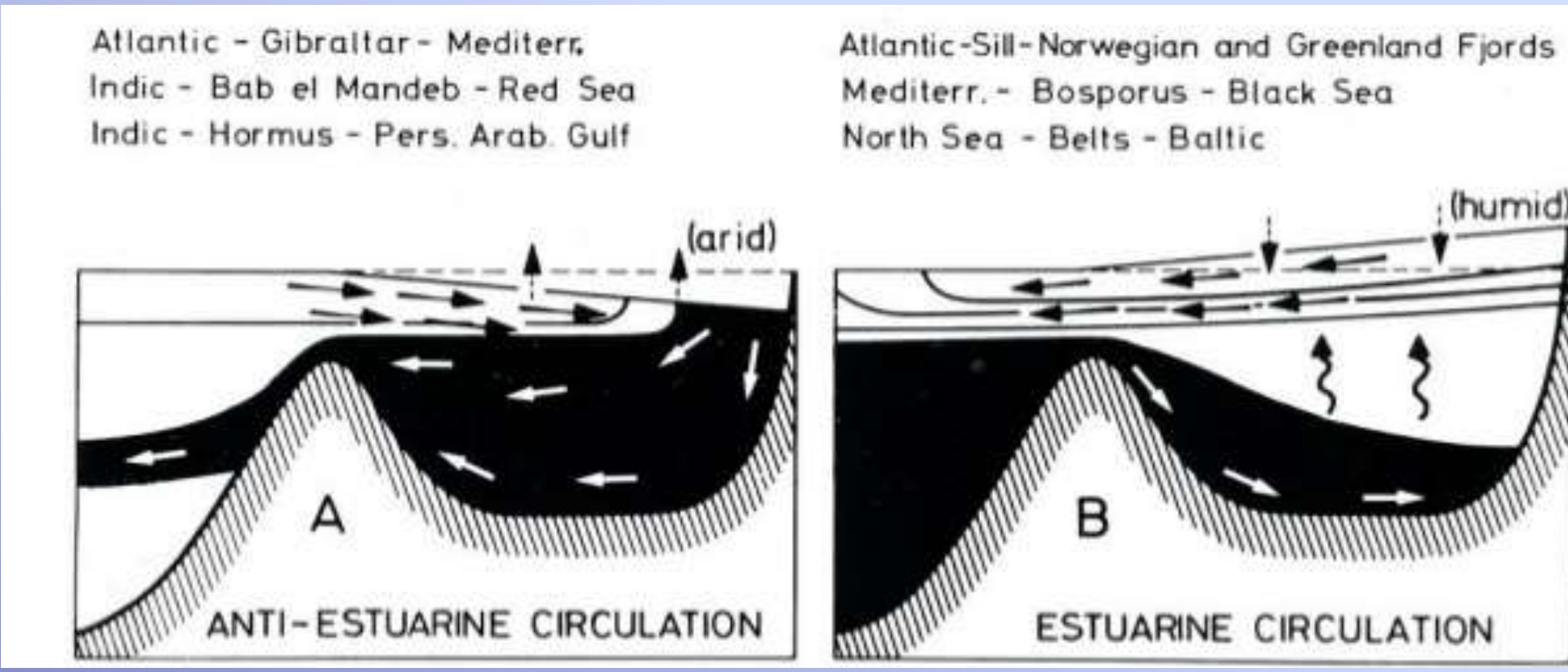

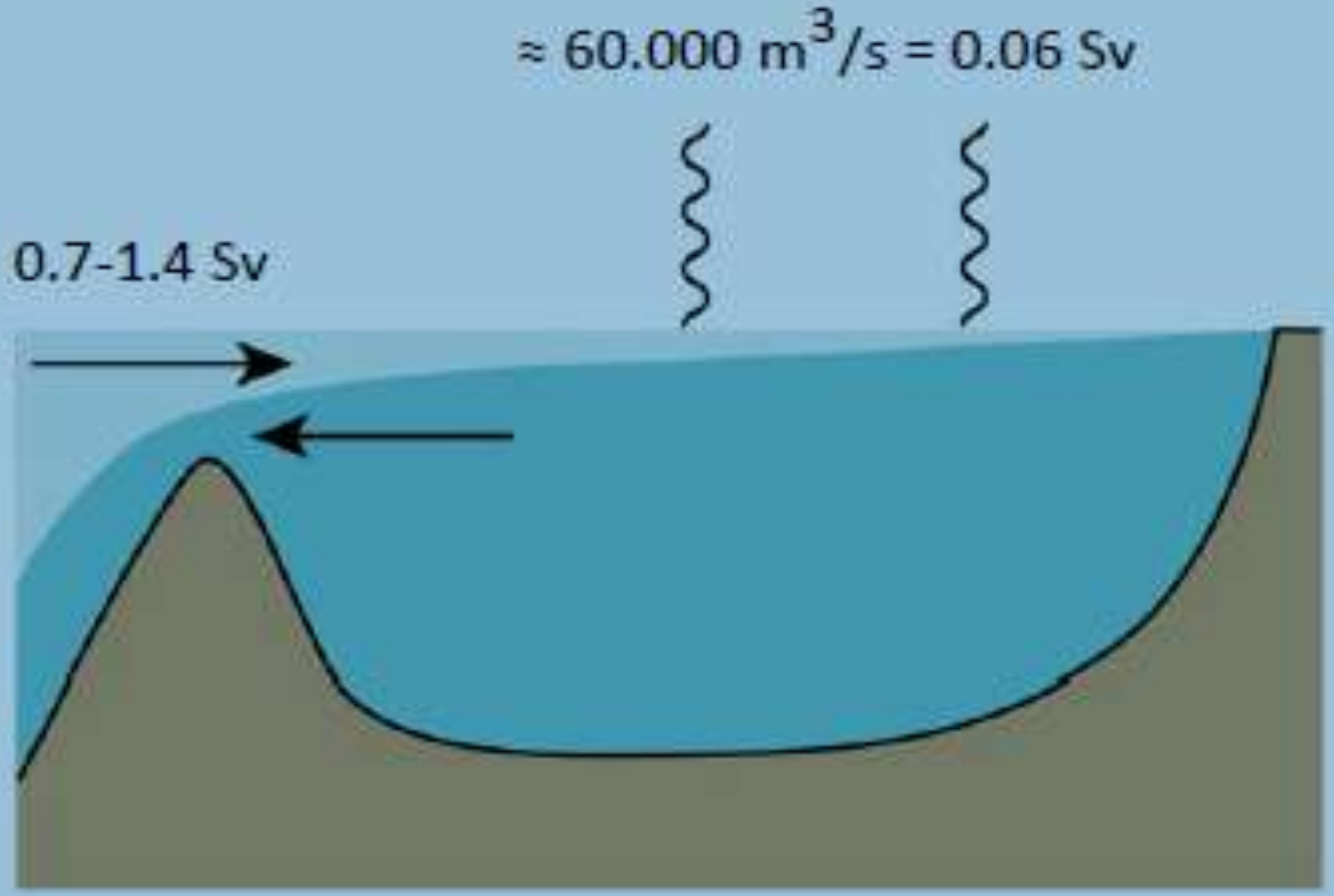

1 Sverdrup = 10^6 m^3/s

Zoutgehalte en stroming

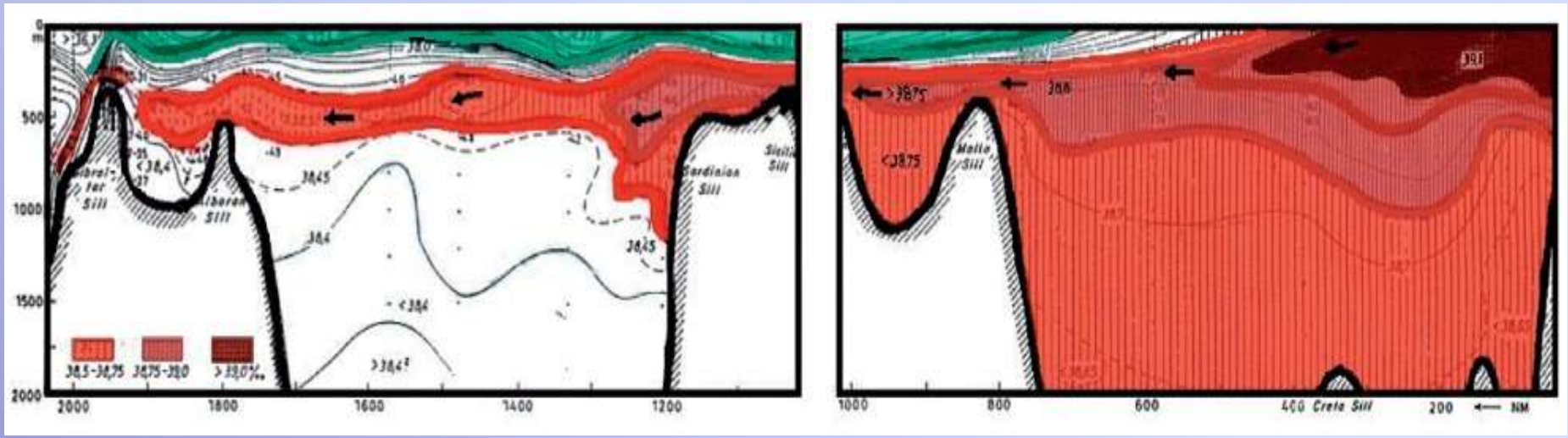

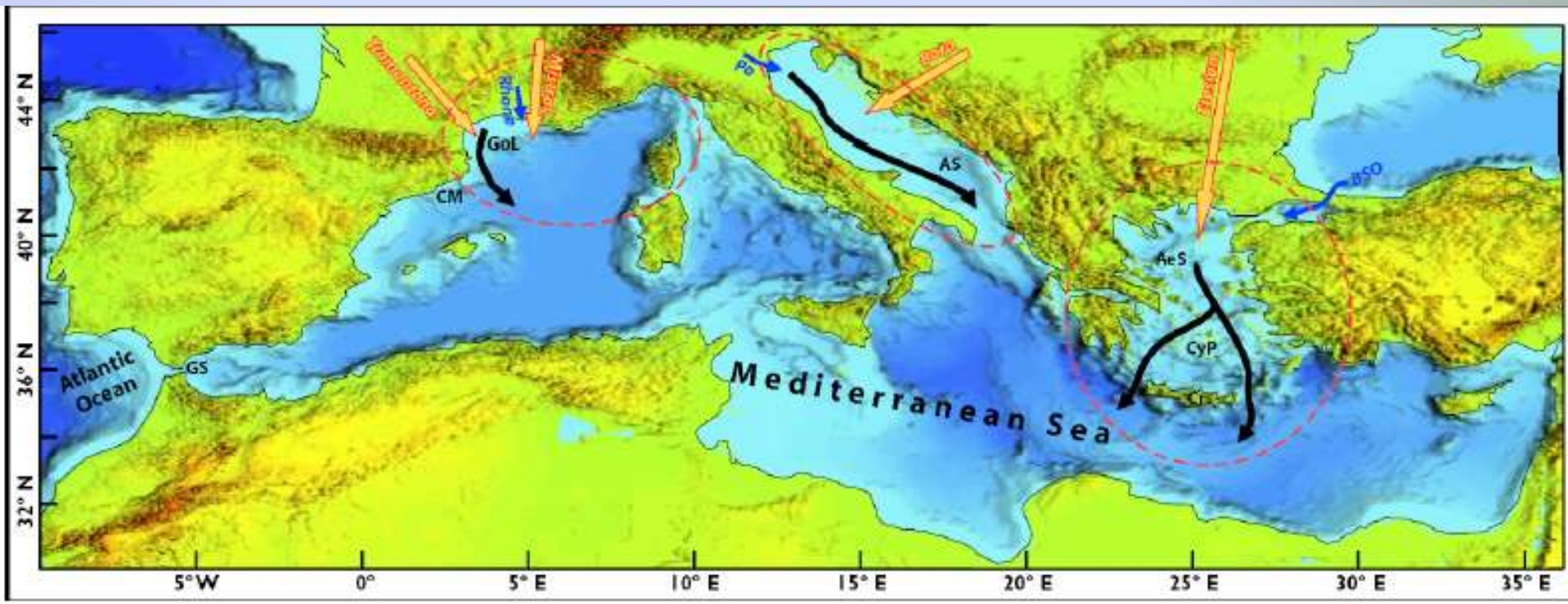

INVLOED RIVIEREN

windrichtingen

reliëf

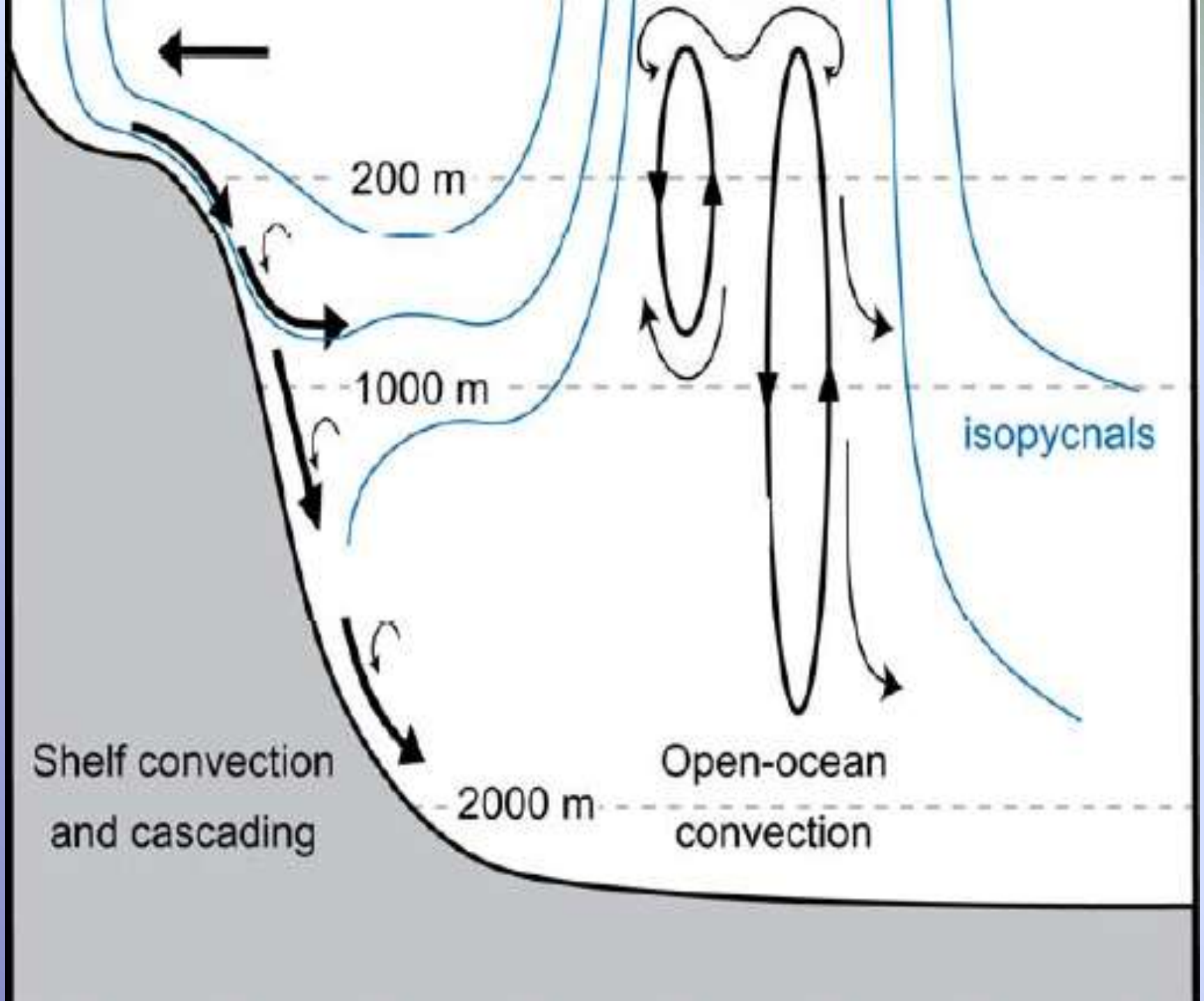
200 m
1000 m
2000 m
isopycnals
Shelf convection
and cascading
Open-ocean
convection

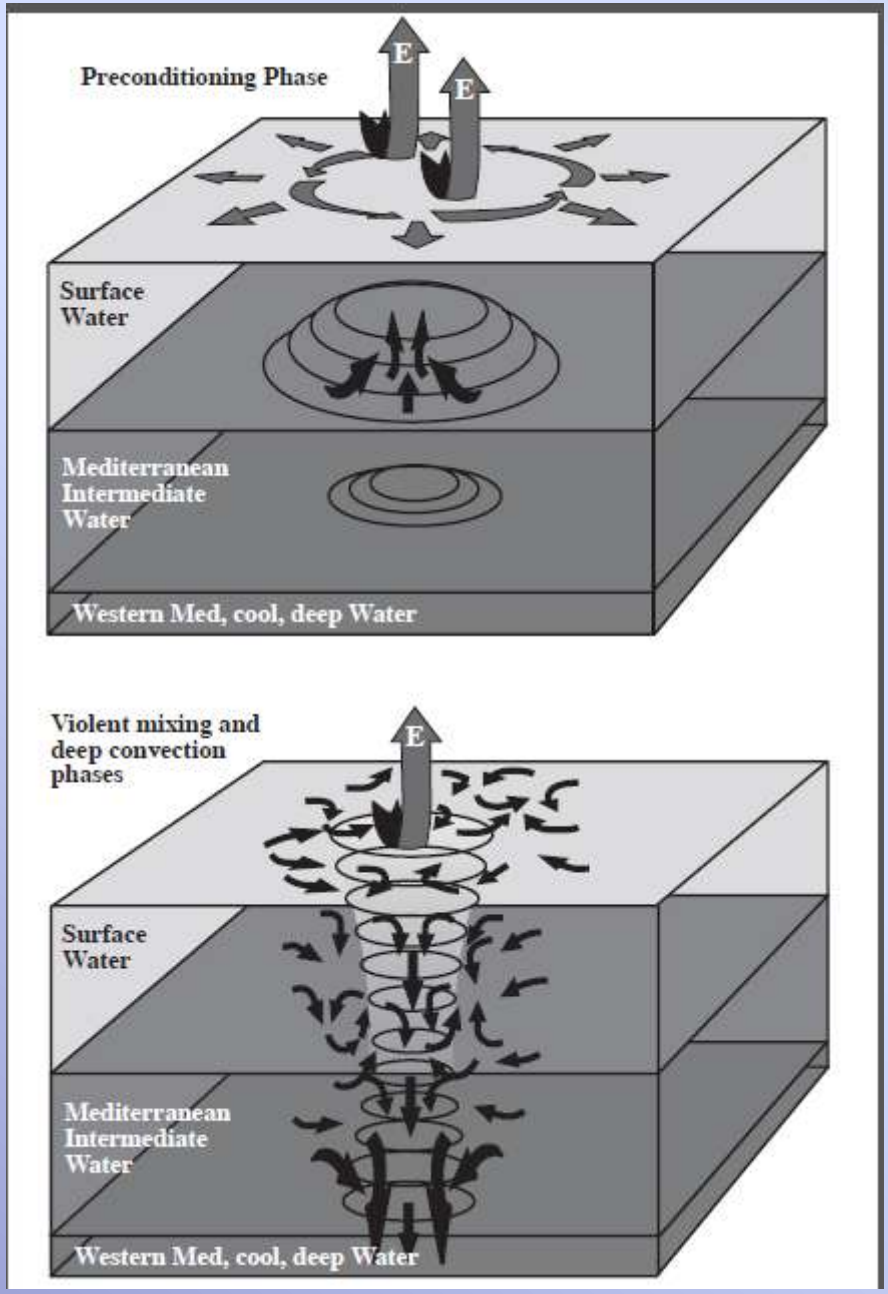
Preconditioning Phase
E
E
Surface
Water
Mediterranean
Intermediate
Water
Western Med, cool, deep Water
Violent mixing and
deep convection
phases
E
Surface
Water
Mediterranean
Intermediate
Water
Western Med, cool, deep Water

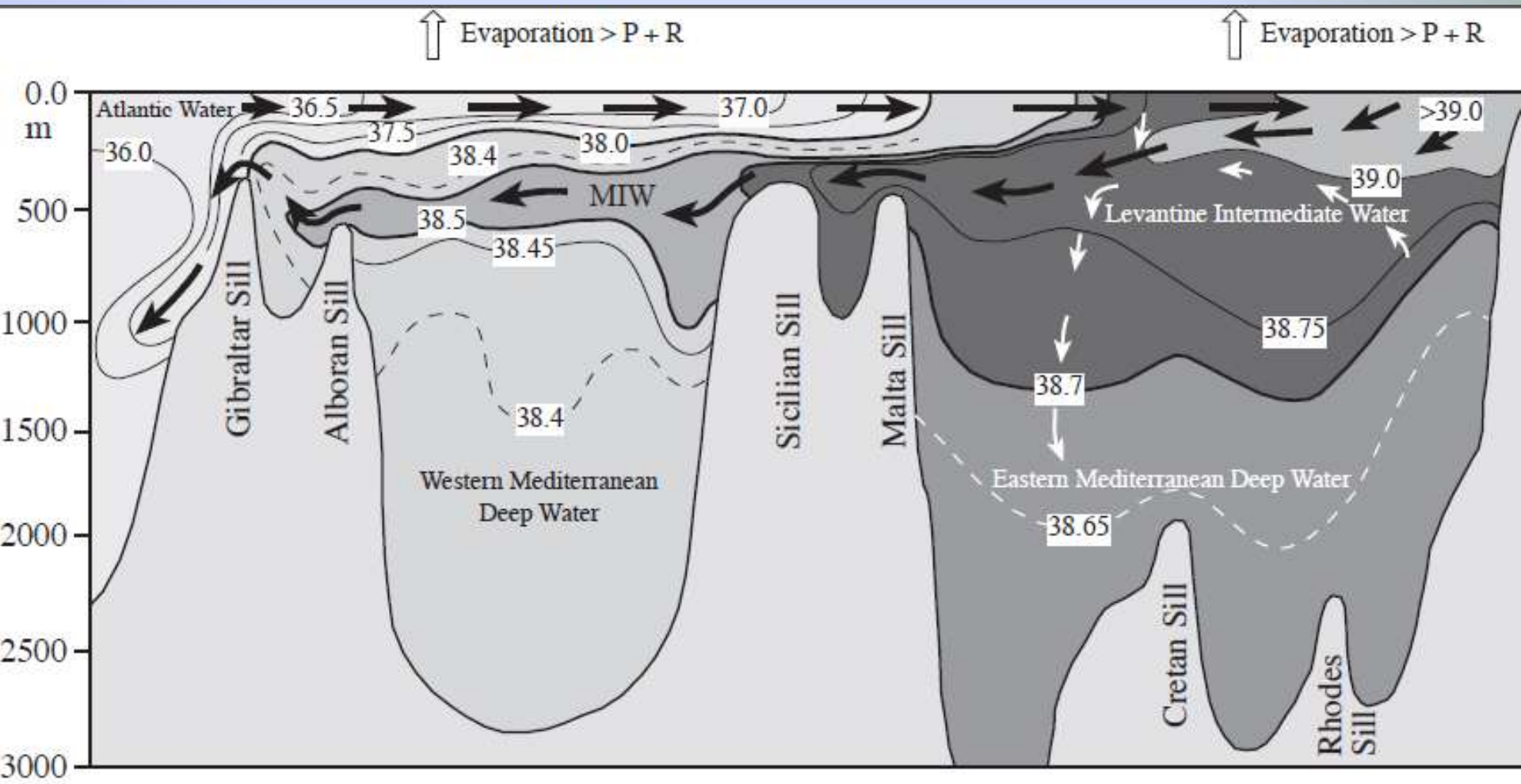
Evaporation > P + R
Evaporation > P + R
0.0
m
500
1000
1500
2000
2500
3000
Atlantic Water
36.0
36.5
37.5
37.0
38.0
38.4
MIW
38.5
38.45
>39.0
39.0
Levantine Intermediate Water
38.75
38.7
38.4
Western Mediterranean
Deep Water
Eastern Mediterranean Deep Water
38.65
Gibraltar Sill
Alboran Sill
Sicilian Sill
Malta Sill
Cretan Sill
Rhodes
Sill

Enkele getallen/richtingen

- Verdamping boven MZ : 4.690 km3
- Aanvoer door rivieren en neerslag: 1.830 km3
- Tekort: 2.860 km3
- Aanvoer vanuit AO: 53.000 km3
- Afvoer naar AO: 50.000 km3
- Neerslag evaporieten in MZ : 10.000.000 km3

- Oppervlakte MZ: 2,5 milj. km2

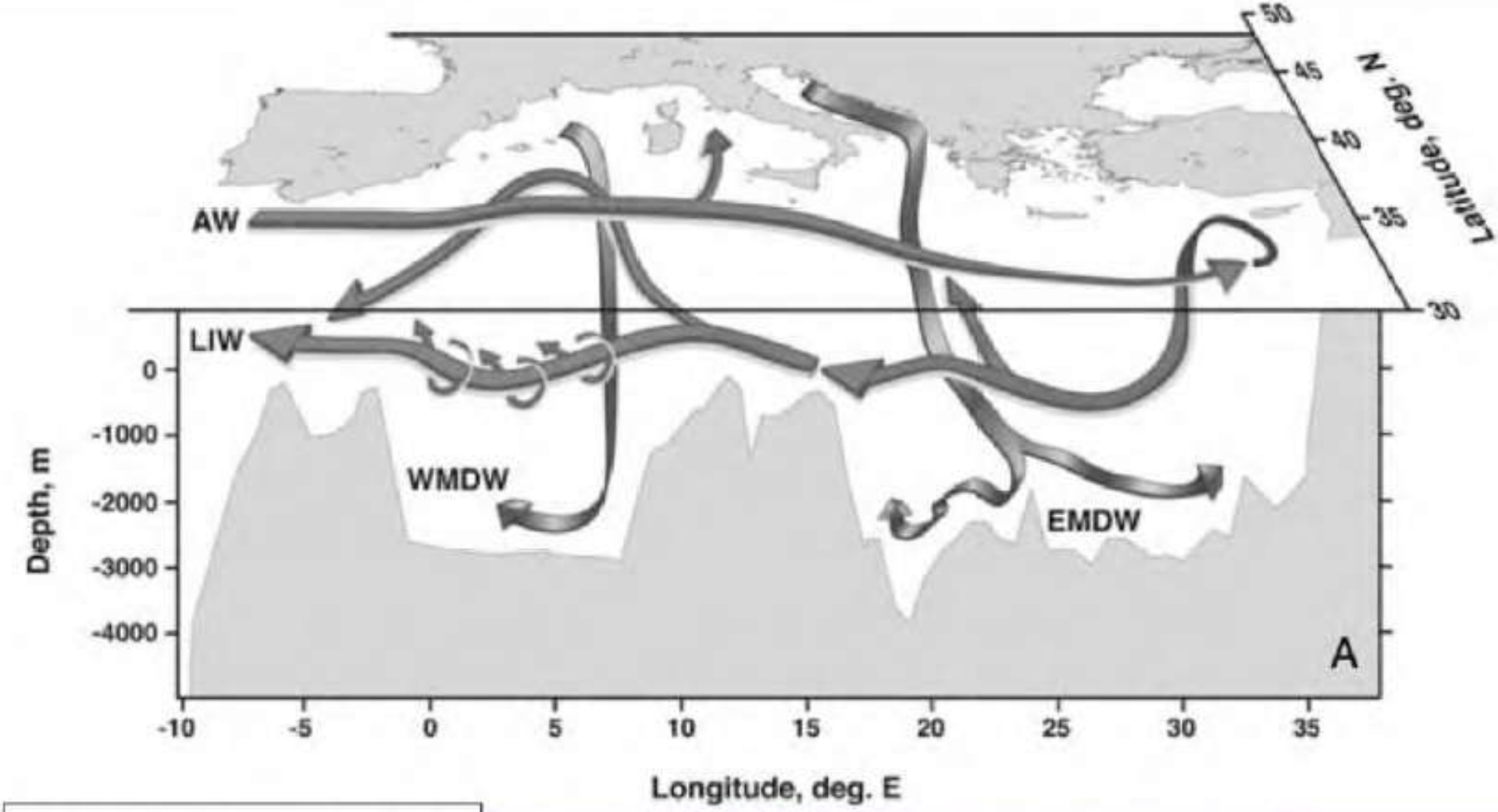

thermohaliene circulatie

Tsimplis et al. (2005)

Onderzoek naar invloed drempelhoogte op stromingen

- Moderate sill (zoals nu)
- Deep sill (ver voor het Messinien)
- Shallow sill (tijdens zoutcrisis)

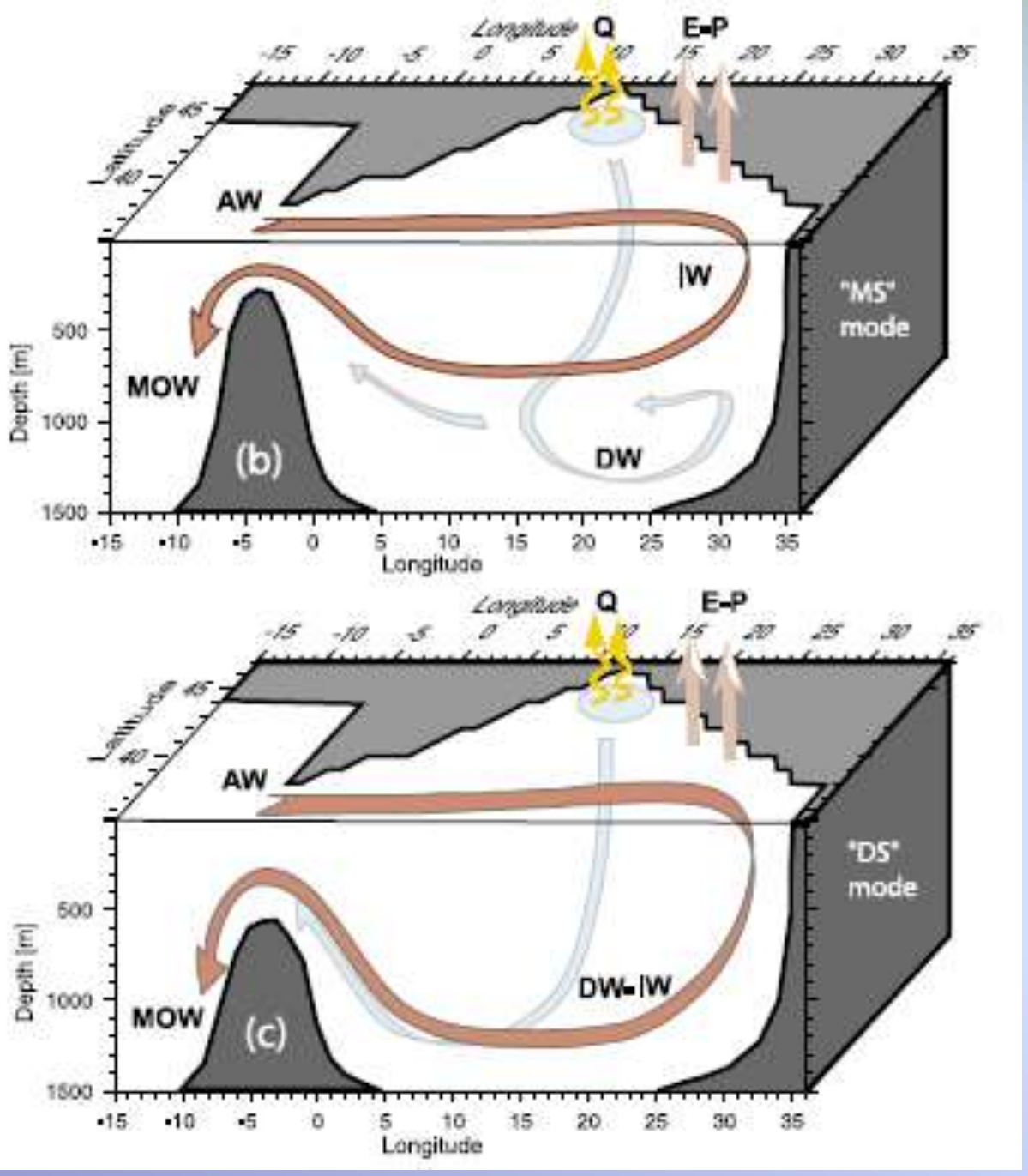
Q
E-P
AW
IW
MOW
DW
(b)
"MS" mode
Depth [m]
500
1000
1500
-15
-10
-5
0
5
10
15
20
25
30
35
Longitude
Q
E-P
AW
DW-IW
MOW
(c)
"DS" mode
Depth [m]
500
1000
1500
Longitude

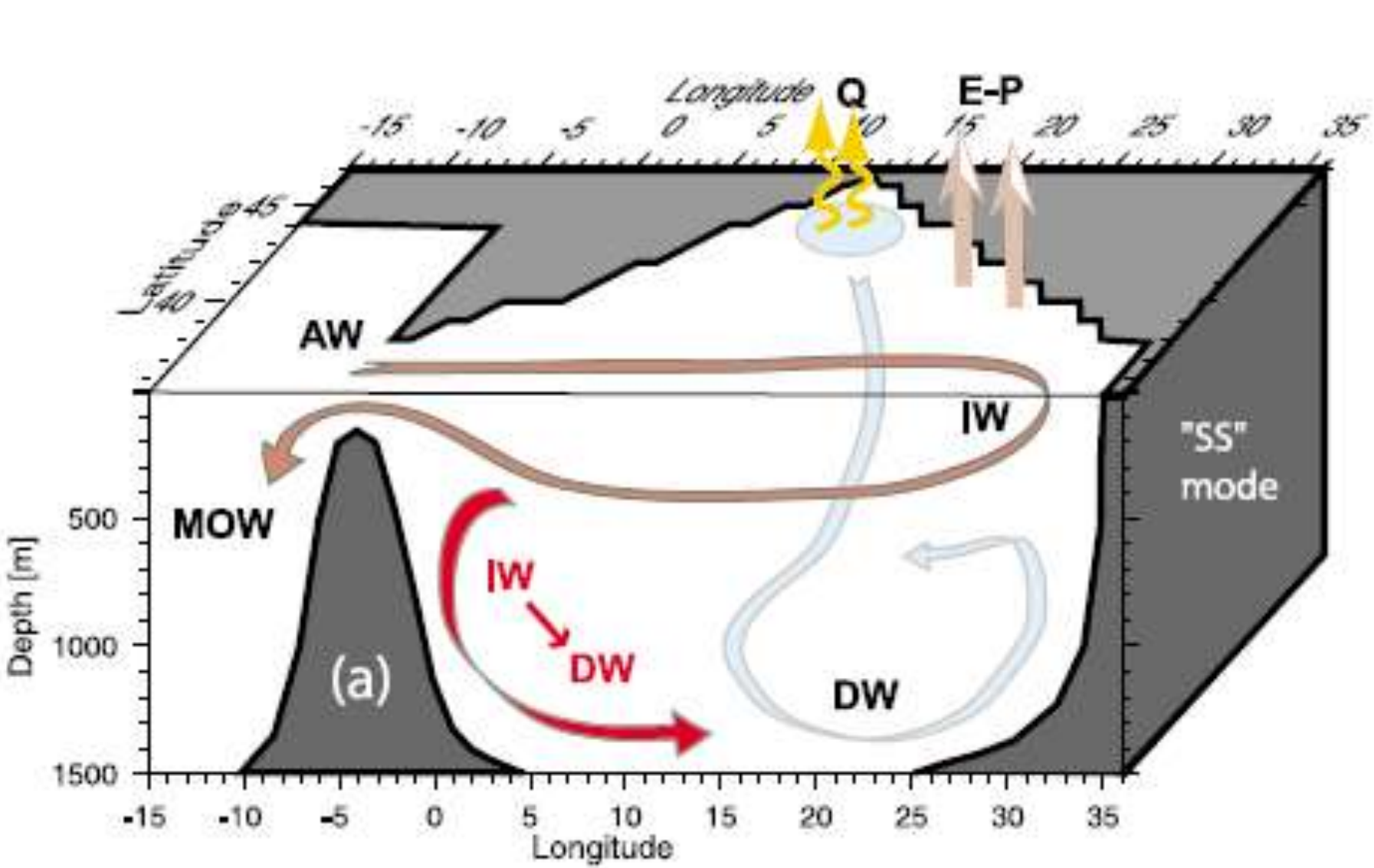
Longitude
Q
E-P
-15
-10
-5
0
5
10
15
20
25
30
35
Latitude @45
40
AW
IW
"SS"
mode
MOW
IW
DW
DW
(a)
Depth [m]
500
1000
1500
-15
-10
-5
0
5
10
15
20
25
30
35
Longitude

Invloed afname drempelhoogte (shoaling)

- De sterkte van de bovenstromingen verminderen
- Uitstroom raakt geblokkeerd hierdoor sterkere circulatie in onderste lagen
- Menging van water wordt minder,vooral in de diepere lagen

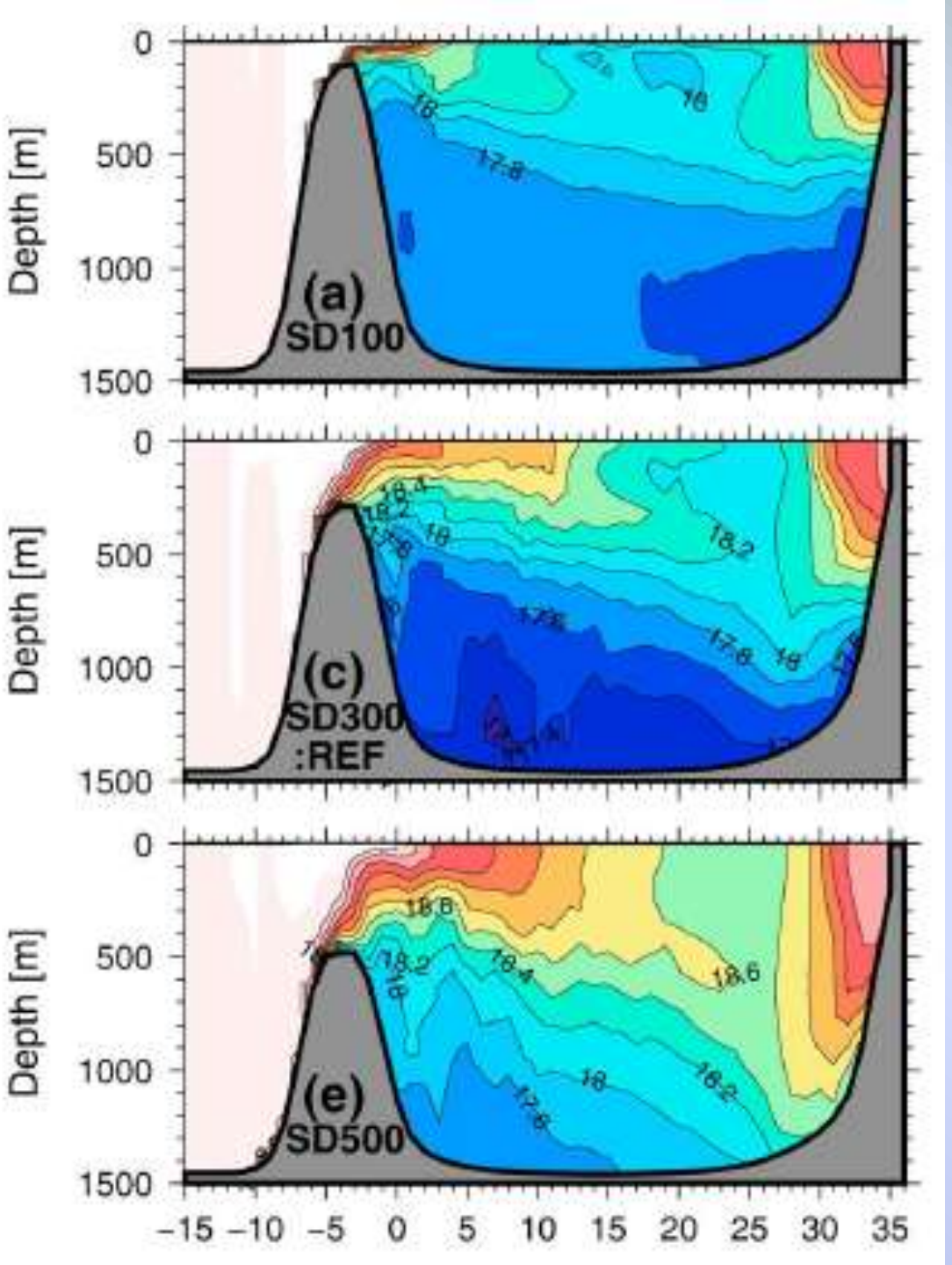
Depth [m]
0
500
1000
1500
(a)
SD100
(c)
SD300
:REF
(e)
SD500
−15 −10 −5 0 5 10 15 20 25 30 35

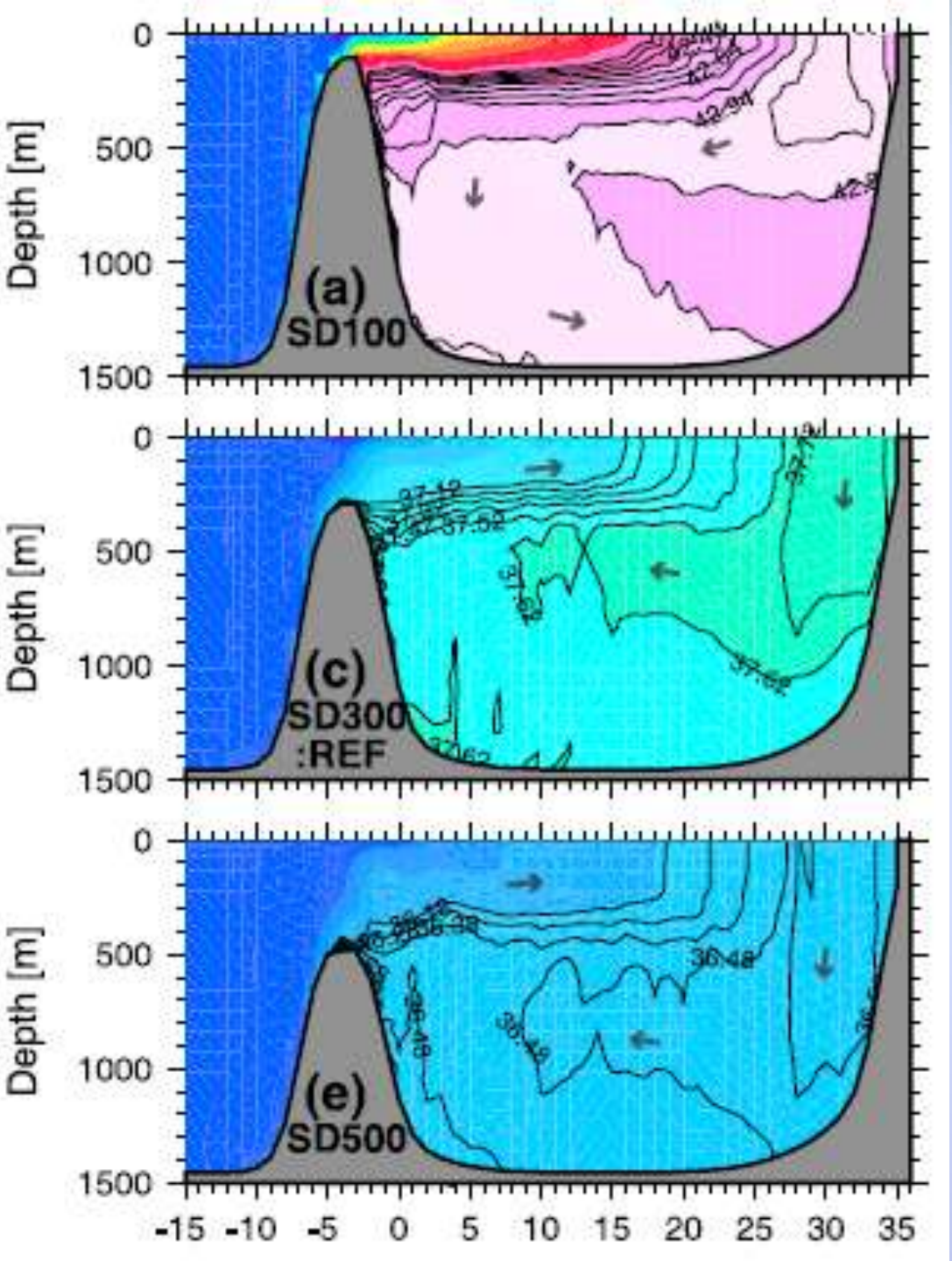
Depth [m]
0
500
1000
1500
(a)
SD100
(c)
SD300
:REF
(e)
SD500
-15 -10 -5 0 5 10 15 20 25 30 35

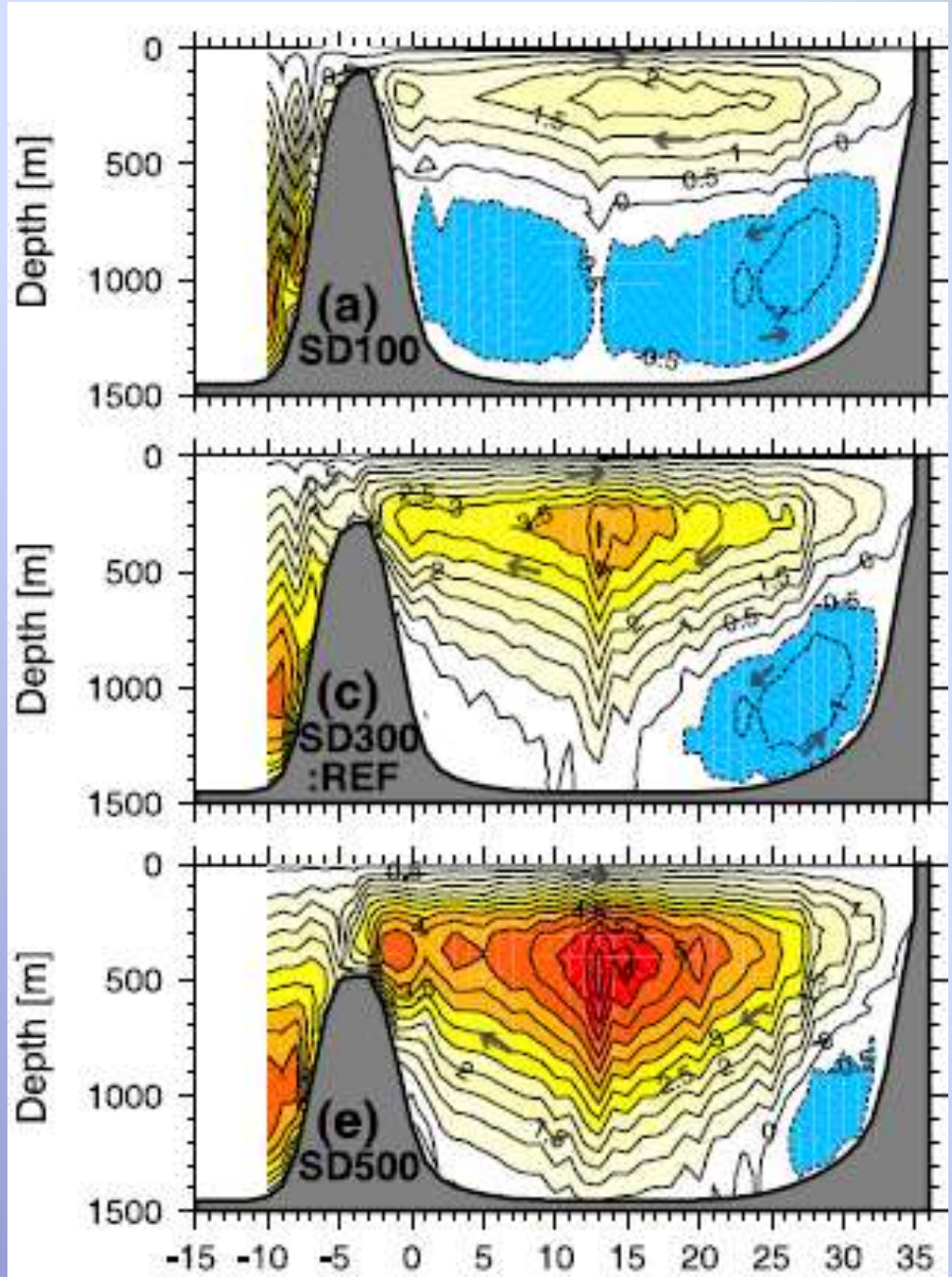
Depth [m]
0
500
1000
1500
(a)
SD100
(c)
SD300
:REF
(e)
SD500
-15 -10 -5 0 5 10 15 20 25 30 35

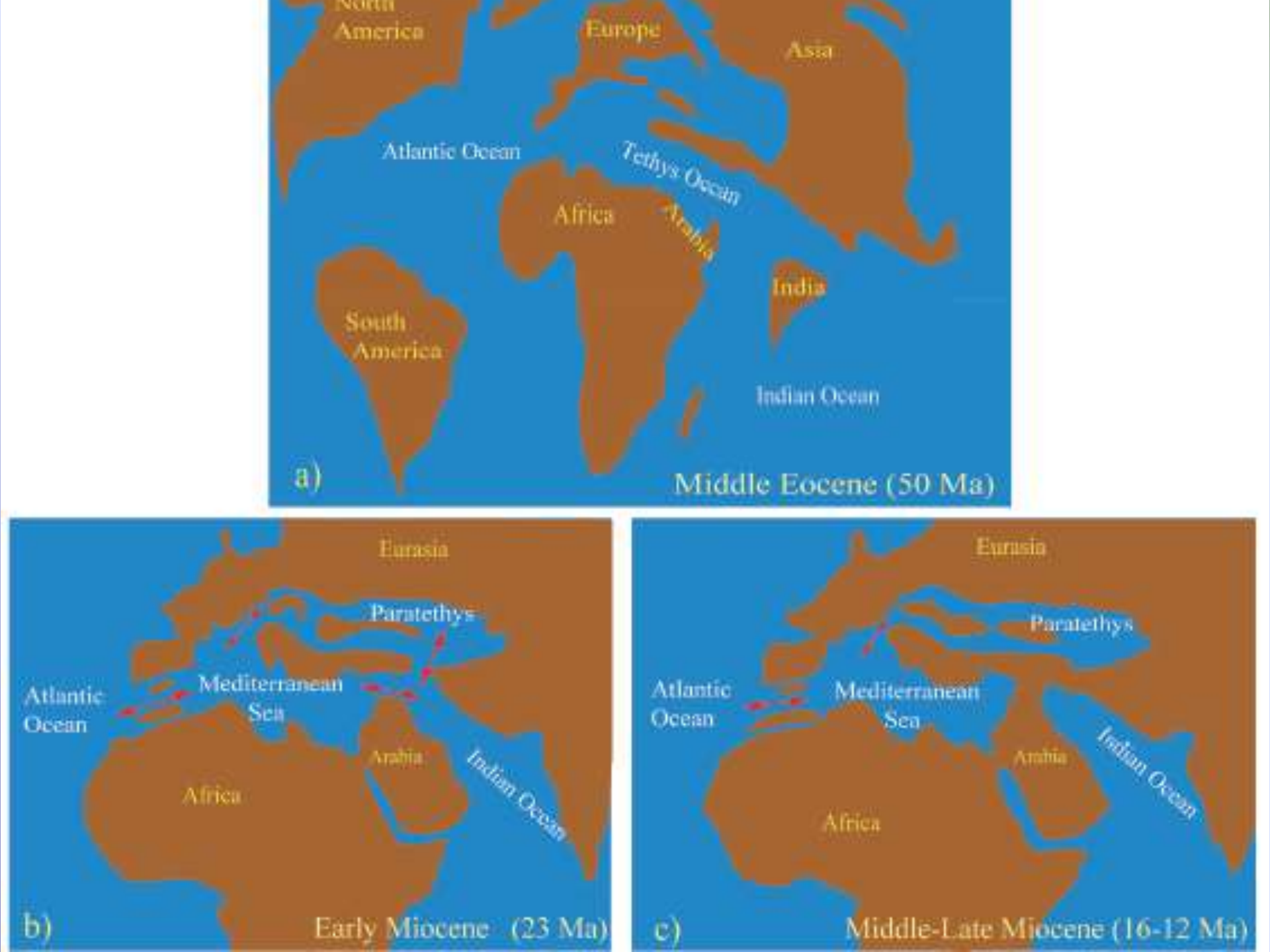
North America
Europe
Asia
Atlantic Ocean
Tethys Ocean
Africa
Arabia
India
South America
Indian Ocean
a)
Middle Eocene (50 Ma)
Eurasia
Paratethys
Atlantic Ocean
Mediterranean Sea
Arabia
Indian Ocean
Africa
b)
Early Miocene (23 Ma)
Eurasia
Paratethys
Atlantic Ocean
Mediterranean Sea
Arabia
Indian Ocean
Africa
c)
Middle-Late Miocene (16-12 Ma)

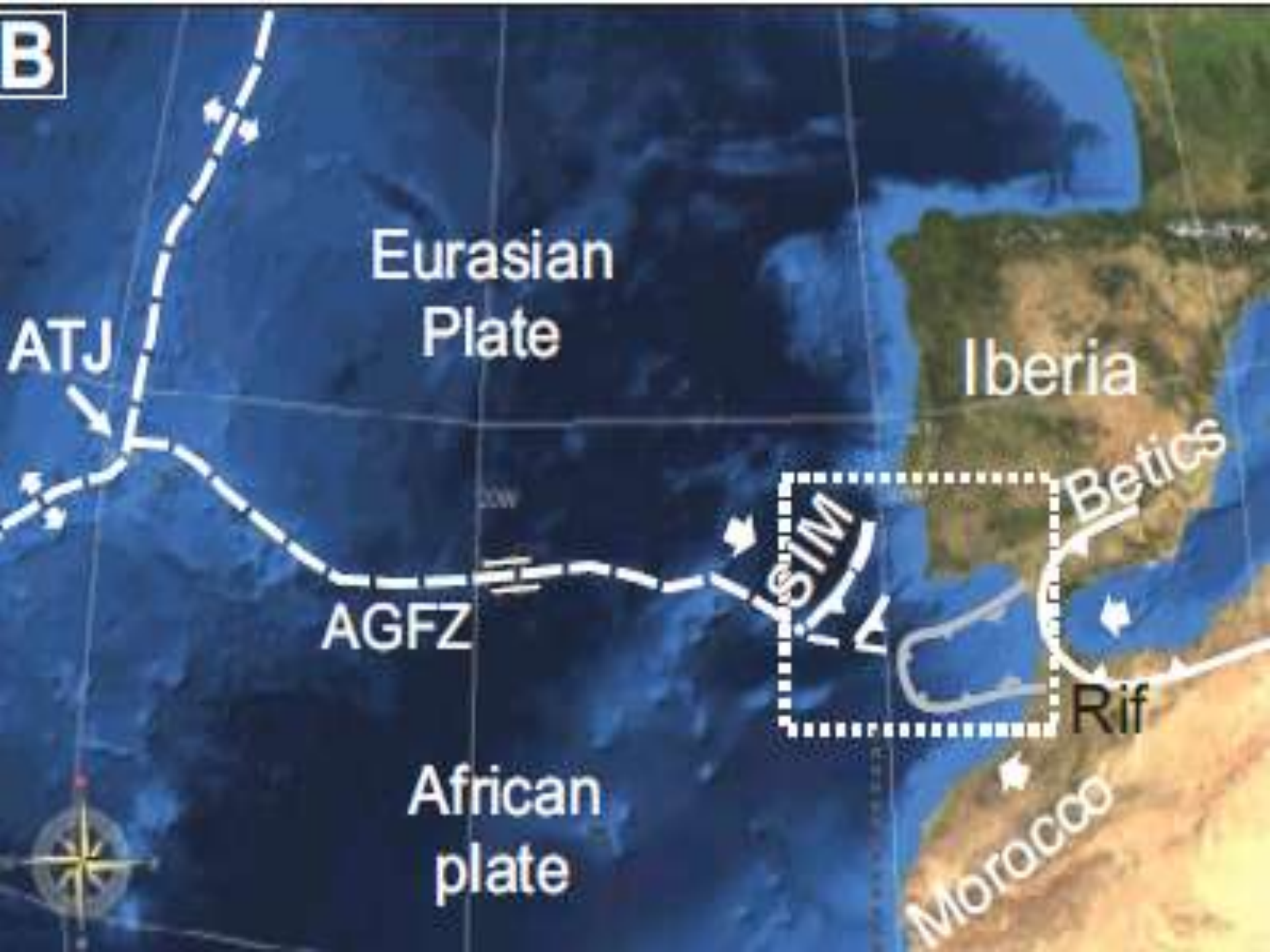
B
Eurasian
Plate
ATJ
Iberia
Betics
SIM
AGFZ
Rif
African
plate
Morocco

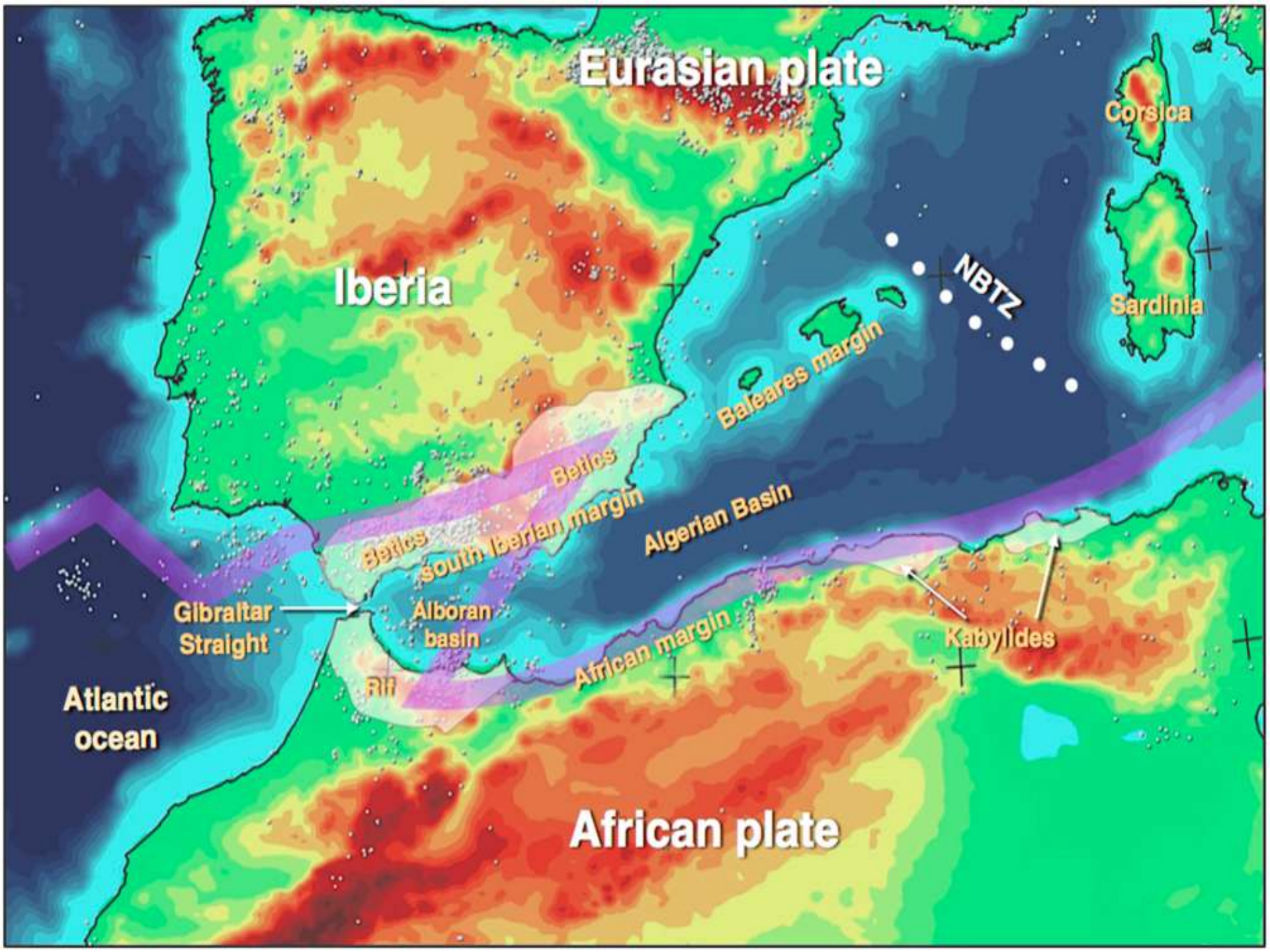
Eurasian plate
Iberia
Corsica
Sardinia
NBTZ
Baleares margin
Algerian Basin
Betics
South Iberian margin
Betics
Gibraltar
Straight
Alboran
basin
Rif
African margin
Kabylides
Atlantic
ocean
African plate

Welke processen spelen een rol in de Alboran regio?

Convergentie
Subductie
Slab roll back
Delaminatie?

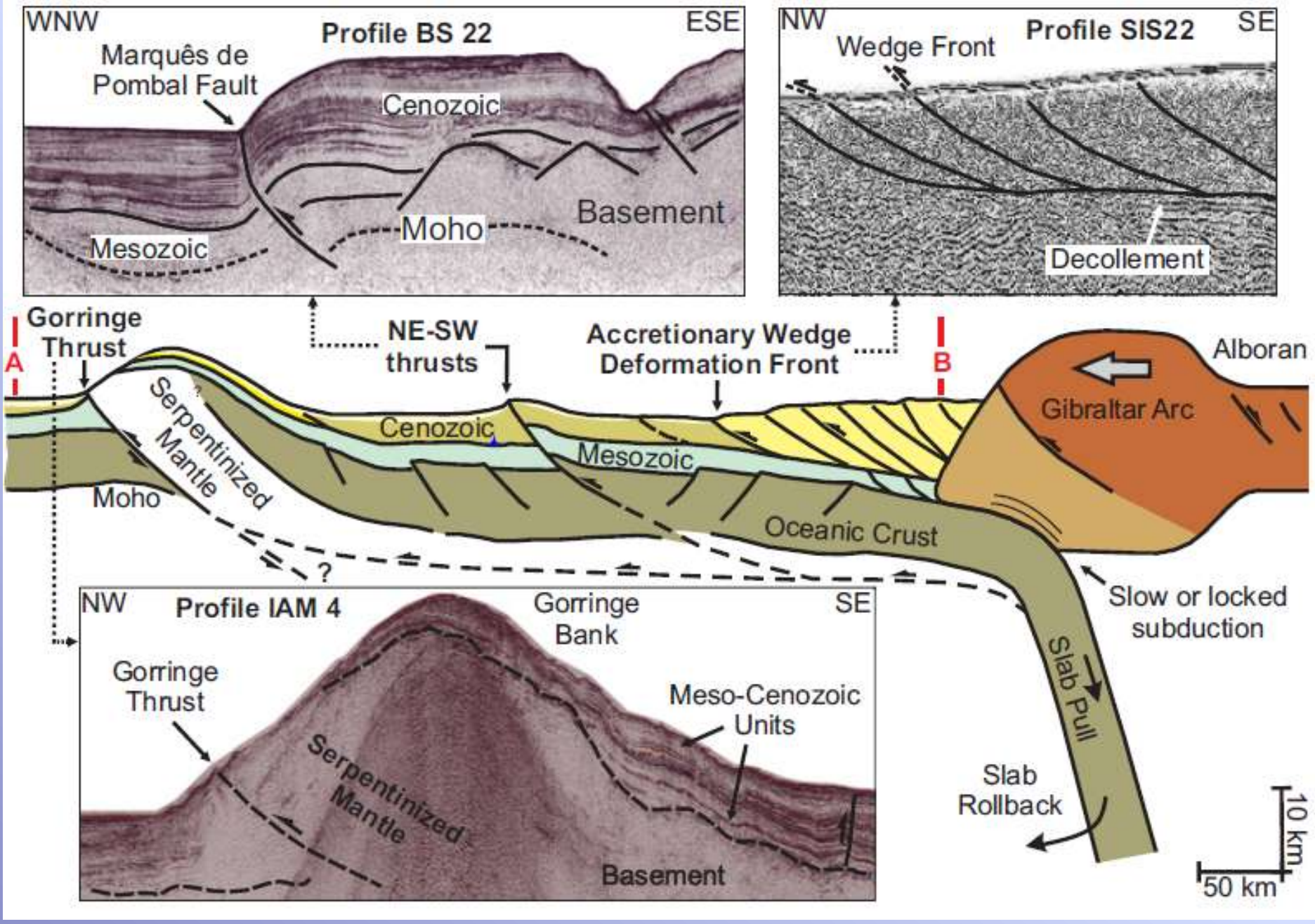
WNW
Profile BS 22
ESE
Marquês de Pombal Fault
Cenozoic
Basement
Moho
Mesozoic
NW
Wedge Front
Profile SIS22
SE
Decollement
Gorringe Thrust
A
NE-SW thrusts
Accretionary Wedge Deformation Front
B
Alboran
Gibraltar Arc
Serpentinized Mantle
Cenozoic
Mesozoic
Moho
Oceanic Crust
?
Slow or locked subduction
Slab Pull
Slab Rollback
10 km
50 km
NW
Profile IAM 4
Gorringe Bank
SE
Gorringe Thrust
Meso-Cenozoic Units
Serpentinized Mantle
Basement

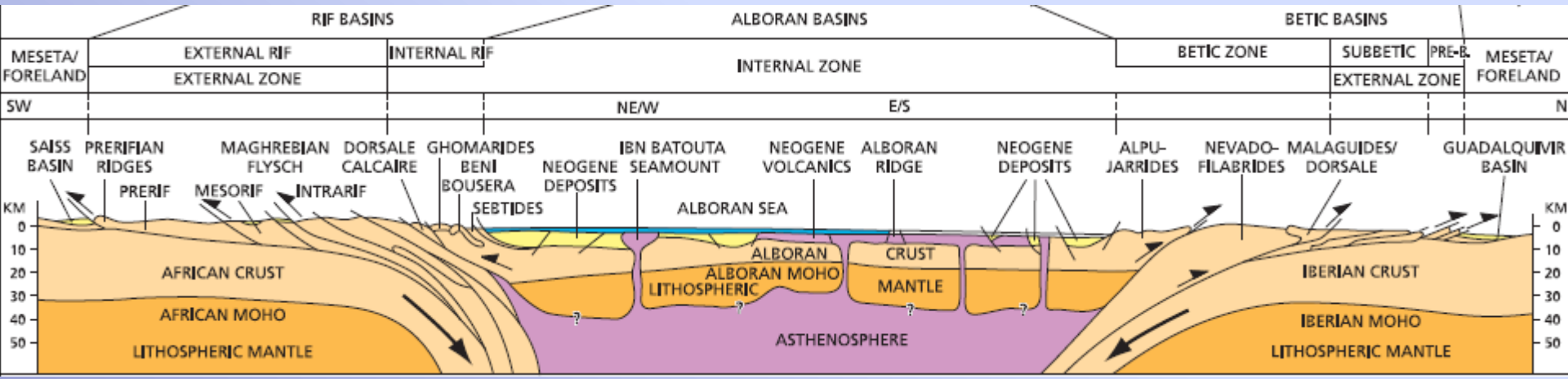
RIF BASINS
ALBORAN BASINS
BETIC BASINS
MESETA/ FORELAND
EXTERNAL RIF
EXTERNAL ZONE
INTERNAL RIF
INTERNAL ZONE
BETIC ZONE
SUBBETIC
EXTERNAL ZONE
PRE-B.
MESETA/ FORELAND
SW
NE/W
E/S
N
SAISS BASIN
PRERIFIAN RIDGES
PRERIF
MAGHREBIAN FLYSCH
MESORIF
INTRARIF
DORSALE CALCAIRE
GHOMARIDES
BENI BOUSERA
SEBTIDES
NEOGENE DEPOSITS
IBN BATOUTA SEAMOUNT
ALBORAN SEA
NEOGENE VOLCANICS
ALBORAN RIDGE
NEOGENE DEPOSITS
ALPU-JARRIDES
NEVADO-FILABRIDES
MALAGUIDES/ DORSALE
GUADALQUIVIR BASIN
KM
0
10
20
30
40
50
AFRICAN CRUST
AFRICAN MOHO
LITHOSPHERIC MANTLE
ALBORAN
ALBORAN MOHO
LITHOSPHERIC
CRUST
MANTLE
ASTHENOSPHERE
IBERIAN CRUST
IBERIAN MOHO
LITHOSPHERIC MANTLE

De Rif Gibraltar Betic Slab

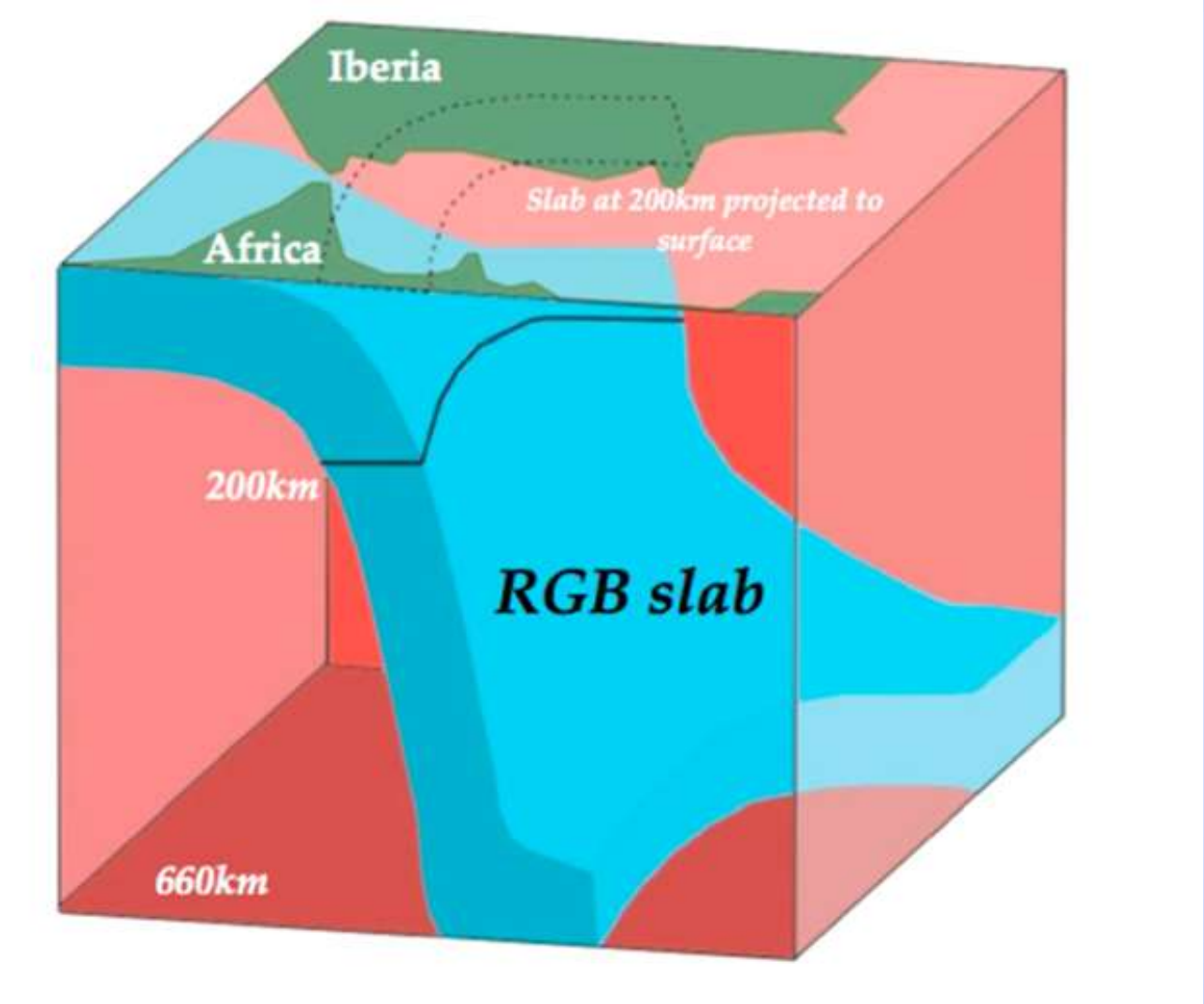

Fantasie?

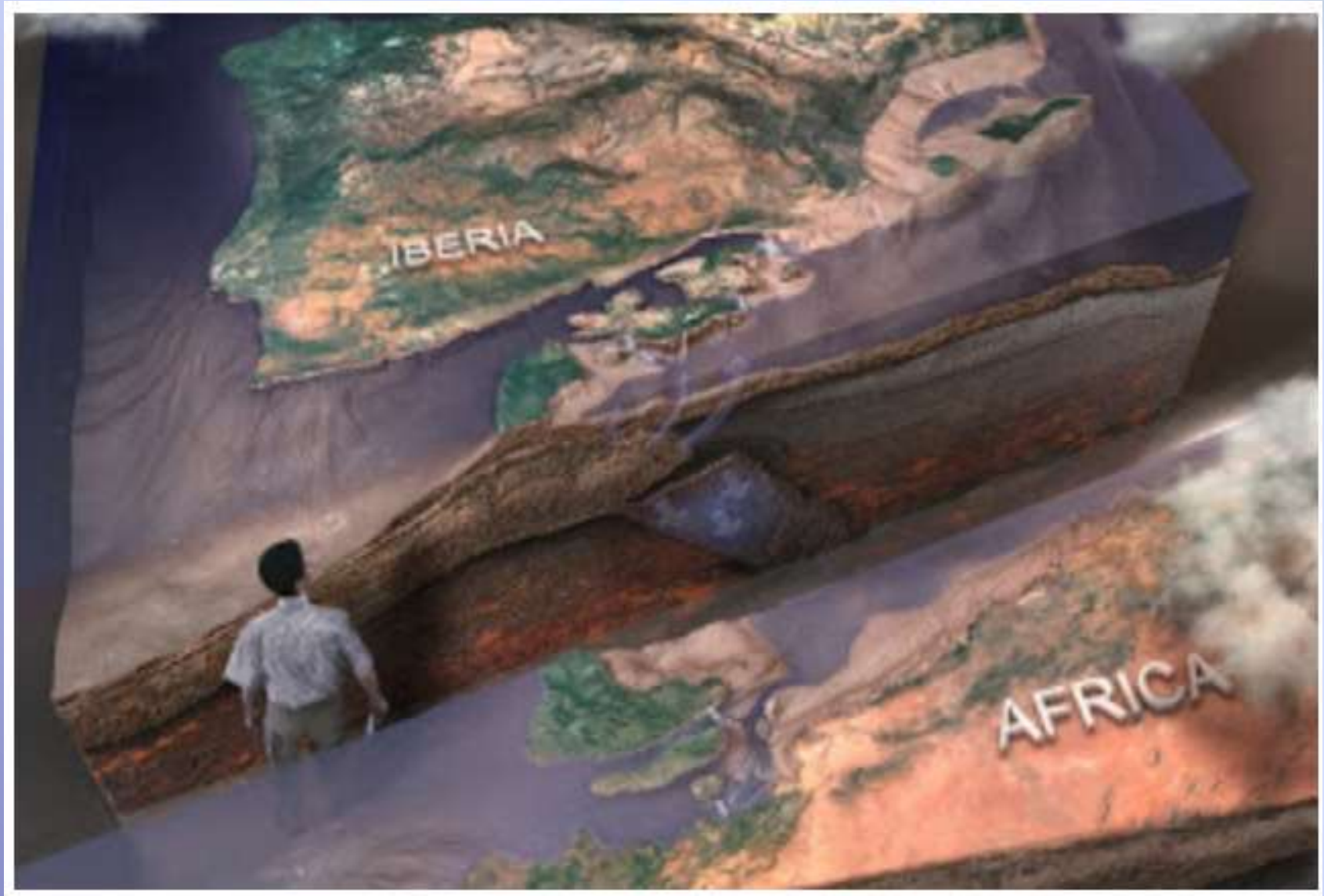

De zeestraten in zuidelijk Spanje en noordelijk Marokko

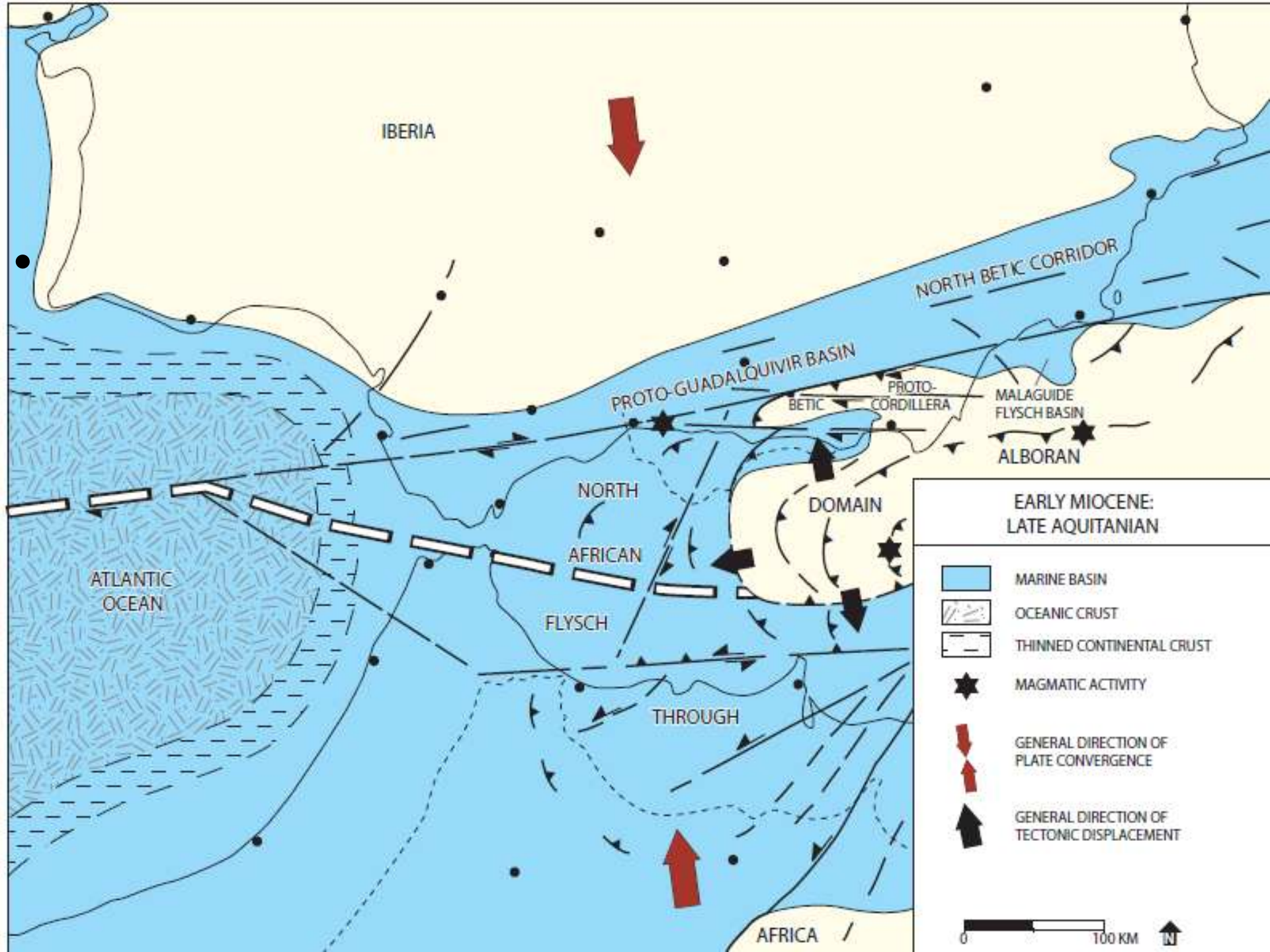
IBERIA
NORTH BETIC CORRIDOR
PROTO-GUADALQUIVIR BASIN
BETIC
PROTO-CORDILLERA
MALAGUIDE FLYSCH BASIN
ALBORAN
DOMAIN
NORTH
AFRICAN
FLYSCH
THROUGH
ATLANTIC OCEAN
AFRICA
EARLY MIOCENE:
LATE AQUITANIAN
MARINE BASIN
OCEANIC CRUST
THINNED CONTINENTAL CRUST
MAGMATIC ACTIVITY
GENERAL DIRECTION OF PLATE CONVERGENCE
GENERAL DIRECTION OF TECTONIC DISPLACEMENT
0
100 KM
N

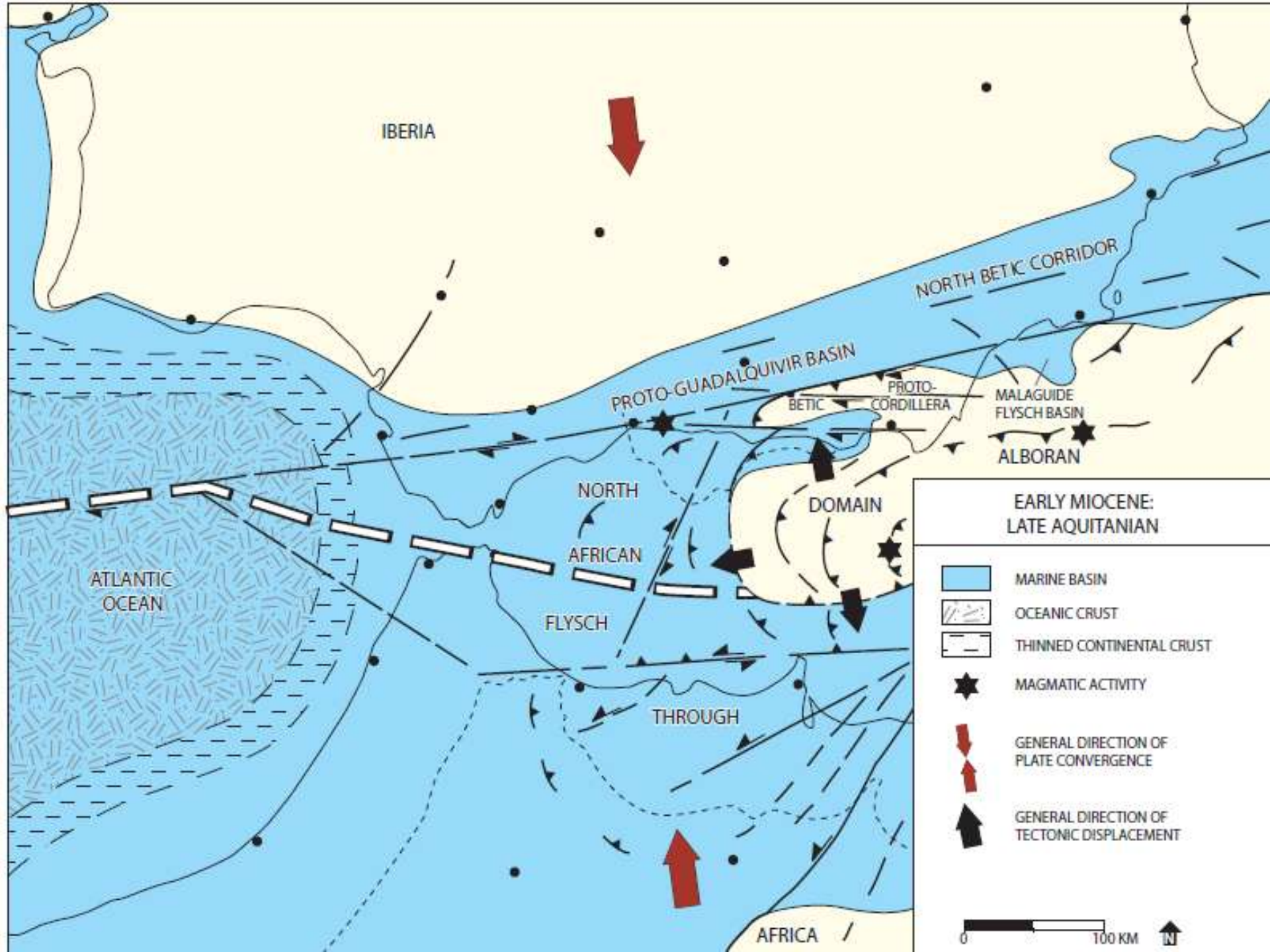
IBERIA
NORTH BETIC CORRIDOR
PROTO-GUADALQUIVIR BASIN
BETIC
PROTO-CORDILLERA
MALAGUIDE FLYSCH BASIN
ALBORAN
DOMAIN
NORTH
AFRICAN
FLYSCH
THROUGH
ATLANTIC OCEAN
AFRICA
EARLY MIOCENE:
LATE AQUITANIAN
MARINE BASIN
OCEANIC CRUST
THINNED CONTINENTAL CRUST
MAGMATIC ACTIVITY
GENERAL DIRECTION OF PLATE CONVERGENCE
GENERAL DIRECTION OF TECTONIC DISPLACEMENT
0
100 KM
N

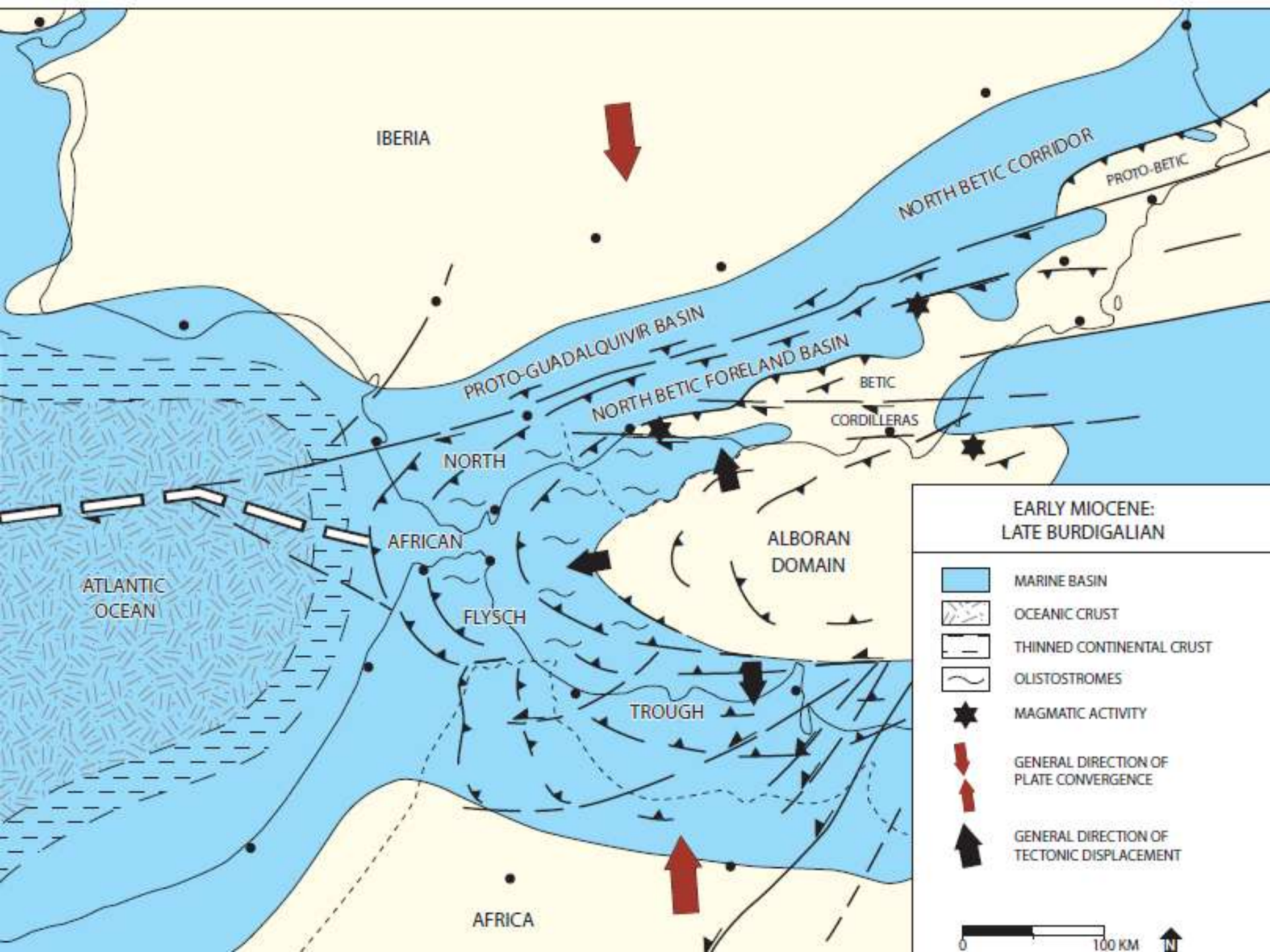
IBERIA
NORTH BETIC CORRIDOR
PROTO-BETIC
PROTO-GUADALQUIVIR BASIN
NORTH BETIC FORELAND BASIN
BETIC
CORDILLERAS
NORTH
AFRICAN
ATLANTIC
OCEAN
FLYSCH
TROUGH
ALBORAN
DOMAIN
AFRICA
EARLY MIOCENE:
LATE BURDIGALIAN
MARINE BASIN
OCEANIC CRUST
THINNED CONTINENTAL CRUST
OLISTOSTROMES
MAGMATIC ACTIVITY
GENERAL DIRECTION OF
PLATE CONVERGENCE
GENERAL DIRECTION OF
TECTONIC DISPLACEMENT
0
100 KM
N

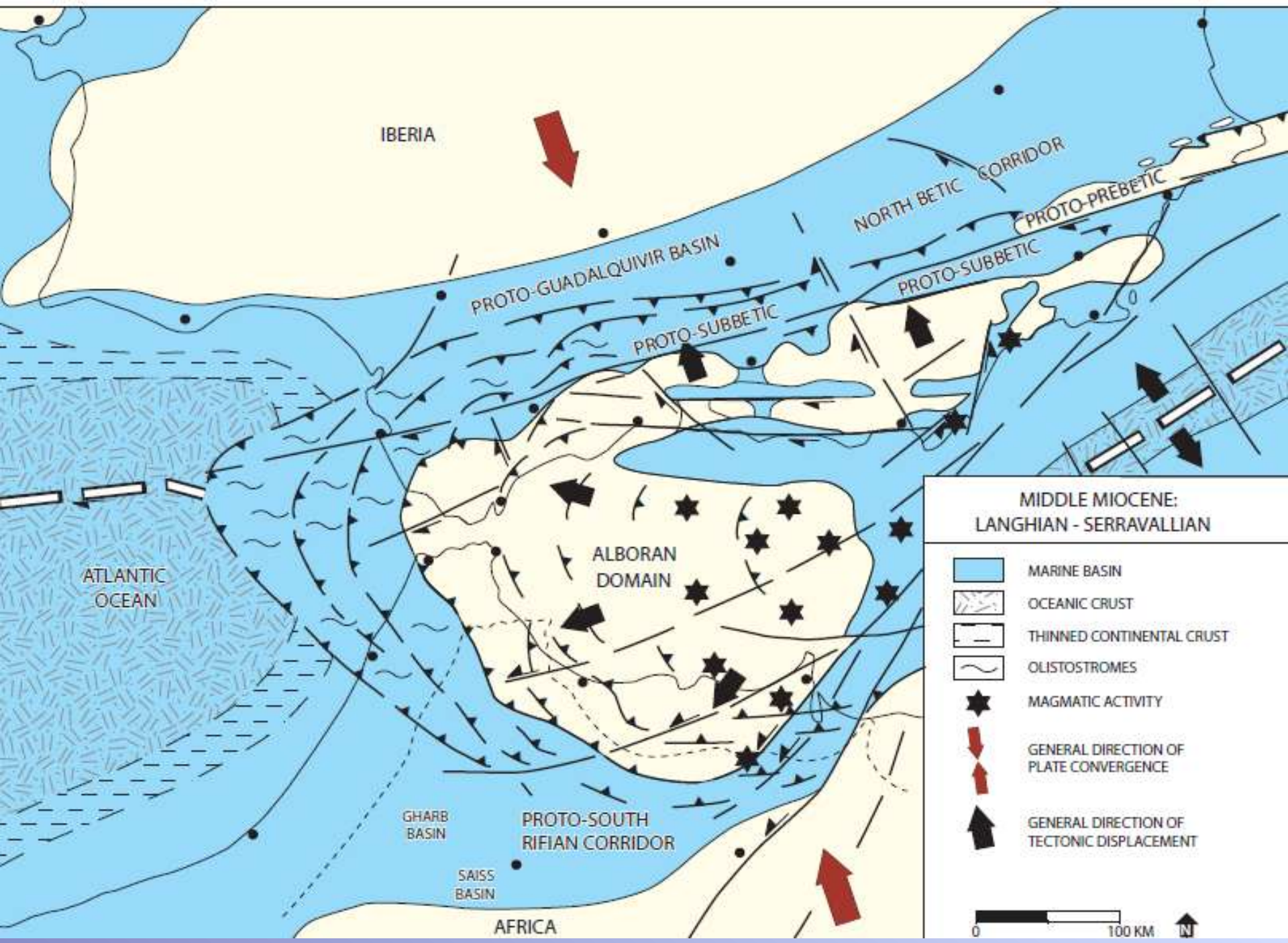
IBERIA
PROTO-GUADALQUIVIR BASIN
NORTH BETIC CORRIDOR
PROTO-PREBETIC
PROTO-SUBBETIC
PROTO-SUBBETIC
ATLANTIC OCEAN
ALBORAN DOMAIN
GHARB BASIN
PROTO-SOUTH RIFIAN CORRIDOR
SAISS BASIN
AFRICA
MIDDLE MIOCENE:
LANGHIAN - SERRAVALLIAN
MARINE BASIN
OCEANIC CRUST
THINNED CONTINENTAL CRUST
OLISTOSTROMES
MAGMATIC ACTIVITY
GENERAL DIRECTION OF PLATE CONVERGENCE
GENERAL DIRECTION OF TECTONIC DISPLACEMENT
0
100 KM
N

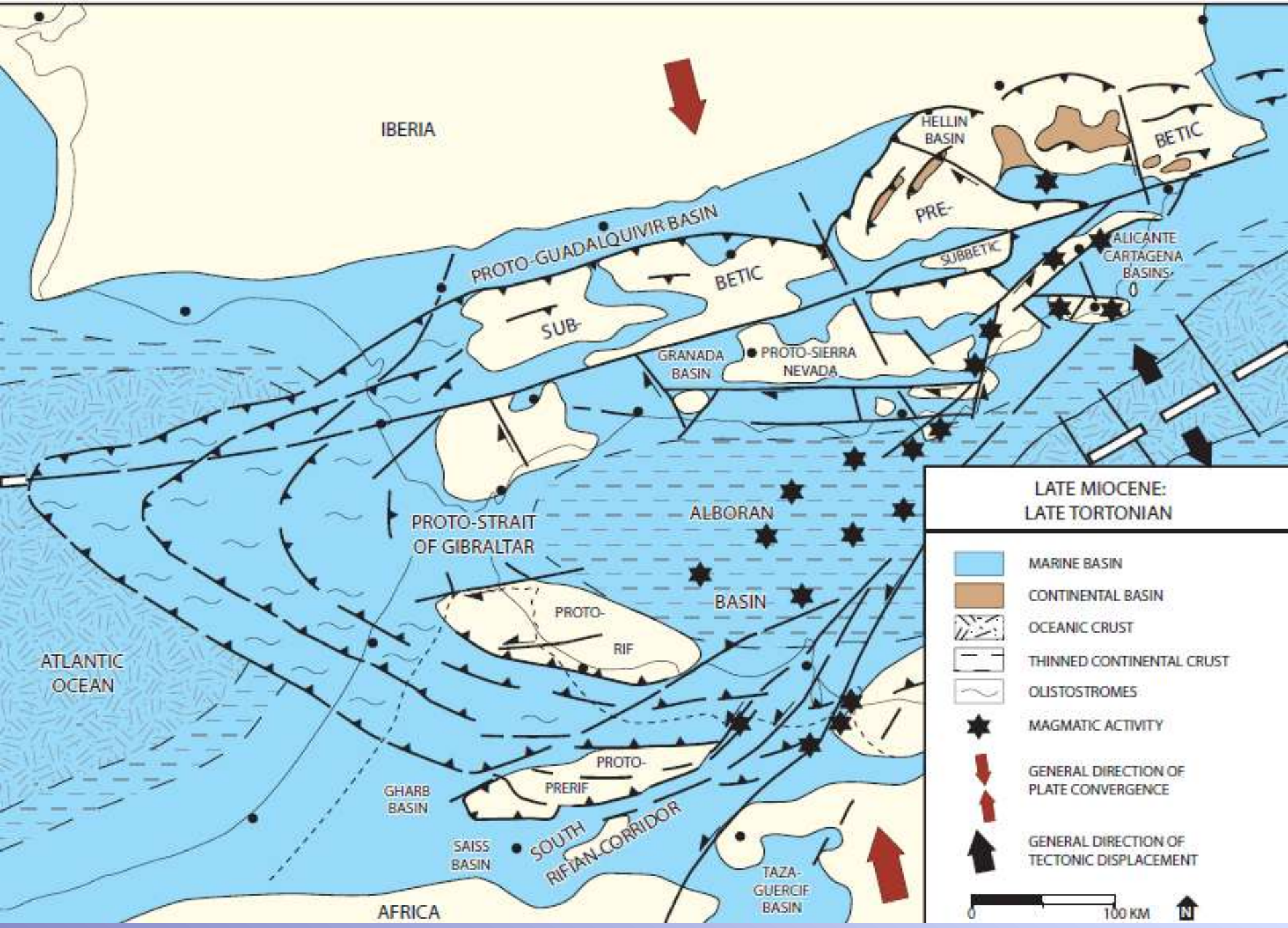
IBERIA
HELLIN BASIN
BETIC
PRE-
SUBBETIC
ALICANTE CARTAGENA BASINS
PROTO-GUADALQUIVIR BASIN
BETIC
SUB-
GRANADA BASIN
PROTO-SIERRA NEVADA
PROTO-STRAIT OF GIBRALTAR
ALBORAN
BASIN
PROTO-
RIF
ATLANTIC OCEAN
PROTO-
PRERIF
GHARB BASIN
SAISS BASIN
SOUTH RIFIAN CORRIDOR
TAZA-GUERCIF BASIN
AFRICA
LATE MIOCENE:
LATE TORTONIAN
MARINE BASIN
CONTINENTAL BASIN
OCEANIC CRUST
THINNED CONTINENTAL CRUST
OLISTOSTROMES
MAGMATIC ACTIVITY
GENERAL DIRECTION OF PLATE CONVERGENCE
GENERAL DIRECTION OF TECTONIC DISPLACEMENT
0
100 KM
N

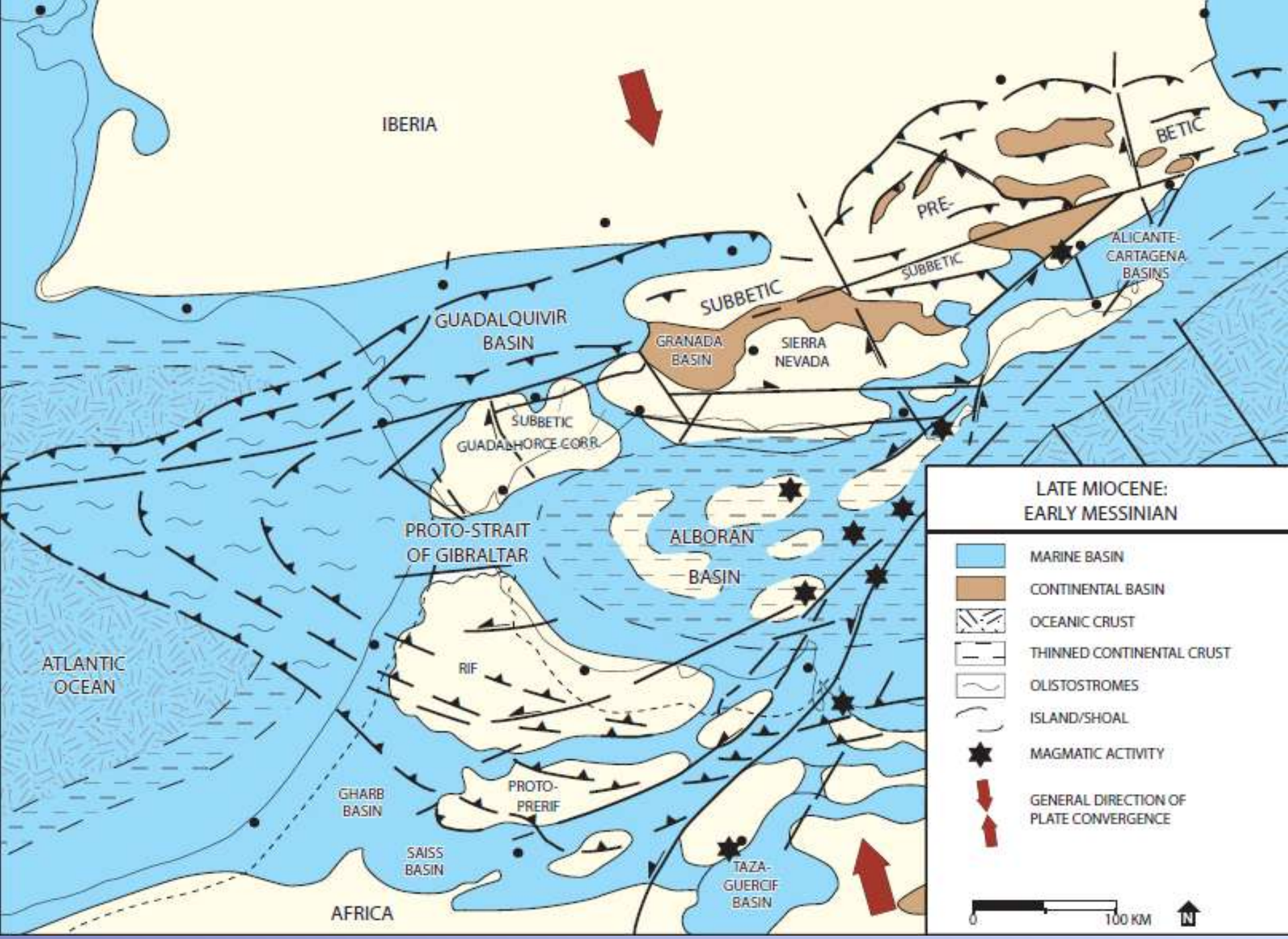
IBERIA
BETIC
PRE-
SUBBETIC
ALICANTE-
CARTAGENA
BASINS
SUBBETIC
GUADALQUIVIR
BASIN
GRANADA
BASIN
SIERRA
NEVADA
SUBBETIC
GUADALHORCE CORR.
PROTO-STRAIT
OF GIBRALTAR
ALBORAN
BASIN
ATLANTIC
OCEAN
RIF
GHARB
BASIN
PROTO-
PRERIF
SAISS
BASIN
TAZA-
GUERCIF
BASIN
AFRICA
LATE MIOCENE:
EARLY MESSINIAN
MARINE BASIN
CONTINENTAL BASIN
OCEANIC CRUST
THINNED CONTINENTAL CRUST
OLISTOSTROMES
ISLAND/SHOAL
MAGMATIC ACTIVITY
GENERAL DIRECTION OF
PLATE CONVERGENCE
0
100 KM
N

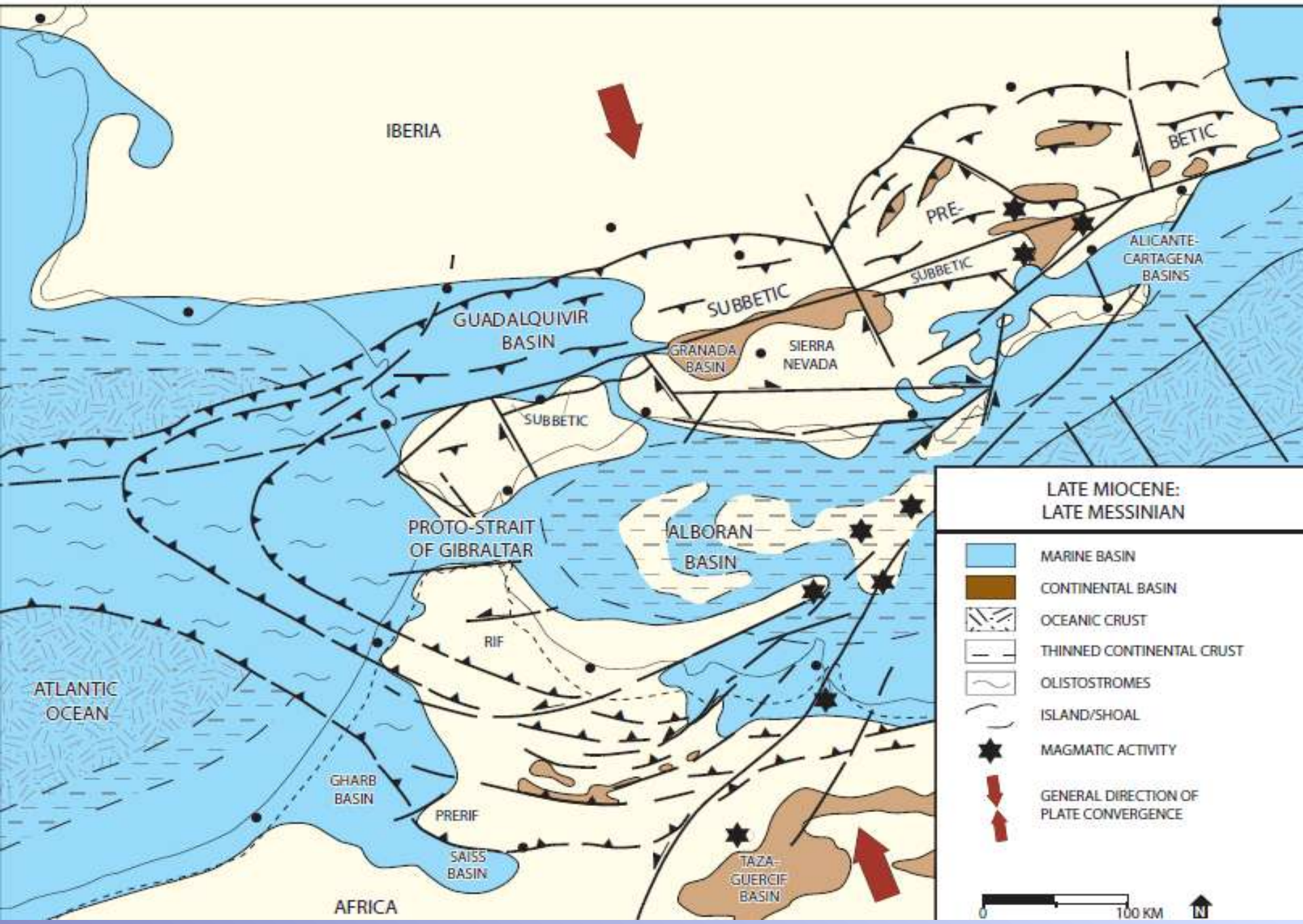
IBERIA
BETIC
PRE-
SUBBETIC
ALICANTE-
CARTAGENA
BASINS
SUBBETIC
GUADALQUIVIR
BASIN
GRANADA
BASIN
SIERRA
NEVADA
SUBBETIC
PROTO-STRAIT
OF GIBRALTAR
ALBORAN
BASIN
RIF
ATLANTIC
OCEAN
GHARB
BASIN
PRERIF
SAISS
BASIN
AFRICA
TAZA-
GUERCIF
BASIN
LATE MIOCENE:
LATE MESSINIAN
MARINE BASIN
CONTINENTAL BASIN
OCEANIC CRUST
THINNED CONTINENTAL CRUST
OLISTOSTROMES
ISLAND/SHOAL
MAGMATIC ACTIVITY
GENERAL DIRECTION OF
PLATE CONVERGENCE
0
100 KM
N

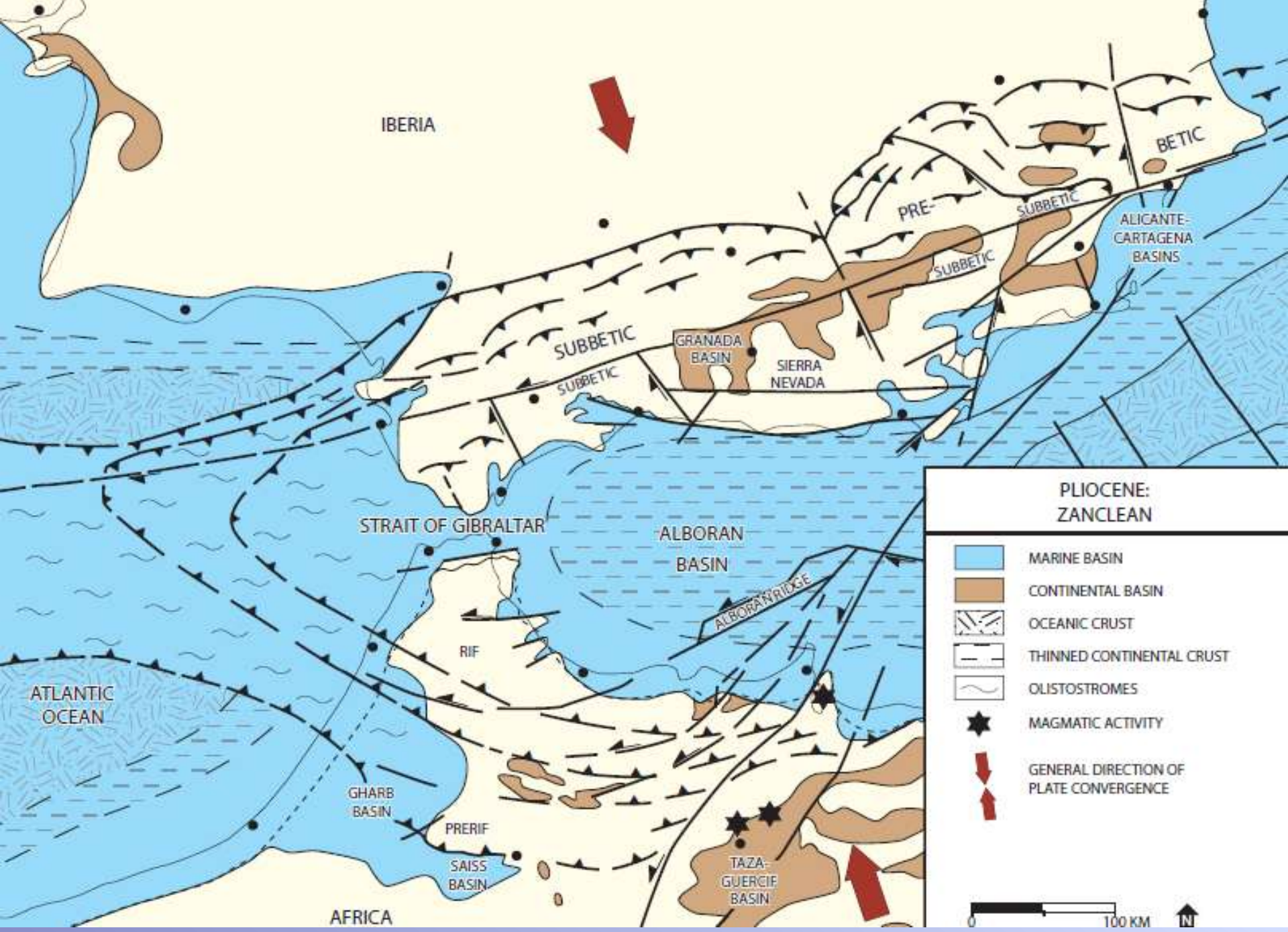
IBERIA
BETIC
PRE-
SUBBETIC
SUBBETIC
ALICANTE-
CARTAGENA
BASINS
SUBBETIC
SUBBETIC
GRANADA
BASIN
SIERRA
NEVADA
STRAIT OF GIBRALTAR
ALBORAN
BASIN
ALBORAN RIDGE
RIF
ATLANTIC
OCEAN
GHARB
BASIN
PRERIF
SAISS
BASIN
TAZA-
GUERCIF
BASIN
AFRICA
PLIOCENE:
ZANCLEAN
MARINE BASIN
CONTINENTAL BASIN
OCEANIC CRUST
THINNED CONTINENTAL CRUST
OLISTOSTROMES
MAGMATIC ACTIVITY
GENERAL DIRECTION OF
PLATE CONVERGENCE
0
100 KM
N

Wat hebben we zojuist gezien?

The Betic Cordillera, lying just between the Atlantic Ocean and the Mediterranean Sea, started to uplift in the Middle Miocene as result of the Alpine collision. First, only certain minor reliefs emerged as small, isolated islands. In Late Miocene, the paleogeography evolved into irregularly trending, interconnected, intermontane marine basins as the emerging reliefs expanded in size and fused together. Some of these basins opened directly to the Atlantic Ocean and others to the Mediterranean Sea (Braga et al., 2003). In the initial stages, numerous marine passages formed between the Atlantic-linked and the Mediterranean-linked basins. These seaways were, however, progressively confined and reduced in number during the uplifting until they finally disappeared.

Straat van Gibraltar

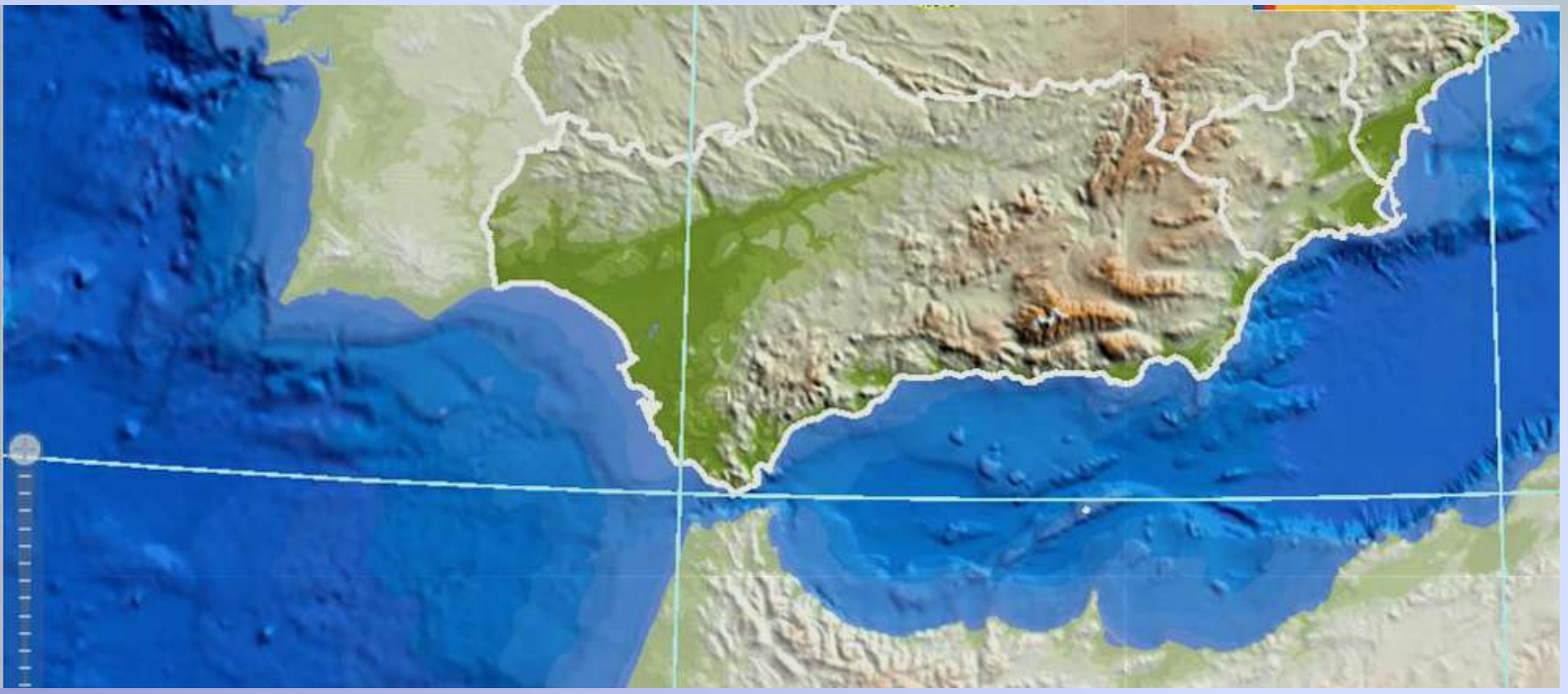

Structuur en topografie

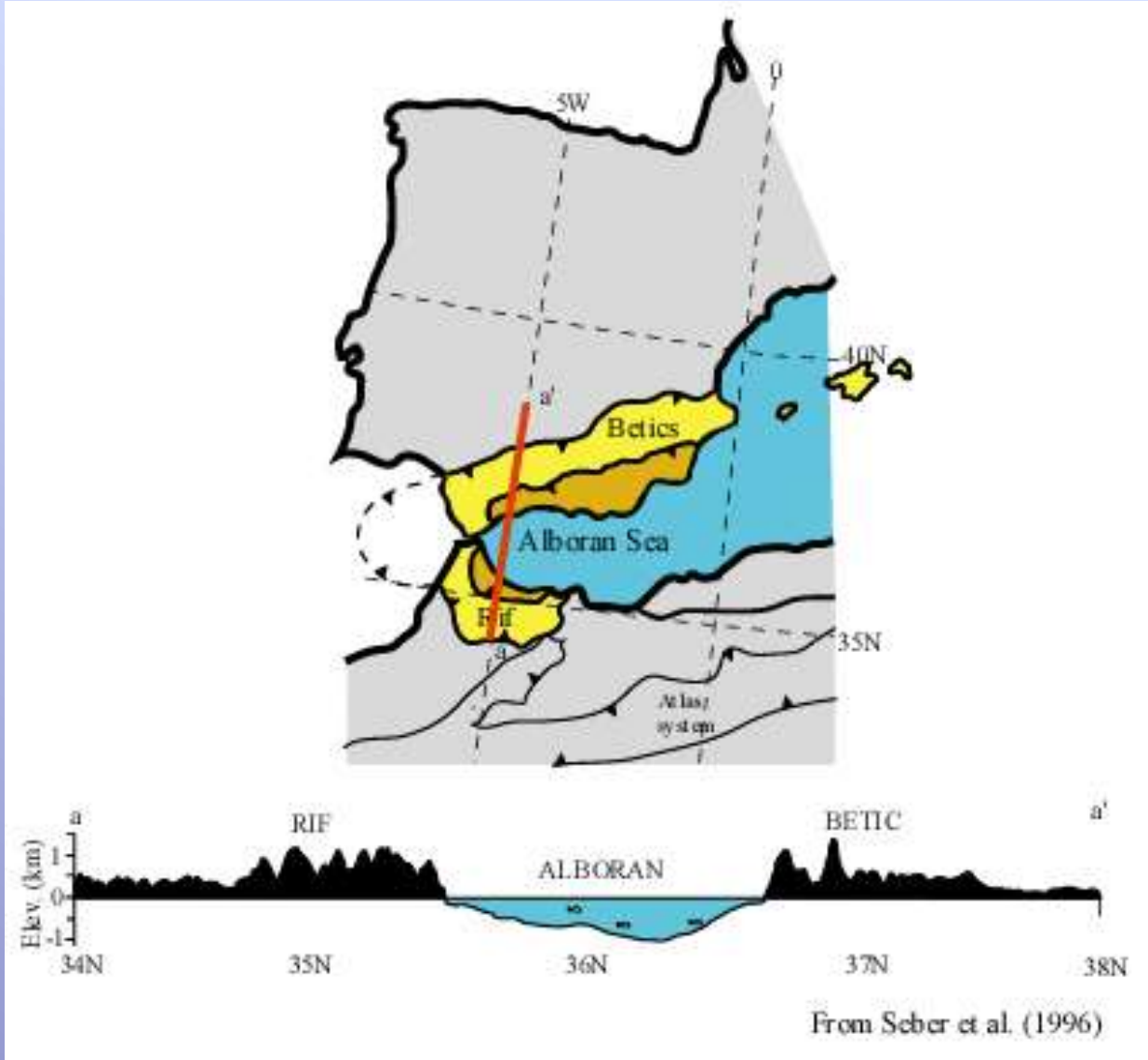

From Seber et al. (1996)

Sierra Nevada

Marokkaanse Mediterrane kust

Rif Chefchaouen mountains

De Spaanse zeestraten in meer detail

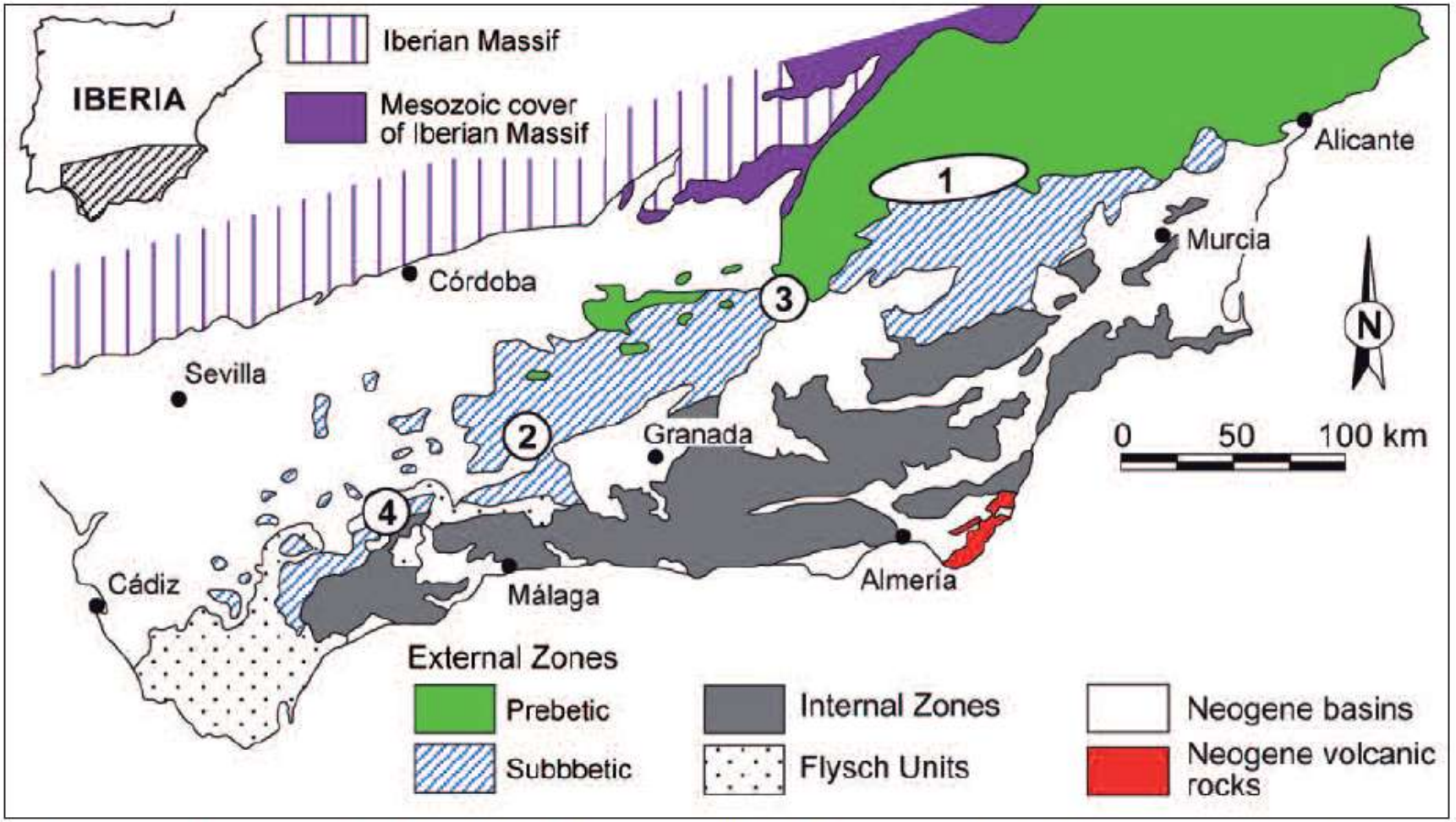

Fig. 1.- Simplified geological map of the Betic Cordillera. The position of the successive Betic straits is marked. 1: North-Betic Strait; 2: Zagra Strait; 3: Dehesas de Guadix Strait; 4: Guadalhorce Strait.

Crossbedding

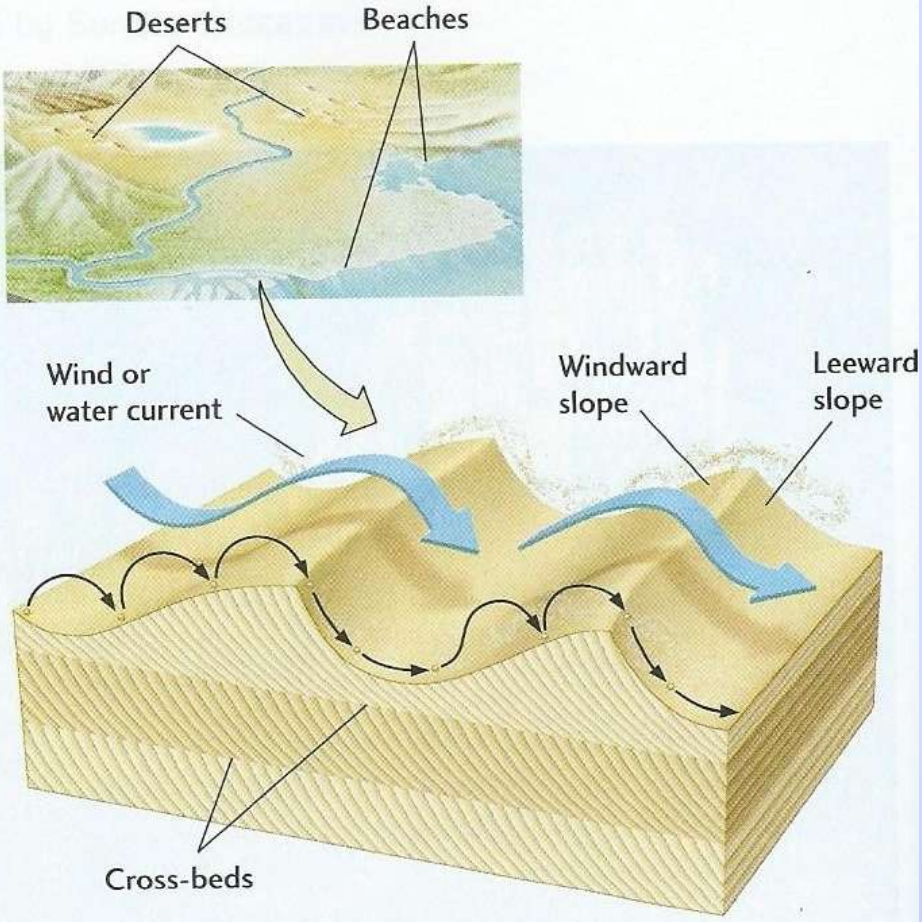

FIGURE 5.11 ■ Sediment particles transported down the steeper, downcurrent slope of a sand dune, sandbar, or ripple form cross-bedding.

De gelaagdheid van de zeestraten

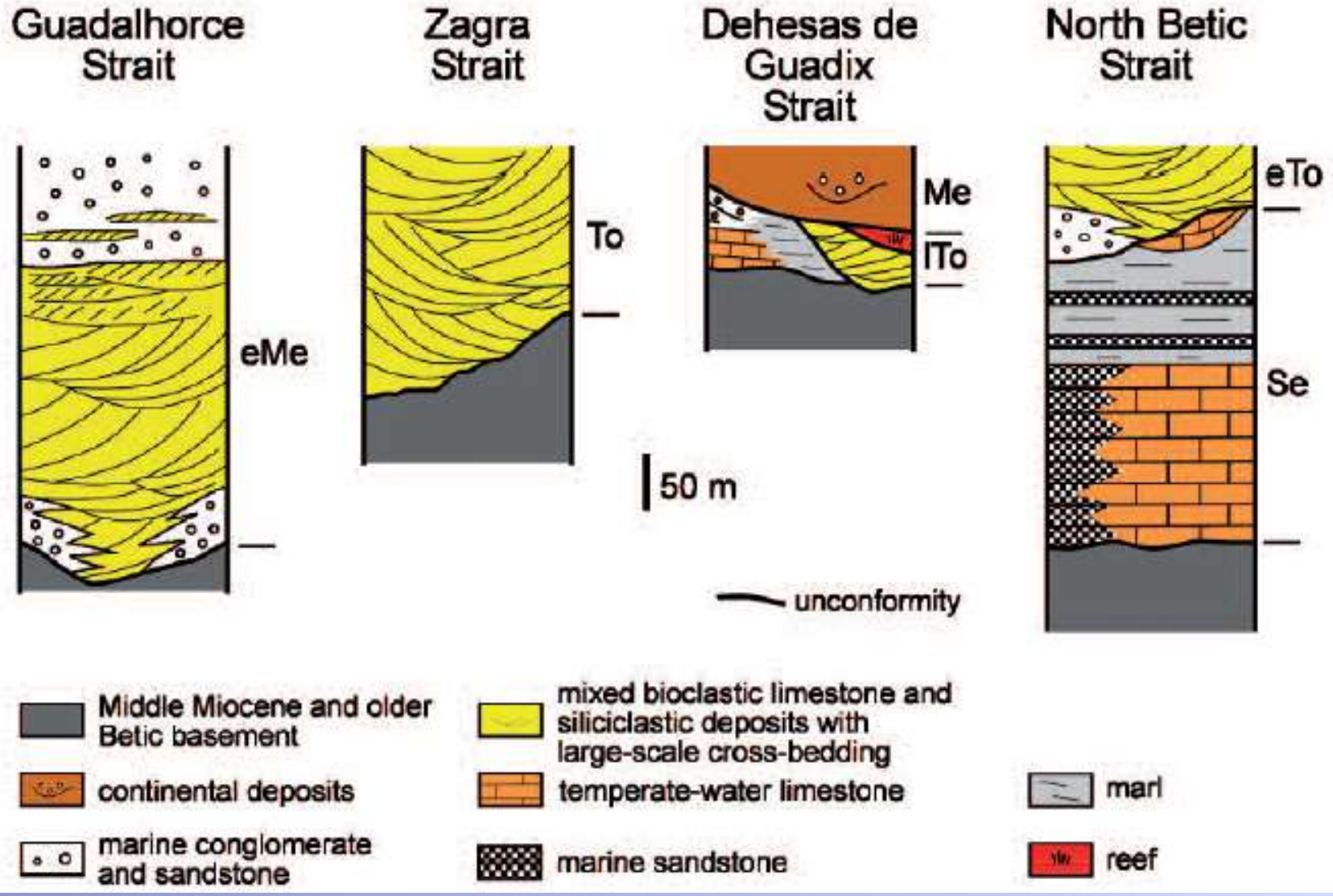


(a)
earliest Tortonian
Northbetic Strait
Alicante
Murcia
Jaén
Granada
Guadalquivir
Basin
Almería
Málaga
100 km
Atlantic Ocean
Mediterranean Sea
N
present-day coast
emergent land

North Betic Strait

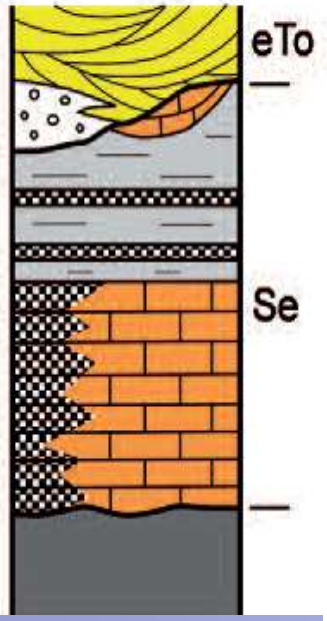

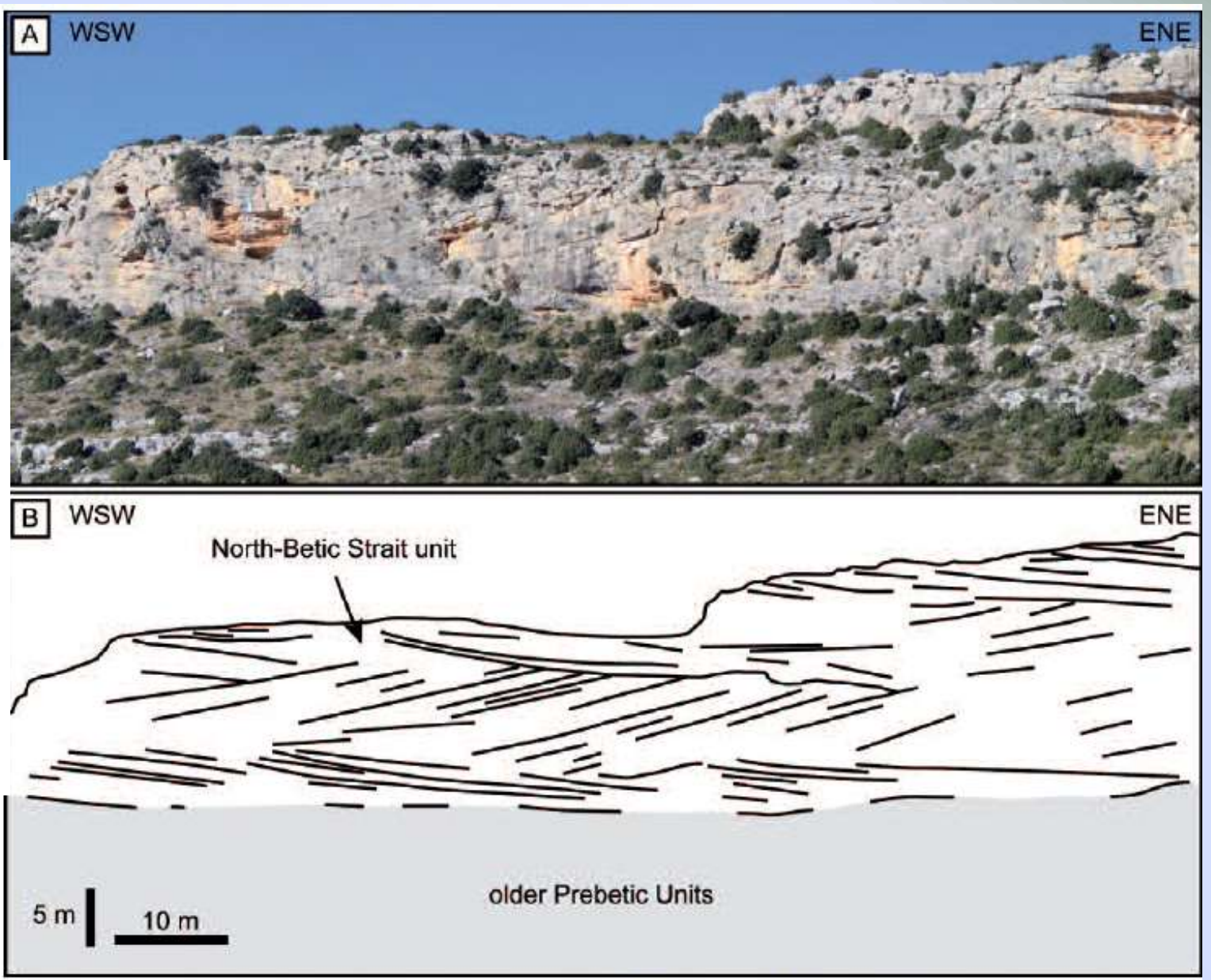

Fig. 3.- Composite structures exhibiting reverse, large-scale cross-bedding are common features in the North-Betic Strait deposits


(b)
Tortonian
DGS
Zagra
Strait
Almeria
Rifian
straits
?
100 km

Fig. 4.- A-B: Huge, cross-bedding structures pointing to the SE. A collapsed dune, exhibiting strongly distorted and folded beds, can be seen at the bottom right of the picture. C: Close-up view of the area marked in A. Fuentes de Cesna (Zagra Strait)

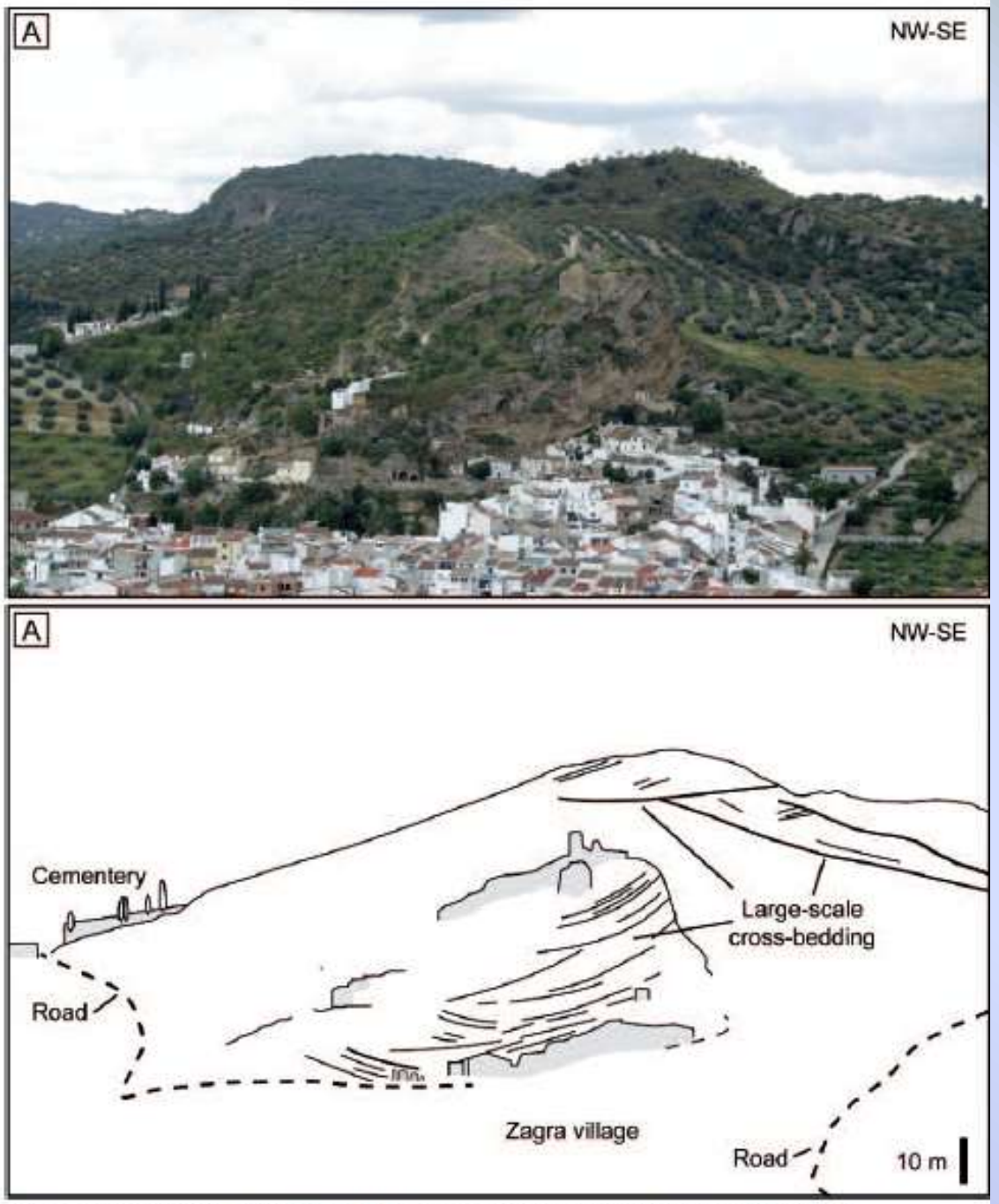

Fig. 5.- S-SE and N-NW dipping giant trough cross-bedding units are ubiquitous in the Zagra Strait.

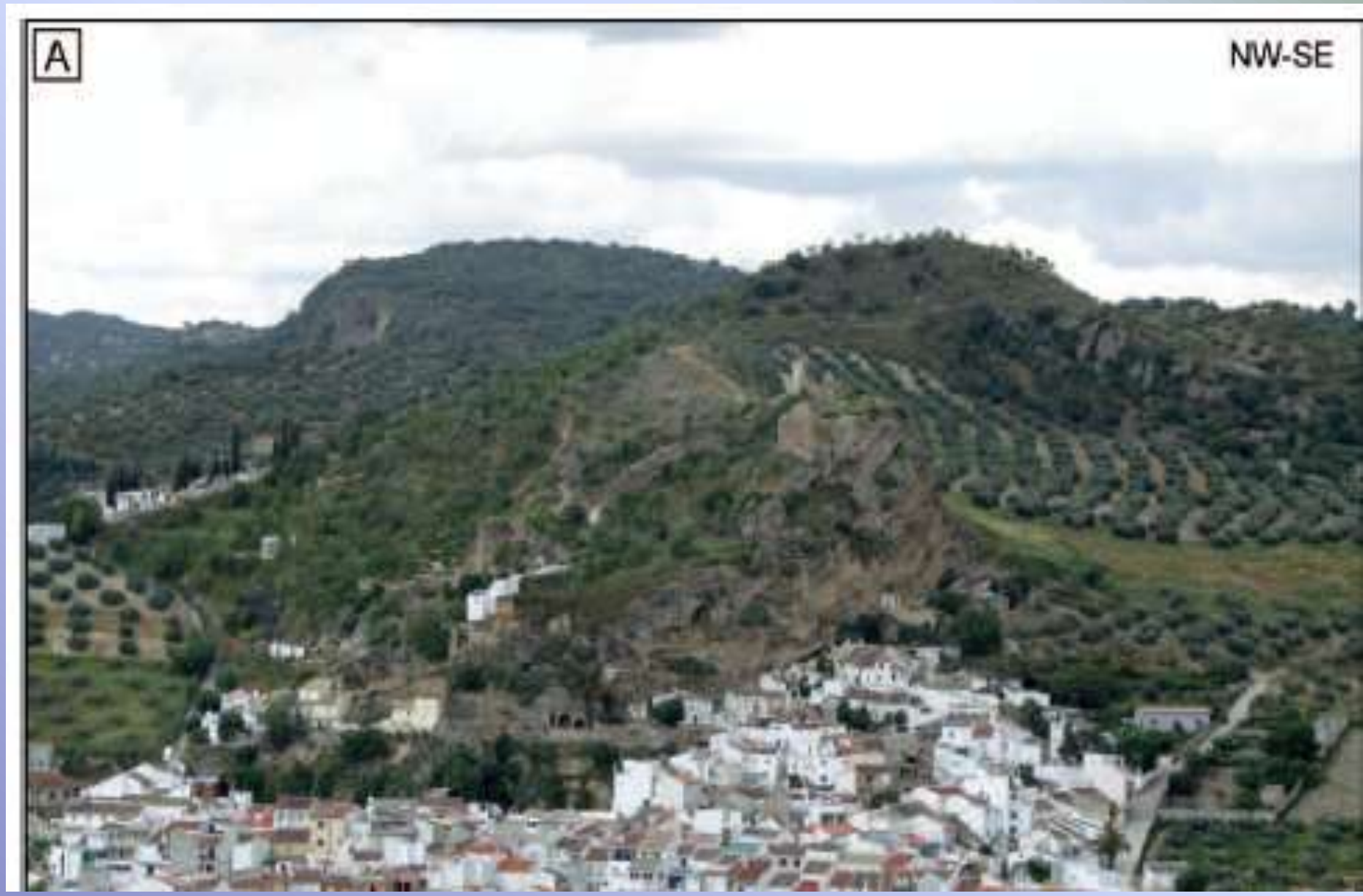
A
NW-SE


(b)
Tortonian
DGS
Zagra
Strait
Almeria
Rifian
straits
?
100 km

Dehesas de Guadix Strait

Fig. 6.- Unidirectional, giant cross-bedding is the most outstanding feature in the Dehesas de Guadix Strait. Man in the picture (encircled) is 1.85 m tall.


(c)
earliest Messinian
Guadalhorce
Strait
Rifian
straits
100 km

Guadalhorce Corridor

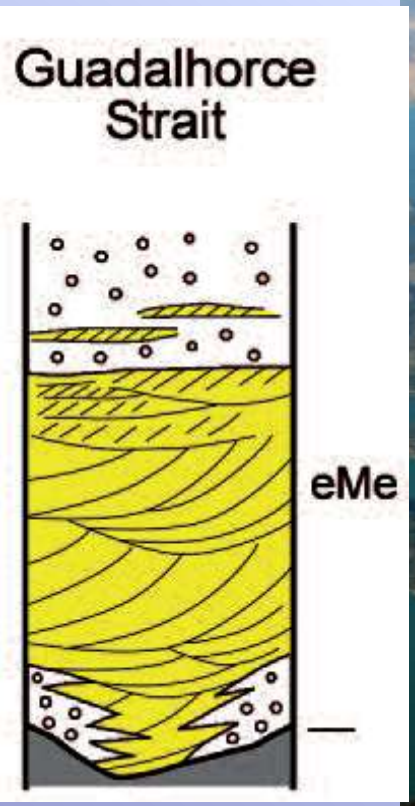

g. 7.- Aerial view of the Guadalhorce Corridor: Horizontal to gently dipping layers of the Messinian strait-infilling stand out in the ntre of the picture. The Miocene beds are limited by Jurassic limestones (upper part of the picture) and by Paleozoic schists (bottom rt of the picture).

Guadalhorce Corridor

Fig. 7.- Aerial view of the Guadalhorce Corridor: Horizontal to gently dipping layers of the Messinian strait-infilling stand out in the centre of the picture. The Miocene beds are limited by Jurassic limestones (upper part of the picture) and by Paleozoic schists (bottom part of the picture).

Rifian corridors

Problemen Evaporieten MSC

- Geen boringen door totale afzettingen in de diepzee, info alleen uit bovenste laag en ondiepere bekkens (in zee of op het land)
- Er was geen adequaat stratigrafisch tijdsframe
- De afzettingen waren zo wie zo complex
- Wel was er een spectaculaire cycliciteit in de gesteente afzettingen van de evaporieten te ontdekken
- Daardoor geschikt voor astro-chronological tuning en gedetailleerde bestudering

Gevolgen van een geleidelijke afsluiting? (de aanloop)

- 7,15 Ma vermindering van de diepzee circulatie
- Daarmee samenhangend een toenemende afzetting van diatomeeën rijke sedimenten de Tripolo formatie op o.a. Sicilië (maar over hele MZ)
- Ook opaal rijke afzettingen in Zuid-Spanje en door de hele MZ (7,15-6,7 MA)
- 6,7 De diversiteit van kalkhoudende plankton vermindert sterk (door zouter oppervlakte water)
- Tussen 6.3 en 5.97 calciet-,dolomiet- en aragonietvorming

Het begin: afzetting van de eerste gipslagen

- Waar komen die afzettingen voor ?
- Hoe ontstaan?
- Hoe zien ze er uit?

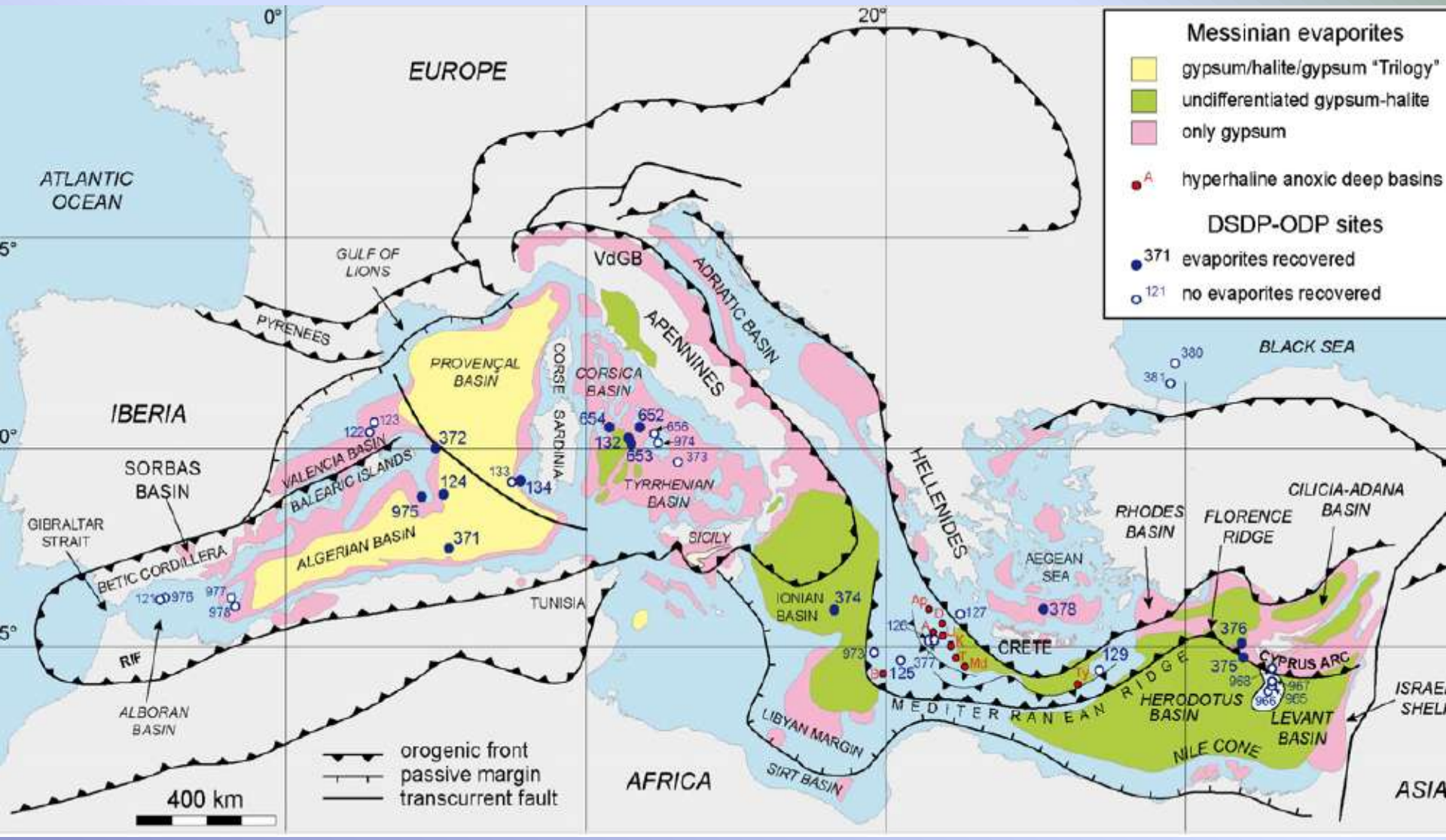
Messinian evaporites
gypsum/halite/gypsum "Trilogy"
undifferentiated gypsum-halite
only gypsum
hyperhaline anoxic deep basins
DSDP-ODP sites
371 evaporites recovered
121 no evaporites recovered
EUROPE
ATLANTIC OCEAN
IBERIA
AFRICA
ASIA
BLACK SEA
GULF OF LIONS
PYRENEES
PROVENÇAL BASIN
CORSE SARDINIA
CORSICA BASIN
APENNINES
ADRIATIC BASIN
VdGB
VALENCIA BASIN
BALEARIC ISLANDS
SORBAS BASIN
GIBRALTAR STRAIT
BETIC CORDILLERA
RIF
ALBORAN BASIN
ALGERIAN BASIN
TYRRHENIAN BASIN
SICILY
TUNISIA
IONIAN BASIN
HELLENIDES
AEGEAN SEA
CRETE
RHODES BASIN
FLORENCE RIDGE
CILICIA-ADANA BASIN
CYPRUS ARC
MEDITERRANEAN RIDGE
HERODOTUS BASIN
LEVANT BASIN
NILE CONE
LIBYAN MARGIN
SIRT BASIN
ISRAEL SHELF
orogenic front
passive margin
transcurrent fault
400 km

Omstandigheden tijdens vorming PLG's

- Relatief homogeen water dat zijn oorsprong vond uit de A.O.
- Er was een beperkte uitstroom van water uit de MZ naar de A.O.
- De instroom van rivierwater was ook belangrijk,significant
- Er was dus verbinding met de A.O.
- Relatief lage drempel tussen MZ en AO
- Continentale invloed en invloed van klimaat

Zeespiegelniveau MZ=AO drempel wordt hoger

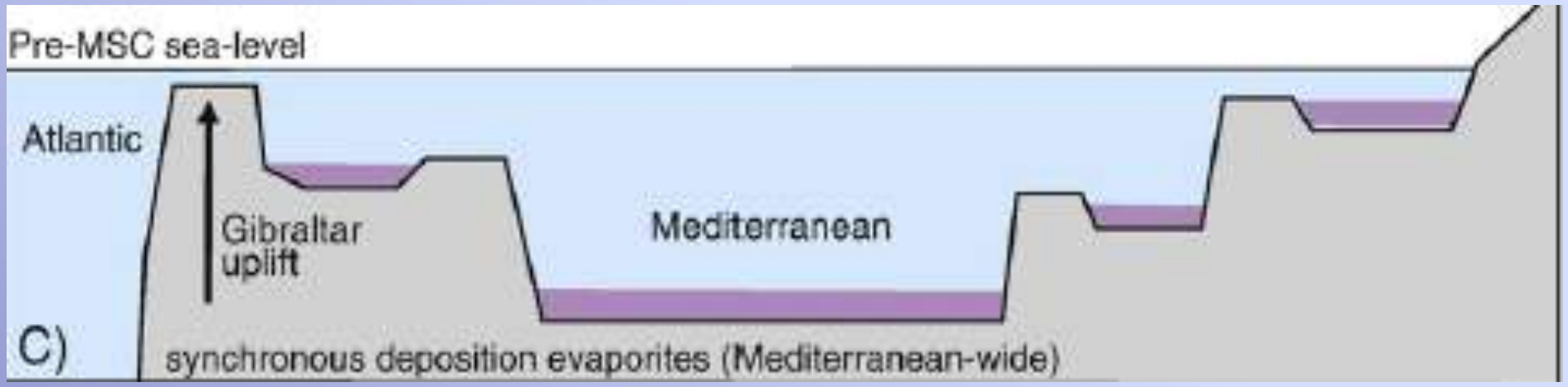

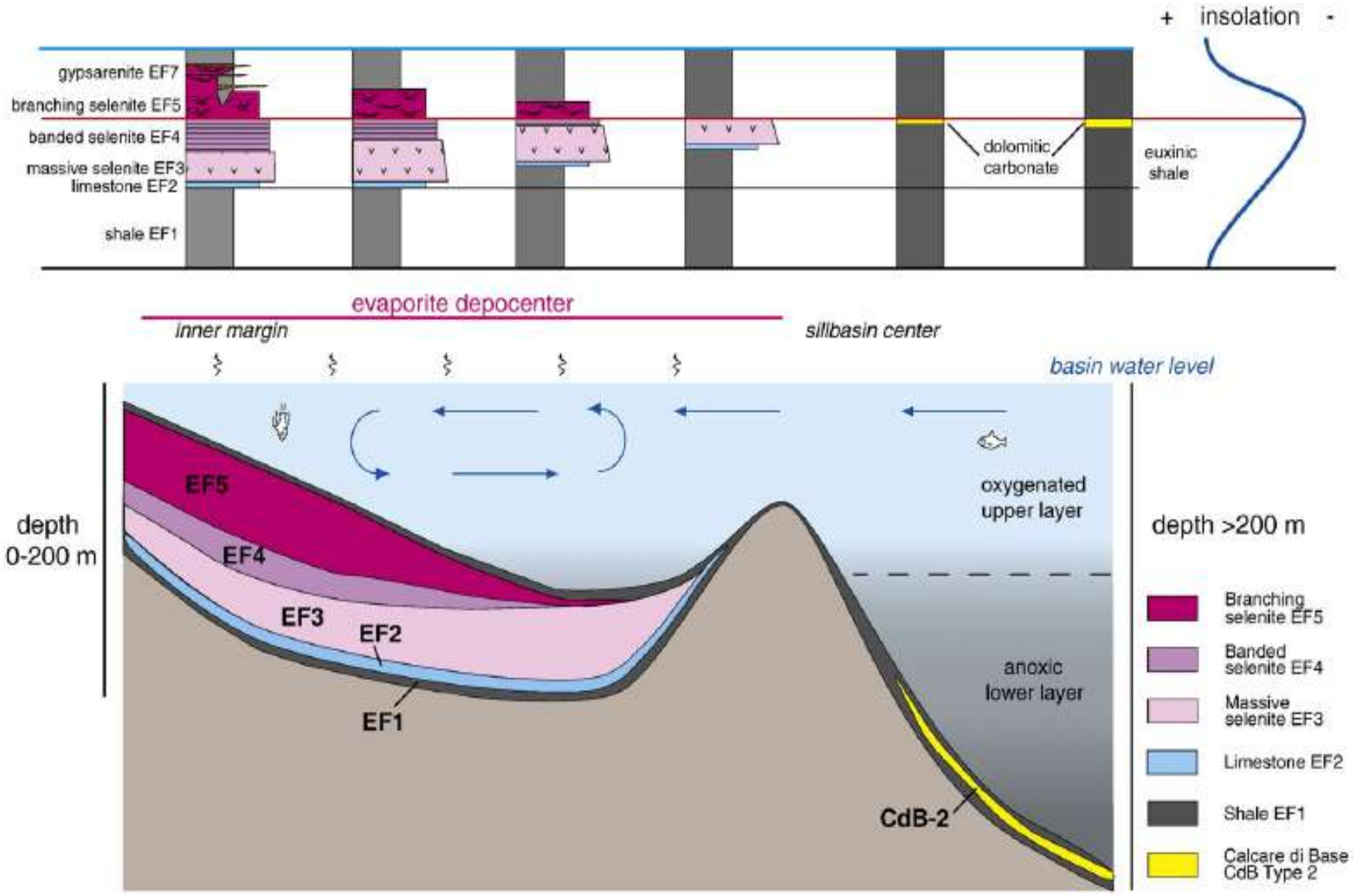
+ insolation -
gypsarenite EF7
branching selenite EF5
banded selenite EF4
massive selenite EF3
limestone EF2
shale EF1
dolomitic carbonate
euxinic shale
evaporite depocenter
inner margin
sillbasin center
basin water level
depth 0-200 m
EF5
EF4
EF3
EF2
EF1
oxygenated upper layer
anoxic lower layer
CdB-2
depth >200 m
Branching selenite EF5
Banded selenite EF4
Massive selenite EF3
Limestone EF2
Shale EF1
Calcare di Base CdB Type 2

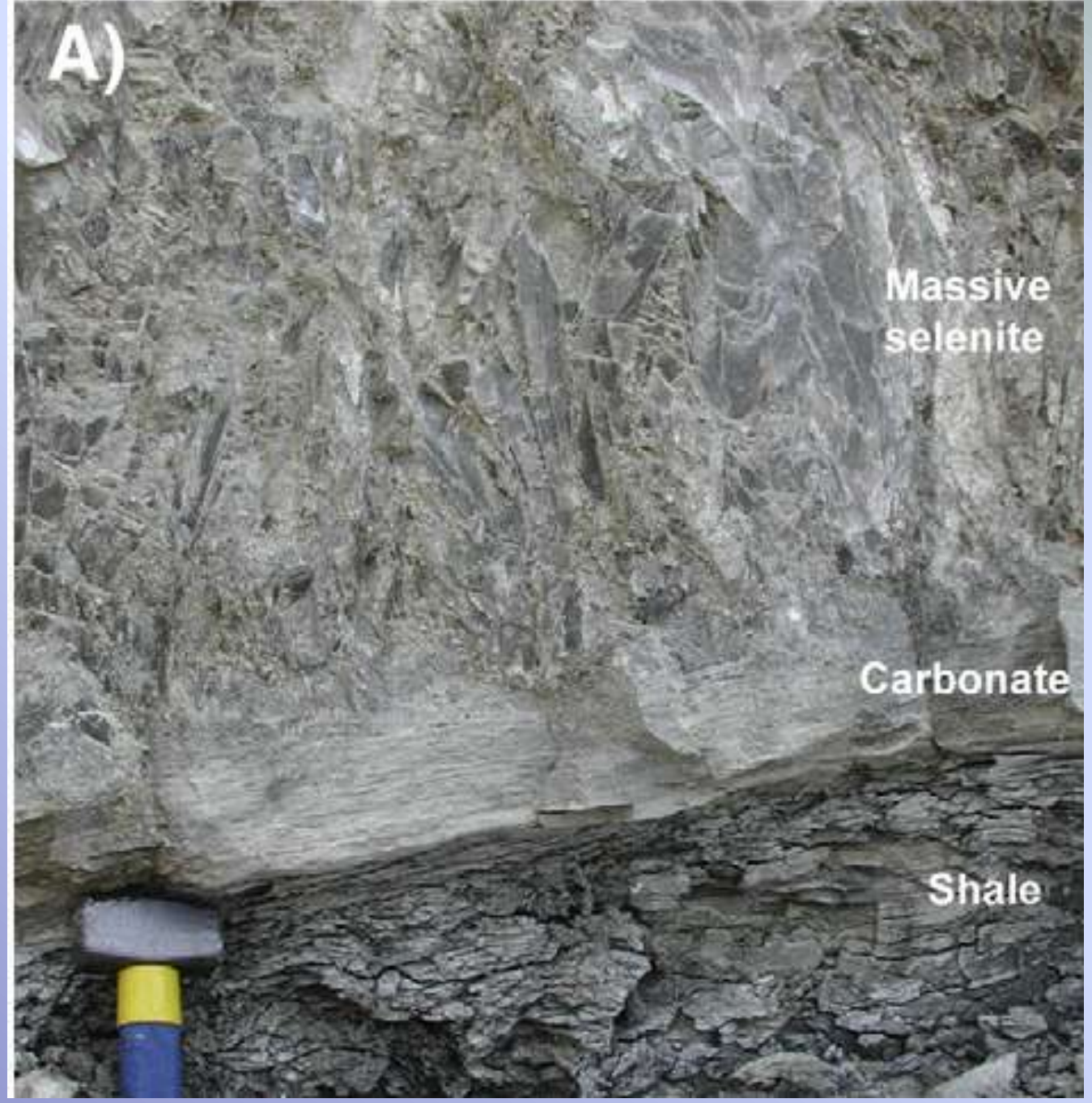
A)
Massive selenite
Carbonate
Shale

Primary Lower Gypsum facies association

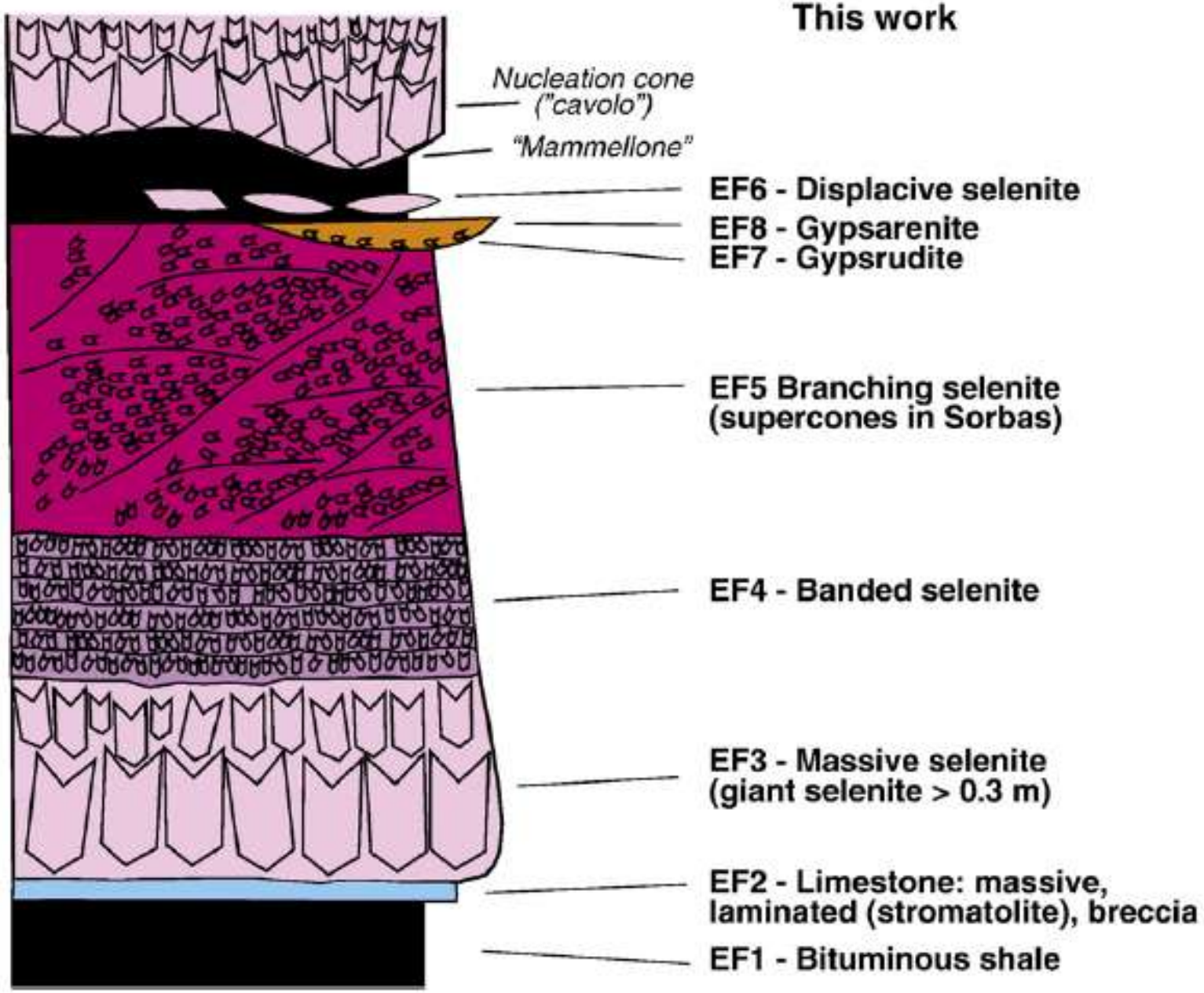

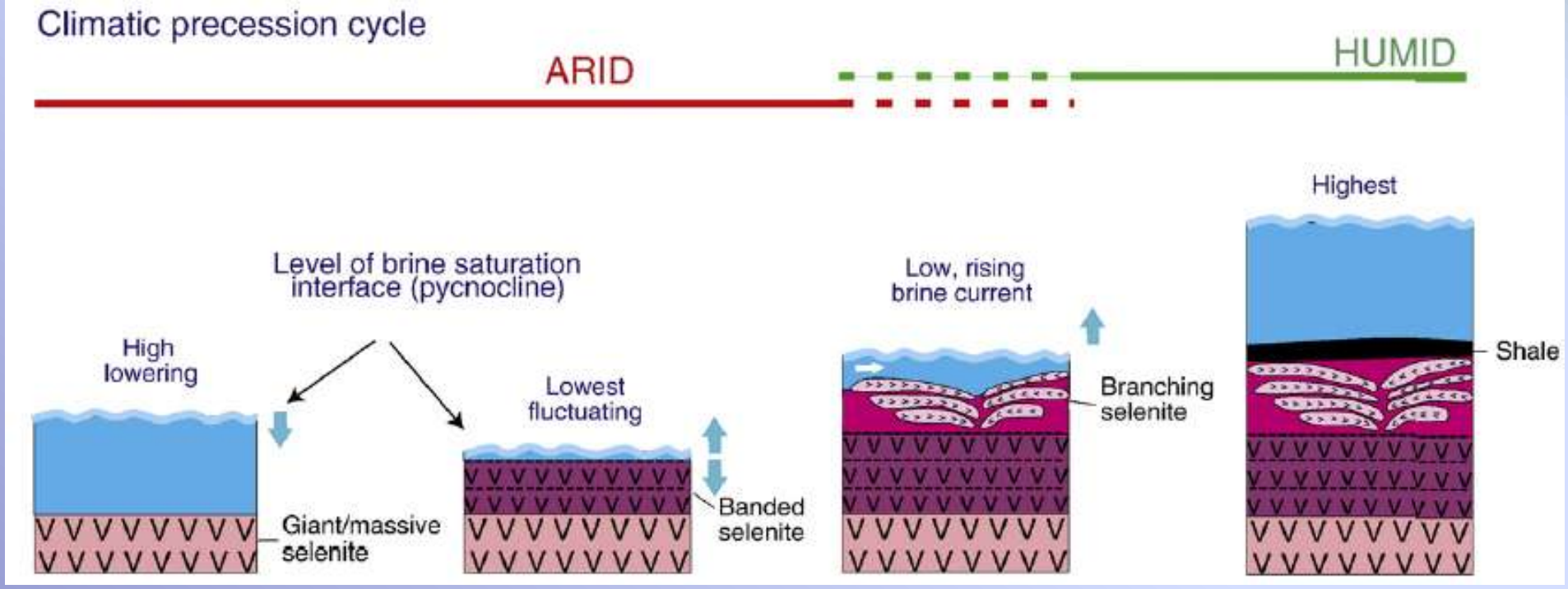
Climatic precession cycle
ARID
HUMID
Level of brine saturation interface (pycnocline)
High lowering
Giant/massive selenite
Lowest fluctuating
Banded selenite
Low, rising brine current
Branching selenite
Highest
Shale

Ontstaan Giant- of Massive Selenite

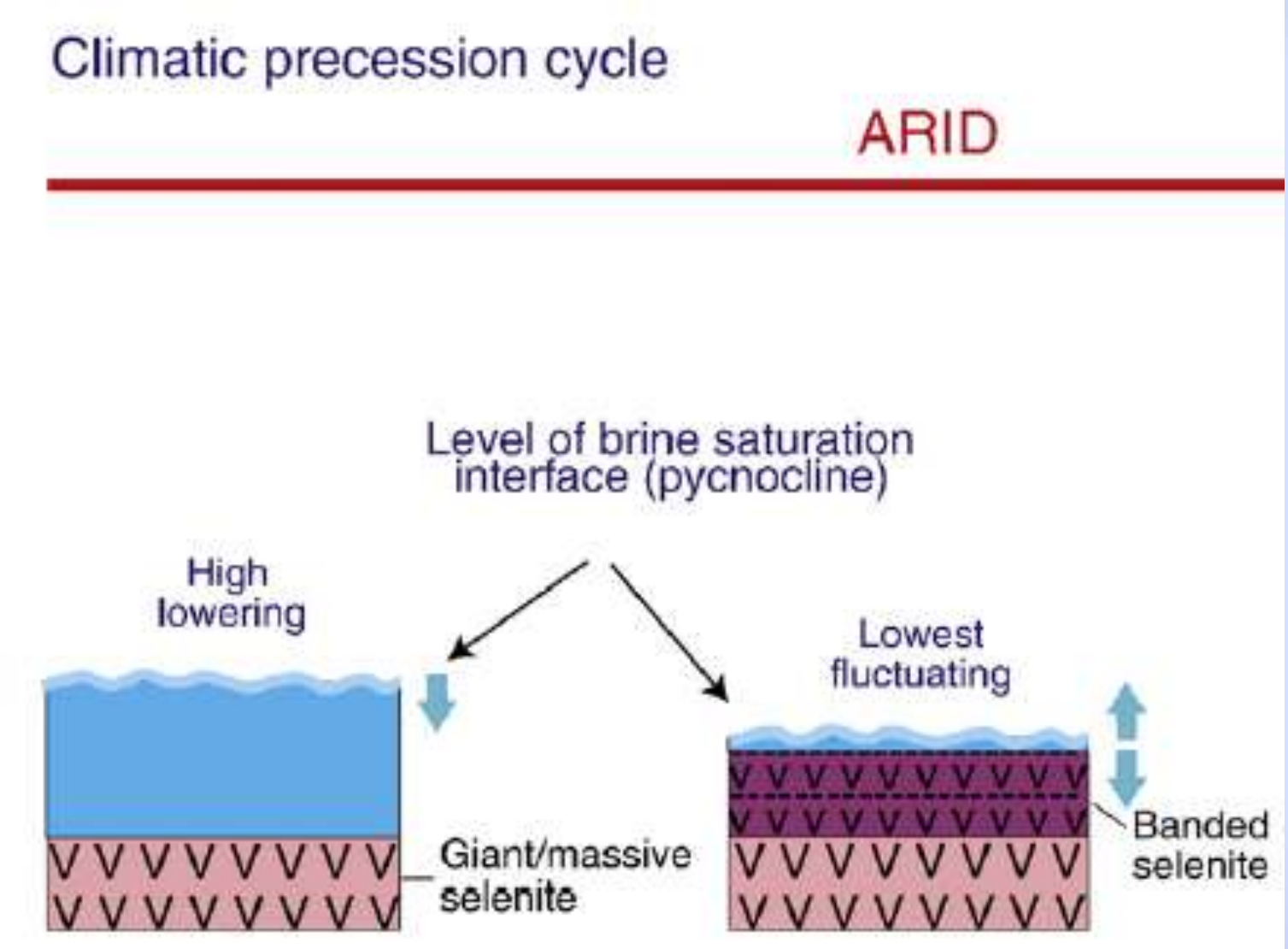

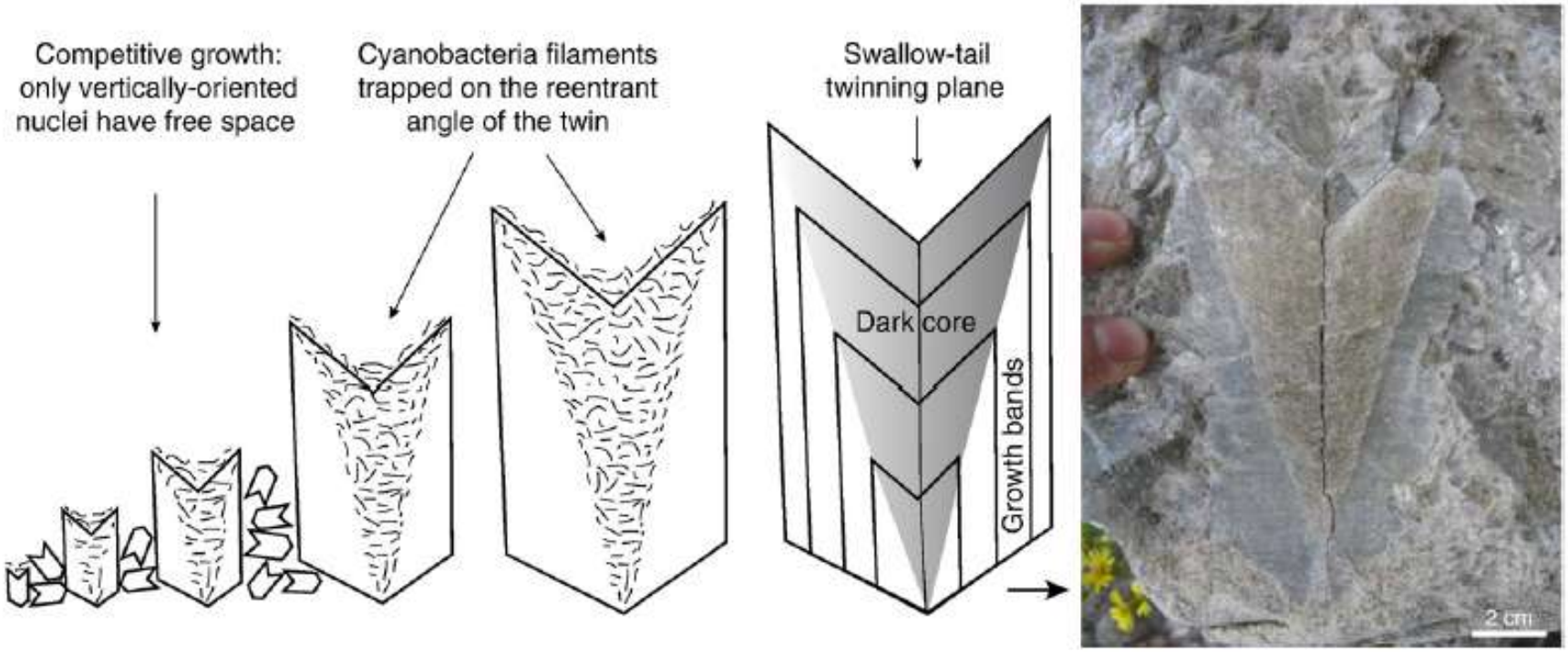

Fig. 8. Diagram showing the competitive growth of selenite determining the typical vertical orientation of the crystals (Mottura's rule) and the trapping mechanism of cyanobacteria filaments on the re-entrant angles of the twins producing the dark triangular core of the swallow-tail crystals.

Ontstaan banded Selenite

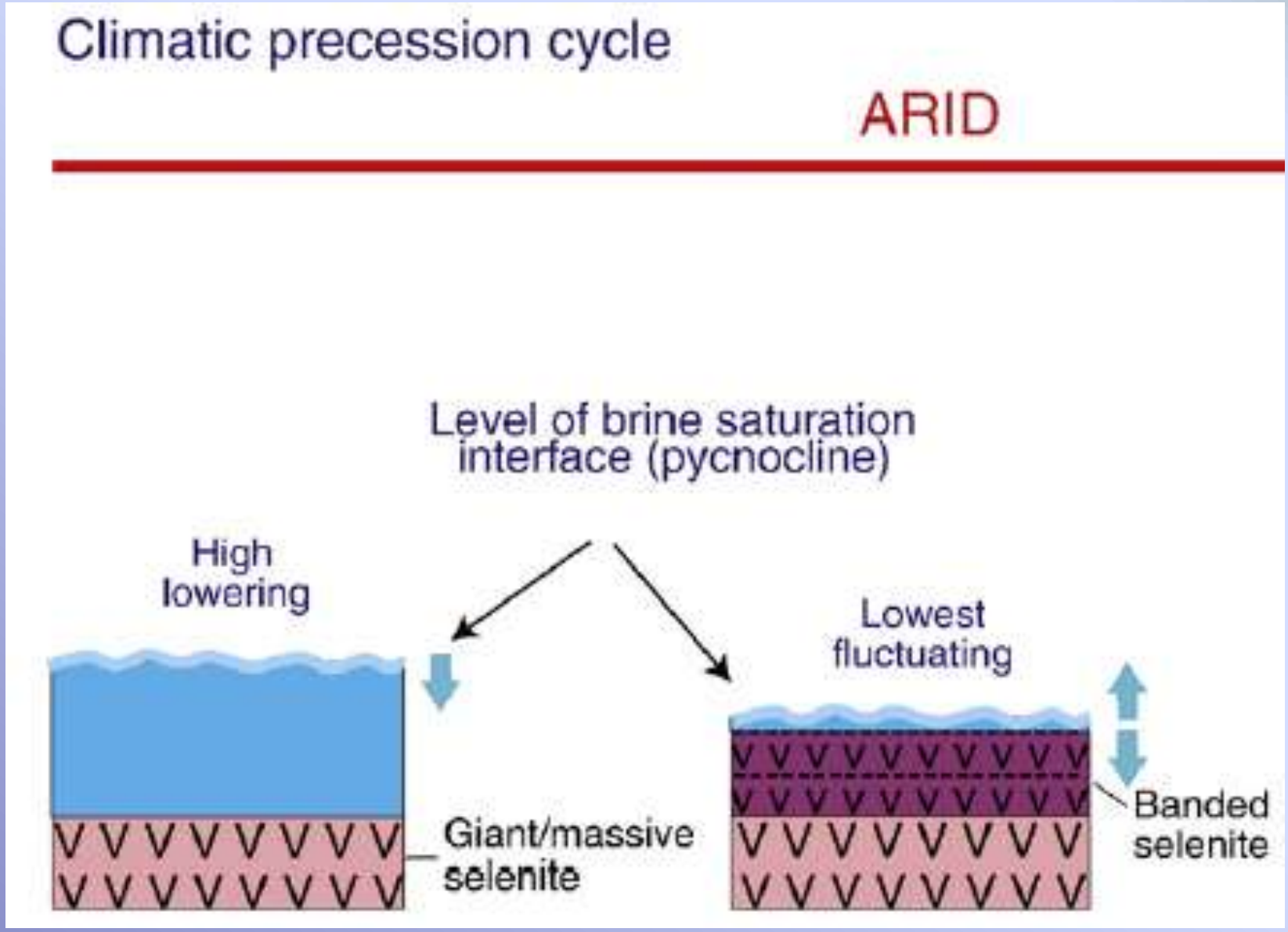


Branching selenite
BED 12
Banded selenite
Massive selenite
Branching selenite
Shale
BED 11
Banded selenite
Massive selenite
BED 10
D)
1 m

Overgang van Massive – naar banded selenite


C)
2 cm

Ontstaan Branching selenite

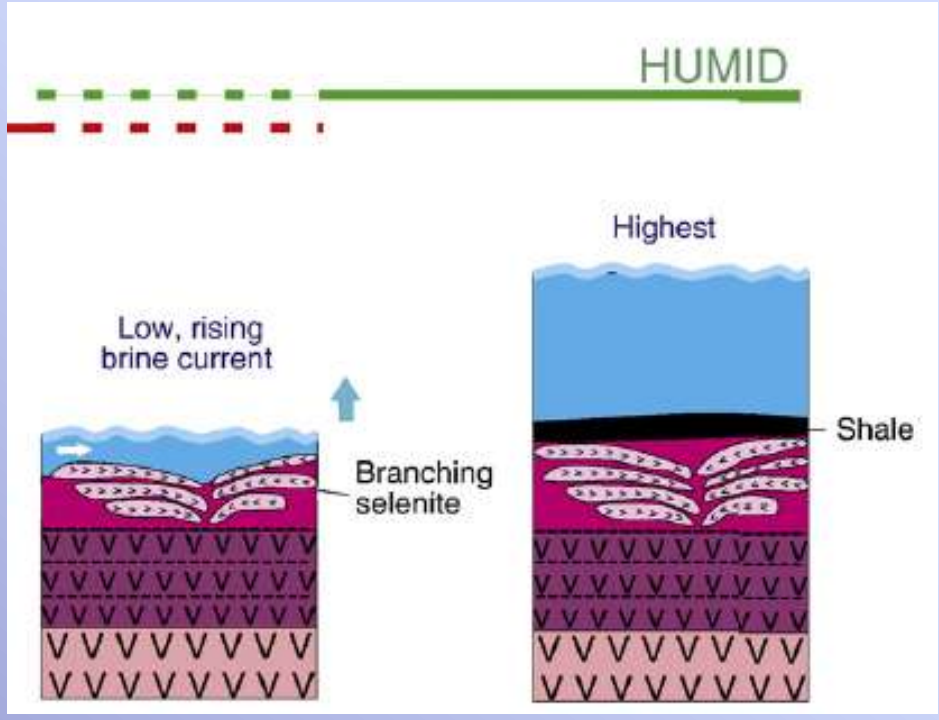

Branching selenite

Geraadpleegde literatuur 1

The Messinian Salinity Crisis: Past and future of a great challenge for marine sciences

Marco Roveri [a,b,*], Rachel Flecker [c], Wout Krijgsman [d], Johanna Lofi [e], Stefano Lugli [f], Vinicio Manzi [a,b], Francisco J. Sierro [g], Adele Bertini [h], Angelo Camerlenghi [i], Gert De Lange [j], Rob Govers [j], Frits J. Hilgen [j], Christian Hübscher [k], Paul Th. Meijer [j], Marius Stoica [l]

carbonate bioconstructions, Salento Peninsula, Italy: record of a microbial/metazoan association. Sedimentary Geology 263–264, 133–143.
Gvirtzman, Z., Reshef, M., Buch-Leviatan, O., Ben-Avraham, B., 2013. Intense salt deformation in the Levant Basin in the middle of the Messinian Salinity Crisis. Earth and Planetary Science Letters 379, 108–119.
Hardie, L.A., Lowenstein, T.K., 2004. Did the Mediterranean Sea dry out during the Miocene? A reassessment of the evaporite evidence from DSDP Legs 13 and 42A cores. Journal of Sedimentary Research 74, 453–461.
Hersey, J.B., 1965. Sedimentary basins of the Mediterranean Sea. In: Whittard, W.F., Bradshaw, R. (Eds.), Submarine Geology and Geophysics. Proceedings 17th Symposium Colston Res. Soc. April 5–9, 1965. Butterworths, London, pp. 75–91.
Hilgen, F.J., Krijgsman, W., 1999. Cyclostratigraphy and astrochronology of the Tripoli diatomite formation (pre-evaporite Messinian, Sicily, Italy). Terra Nova 11, 16–22.
Hilgen, F.J., Krijgsman, W., Langereis, C.G., Lourens, L.J., Santarelli, A., Zachariasse, W.J., 1995. Extending the astronomical (polarity) time scale into the Miocene. Earth and Planetary Science Letters 136, 495–510.
Hilgen, F.J., Bissoli, L., Iaccarino, S., Krijgsman, W., Meijer, R., Negri, A., Villa, G., 2000. Integrated stratigraphy and astrochronology of the Messinian GSSP at Oued Akrech (Atlantic Morocco). Earth and Planetary Science Letters 182, 237–251.
Hilgen, F.J., Kuiper, K., Krijgsman, W., Snel, E., van der Laan, E., 2007. Astronomical tuning as the basis for high resolution chronostratigraphy: the intricate history of the Messinian Salinity Crisis. Stratigraphy 4, 231–238.
Hodell, D.A., Curtis, J.H., Sierro, F.J., Raymo, M.E., 2001. Correlation of the Miocene to early Pliocene sequences between the Mediterranean and North Atlantic. Paleoceanography 16, 164–178.
Hsü, K.J., 1972. Origin of Saline Giants: a critical review after the discovery of the Mediterranean evaporite. Earth-Science Reviews 8, 371–396.
Hsü, K.J., 1973. The desiccated deep-basin model for the Messinian events. In: Drooger, C.W. (Ed.), Messinian Events in the Mediterranean. North-Holland Publ. Co., Amsterdam, pp. 60–67.
Hsü, K.J., 1984. The Mediterranean was a DesertPrinceton University Press, Princeton, NJ 1–197.
Ivanovic, R.F., Valdes, P.J., Flecker, R., Gregoire, L.J., Gutjahr, M., 2013b. The parameterisation of Mediterranean–Atlantic water exchange in the Hadley Centre model HadCM3, and its effect on modelled North Atlantic climate. Ocean Modelling 62, 11–16.
Ivanovic, R.F., Valdes, P.J., Flecker, R., Gutjahr, M., 2014. Modelling global-scale climate impacts of the late Miocene Messinian Salinity Crisis. Climate of the Past Discussions 9, 4807–4853.
Jauzein, A., Hubert, P., 1984. Les bassins oscillants: un modèle de genèse des séries salines. Bulletin des Sciences Géologiques, Strasbourg 37, 267–282.
Jimenez-Moreno, G., Pérez-Asensio, J.N., Larrasoaña, J.C., Aguirre, J., Civis, J., Rivas-Carballo, M.R., Valle-Hernàndez, M.F., Gonzàlez-Delgado, J.A., 2013. Vegetation, sea-level, and climate changes during the Messinian salinity crisis. Geological Society of America Bulletin 125, 432–444.
Jolivet, L., Augier, R., Robin, C., Suc, J.-P., Rouchy, J.M., 2006. Lithospheric-scale geodynamic context of the Messinian salinity crisis. Sedimentary Geology 188–189, 9–33.
Jongsma, D., Fortuin, A.R., Huson, W., Troelstra, S.R., Klaver, G.T., Peters, J.M., Van Harten, D., De Lange, G.J., Ten Haven, H.L., 1983. Discovery of an anoxic basin within the Strabo Trench, eastern Mediterranean. Nature 305 (795), 797.
Just, J., Hübscher, C., Betzler, C., Lüdmann, T., Reicherter, K., 2011. Erosion of continental margins in the Western Mediterranean due to sea-level stagnancy during the Messinian Salinity Crisis. Geo-Marine Letters 31, 51–64.
Kahana, R., 2005. Modelling the Interactions Between the Mediterranean and the Global Thermhaline Circulations. (Ph.D. thesis) University of East Anglia.
Karakitsios, V., Roveri, M., Lugli, S., Manzi, V., Gennari, R., Antonarakou, A., Triantaphyllou, M., Agiadi, K., Kontakiotis, G., 2013. Remarks on the Messinian evaporites of Zakynthos Island (Ionian Sea, eastern Mediterranean). Bulletin of the Geological Society of Greece 47.
Kastens, K., 1992. Did a glacio-eustatic sealevel drop trigger the Messinian salinity crisis? New evidence from ODP Site 654 in the Tyrrehnian Sea. Paleoceanography 7, 333–356.
Kontopoulos, N., Zelilidis, A., Piper, D.J.W., Mudie, P.J., 1997. Messinian evaporites in Zakynthos, Greece. Palaeogeography, Palaeoclimatology, Palaeoecology 129, 361–367.

Geraadpleegde literatuur 2

The Messinian Salinity Crisis: Past and future of a great challenge for marine sciences

Marco Roveri [a,b,*], Rachel Flecker [c], Wout Krijgsman [d], Johanna Lofi [e], Stefano Lugli [f], Vinicio Manzi [a,b], Francisco J. Sierro [g], Adele Bertini [h], Angelo Camerlenghi [i], Gert De Lange [j], Rob Govers [j], Frits J. Hilgen [j], Christian Hübscher [k], Paul Th. Meijer [j], Marius Stoica [l]

Hsü, K.J., Giovanoli, F., 1979. Messinian event in the Black Sea. Palaeogeography, Palaeoclimatology, Palaeoecology 29, 75–93.

Hsü, K., Ryan, W.B.F., Cita, M., 1973a. Late Miocene desiccation of the Mediterranean. Nature 242, 240.

Hsü, K.J., Cita, M.B., Ryan, W.B.F., 1973b. The origin of the Mediterranean evaporites. In: Ryan, W.B.F., Hsü, K.J., Cita, M.B. (Eds.), Initial Reports of the Deep Sea Drilling Project 13, Part 2. U.S. Government Printing Office, Washington D.C., pp. 1203–1231.

Hsü, K.J., Montadert, L., Bernoulli, D., Cita, M.B., Erikson, A., Garrison, R.E., Kidd, R.B., Melieres, F., Muller, C., Wright, R.H., 1978. Initial report of Deep Sea Drilling Project. Mediterranean Sea, 42. U.S. Government Printing Office, Washington, DC.

Hübscher, C., Dümmong, S., 2011. Levant Basin — salt and fluid dynamic. In: J.L., Déverchère, J., Gaullier, V., Gillet, H., Guennoc, P., Gorini, C., Loncke, L., Maillard, A., Sage, F., Thinon, I. (Eds.), Seismic Atlas of the "Messinian Salinity Crisis" Markers in the Mediterranean and Black Seas. Commission for the Geological Map of the World and Mémoires de la Société Géologique de France, nouvelle série, p. 60.

Hübscher, C., Netzeband, G., 2007. Evolution of a young salt giant: the example of the Messinian evaporites in the Levantine Basin. In: Wallner, M., Lux, K.-H., Minkley, W., Hardy, J., H.R. (Eds.), The Mechanical Behaviour of Salt — Understanding of THMC Processes in Salt. Taylor&Francis Group, London, pp. 175–184.

Kouwenhoven, T.J., Seidenkrantz, M.S., van der Zwaan, G.J., 1999. Deep-water changes: the near-synchronous disappearance of a group of benthic foraminifera from the Late Miocene Mediterranean. Palaeogeography, Palaeoclimatology, Palaeoecology 152, 259–281.

Kouwenhoven, T.J., Hilgen, F.J., van der Zwaan, G.J., 2003. Late Tortonian–early Messinian stepwise disruption of the Mediterranean–Atlantic connections: constraints from benthic foraminiferal and geochemical data. Palaeogeography, Palaeoclimatology, Palaeoecology 18, 303–319.

Krijgsman, W., Meijer, P.Th., 2008. Depositional environments of the Mediterranean "Lower Evaporites" of the Messinian salinity crisis: Constraints from quantitative analyses. Marine Geology 253, 73–81.

Krijgsman, W., Hilgen, F.J., Marabini, S., Vai, G.B., 1999a. New paleomagnetic and cyclostratigraphic age constraints on the Messinian of the Northern Apennines (Vena del Gesso Basin, Italy). Memorie della Società Geologica Italiana 54, 25–33.

Krijgsman, W., Hilgen, F.J., Raffi, I., Sierro, F.J., Wilson, D.S., 1999b. Chronology, causes, and progression of the Messinian salinity crisis. Nature 400, 652–655.

Krijgsman, W., Fortuin, A.R., Hilgen, F.J., Sierro, F.J., 2001. Astrochronology for the Messinian Sorbas basin (SE Spain) and orbital (precessional) forcing for evaporite cyclicity. Sedimentary Geology 140, 43–60.

Krijgsman, W., Blanc-Valleron, M.M., Flecker, R., Hilgen, F.J., Kouwenhoven, T.J., Orszag-Sperber, F., Rouchy, J.M., 2002. The onset of the Messinian salinity crisis in the eastern

Met dank aan

1 dr. Paul Th. Meijer

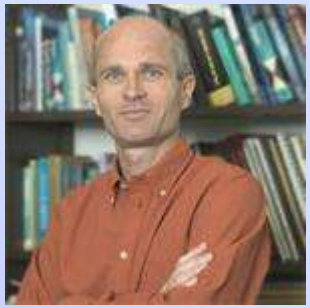

4 dr. Rob Govers

7 prof. dr. M.J.R. Wortel

2 Marco Roveri

3 prof. dr. Wout Krijgsman

5 Vinicio Manzi

6 D. Garcia-Castellanos

Einde